



**HAL**  
open science

# Polymer networks architecture using supramolecular interactions

Yiping Ni

► **To cite this version:**

Yiping Ni. Polymer networks architecture using supramolecular interactions. Other. Université Jean Monnet - Saint-Etienne, 2012. English. NNT : 2012STET4005 . tel-00952090

**HAL Id: tel-00952090**

**<https://theses.hal.science/tel-00952090>**

Submitted on 26 Feb 2014

**HAL** is a multi-disciplinary open access archive for the deposit and dissemination of scientific research documents, whether they are published or not. The documents may come from teaching and research institutions in France or abroad, or from public or private research centers.

L'archive ouverte pluridisciplinaire **HAL**, est destinée au dépôt et à la diffusion de documents scientifiques de niveau recherche, publiés ou non, émanant des établissements d'enseignement et de recherche français ou étrangers, des laboratoires publics ou privés.

# **THESE**

Présentée à

**L'Université Jean Monnet, Saint Etienne**

**Ecole doctorale de Saint Etienne**

Pour obtenir le diplôme de

**DOCTEUR**

**Spécialité Chimie et Science des Matériaux**

Par

**Yiping NI**

---

## **Polymer networks architecture using supramolecular interactions**

---

Directeur de Thèse: Professeur Mohamed TAHA

Co-directeur de Thèse : Dr Frédéric BBECQUART

Soutenu le : 20 Novembre 2012

Devant le jury composé par :

Mihail BARBOIU	Rapporteur
Jianding CHEN	Rapporteur
Mohamed TAHA	Examineur
Frédéric BECQUART	Examineur
Françoise MECHIN	Examinatrice

## Remerciements

The experiments in the present study were realized in the LABORATOIRE D'INGENIERIE DES MATERIAUX POLYMERES, CNRS UMR 5223, in site UNIVERSITE JEAN MONNET, SAINT ETIENNE, FRANCE.

I feel grateful to the Professor Christian CARROT, for welcoming me to his laboratory, and treating me friendly in my three years of doctoral study.

My deepest gratitude greatly to Professor Mohamed TAHA, my director of thesis, for his constant encouragement and guidance. He has walked me through all the stages of the writing of this thesis. Without his consistent and illuminating instruction, this thesis could not have reached its present form.

I would like to express my heartfelt gratitude to Mr Frédéric BECQUART, who offered a lot of help to let me accommodate myself to this new circumstance in France. He is always conscientious to all the details of my experiments in spectroscopic analyses, and willing to point out and correct the flaws in my thesis.

I am also greatly indebted to the professors Professor Jianding CHEN, from EAST CHINA UNIVERSITY OF SCIENCE AND TECHNOLOGY, CHINA. Each time she came visiting here, I received constructive suggestions from the group discussion between supervisors from CHINA and FRANCE. I also want to thank the financial support from China scholarship council (state scholarship fund) for their sponsorship during three years.

I am honored and appreciative to the participation of jury: Mr Monsieur Mihail BARBOIU and Madam Jianding CHEN as the reporters of thesis, and Madam Françoise MECHIN as the examiner.

I would like to express my appreciations to all those who helped me in the laboratory during the writing of in this thesis: Ouissam ADIDOU, Jean-Charles MAJESTE, Caroline PILLON. I owe my sincere gratitude to all the friends I met here and in CHINA: Céline, Nidhal, Hang, Méral, Dominico, Shengmiao, and so on, for gave me their help and time in listening to me

and helping me work out my problems during the difficult course of the thesis, also for the happy and great time that we had spent together in the past three years.

Last my thanks would go to my beloved family and BFFs: my father and mother for their loving considerations and great confidence in me all through these years; Momo, Suzey and Kathy for their consistent support, trust and love; my cat P for his cuteness that consoled my slump.

## Publicatons et communications

### Publications:

Yiping NI, Frédéric BECQUART, Mohamed TAHA, Jean-Charles MAJESTE, Jianding CHEN. Poly(butyl methacrylate-co-methacrylic acid) copolymers with calcium carbonate supramolecular networks (submitted)

Yiping NI, Frédéric BECQUART, Mohamed TAHA, Ouissam ADIDOU, Jean-Charles MAJESTE, Jianding CHEN. Polystyrene supramolecular networks based on DA-AD hydrogen bonds (submitted)

Yiping NI, Frédéric BECQUART, Mohamed TAHA, Jianding CHEN. Construction and controlling of novel polyurea-urethane networks based on urea/biuret through hydrogen bonds (submitted)

### Communications :

Poster: Yiping NI, Frédéric BECQUART, Jianding CHEN, Mohamed TAHA, Supramolecular Interactions in PBMA/MAA/CaCO<sub>3</sub> Copolymers, **Frontiers in Polymer Sciences**, May 29-31, 2011, Lyon, France.

Oral presentation: Yiping NI, Frédéric BECQUART, Jianding CHEN, Mohamed TAHA, Supramolecular Interactions in PBMA/MAA/CaCO<sub>3</sub> Copolymers, **39èmes Journées d'Etudes des Polymères** , October 16-21, 2011, Val joly, France.

Oral presentation: Yiping NI, Ouissam ADIDOU, Frédéric BECQUART, Jianding CHEN, and Mohamed TAHA. Construction and characterization of supramolecular networks based on DA-AD hydrogen bonds in poly(styrene-co-2-methacrylamidopyridine) copolymers, **7<sup>th</sup> International Conference on Nanostructured Polymers and Nanocomposites**, April 24-27, 2012, Prague, Czech Republic.

# Index

General Introduction .....	9
Introduction générale .....	11
Chapter A .....	14
Bibliography .....	14
1. Introduction of supramolecular polymer .....	15
1.1 What is supramolecular chemistry? .....	15
1.2 What is supramolecular polymer? .....	16
1.3 Different categories of supramolecular interaction.....	17
1.3.1 Hydrogen bonds interaction.....	17
1.3.2 Ionic interaction .....	20
1.3.3 Coordinate interaction.....	22
1.3.4 $\pi$ -conjugated interaction.....	23
1.4 Conclusion .....	25
2. Determination of supramolecular bonding .....	26
2.1 Binding constant determination by NMR titration <sup>[24]</sup> .....	26
2.1.1 Host-guest 1:1 complex (heterodimers) system with fast exchange kinetics .....	26
2.1.2 Self-dimerization (homodimer) systems with fast exchange kinetics ..	31
2.1.3 Examples of curve fitting by using NMR methods .....	33
2.2 Binding constant by UV-vis titration <sup>[24]</sup> .....	35
2.2.1 General view of binding constant calculation.....	35
2.2.1 Examples of data treatments by using UV-Vis titration.....	37
2.3 Alternative spectroscopic methods .....	38
2.4 Conclusion .....	39
3. Ionic supramolecular interaction: application of CaCO <sub>3</sub> in polymer materials.....	40
3.1 Introduction of nano inorganic fillers .....	40
3.2 Use calcium carbonate: advantage and disadvantage .....	41
3.3 Modifications of Calcium carbonate (PCC) .....	41
3.3.1 Physical modifications .....	42
3.3.2 Micro-emulsion modification .....	42
3.3.3 High-energy surface modification .....	42

3.3.4	Mechanical force modification .....	43
3.3.5	Chemical modifications .....	43
3.4	Surface modifier.....	44
3.4.1	Organic acids .....	44
3.4.2	Coupling agents .....	45
3.4.3	Phosphate modifier .....	45
3.5	The ionic state ( $\text{Ca}^{2+}$ ) dispersion based from $\text{CaCO}_3$ .....	46
3.5.1	Morphology: Eisenberg model .....	46
3.5.2	Influence of ionic interactions to the mechanical properties of polymers 48	
3.6	$\text{CaCO}_3$ / acid / polybutyl methacrylate composite.....	52
3.6.1	Why PBMA?.....	52
3.6.2	$\text{CaCO}_3$ influence to polymer.....	52
3.7	Conclusion .....	55
4.	Nonionic supramolecular interaction: hydrogen bonding polymer .....	56
4.1	Why double hydrogen bonding moiety?.....	56
4.2	The motifs based on aminopyridine derivatives .....	57
4.3	The moieties based on amide blocks .....	58
4.4	The moieties based on urea blocks .....	60
4.5	Conclusion .....	63
	References.....	64
Chapter B	.....	71
Poly(butyl methacrylate-co-methacrylic acid) copolymers with calcium carbonate supramolecular networks .....		71
Résumé.....		72
Abstract.....		73
B-1. INTRODUCTION .....		74
B-2. EXPERIMENTAL .....		77
B-2.1. Materials .....		77
$\text{CO}_2$ formation and quantification.....		78
Samples preparation.....		78
Preparation in tubes.....		79
Plates preparation.....		79
B-2.2 Characterizations.....		80

Rheology .....	80
Thermal analysis .....	80
Thermodegradation analyses .....	81
Microscopy analyses .....	81
X-ray diffraction .....	81
<b>B-3. RESULTS AND DISCUSSION.....</b>	<b>81</b>
B-3.1 Calcium carbonate reactivity and decomposition.....	81
Cluster structuration from CaCO <sub>3</sub> decomposition .....	83
Crystalline peaks.....	83
Ionic peak.....	83
B-3.2 Thermal properties.....	85
B-3.3 Calcium Carbonate dispersion.....	88
B-3.4 Solubility of PBMA-co-PMA/CaCO <sub>3</sub> systems .....	90
B-3.5 Structural analyses .....	92
Filler content effect above the glass transition.....	92
MA content in the copolymer above the glass transition.....	97
<b>B-4 CONCLUSION.....</b>	<b>98</b>
<b>REFERENCES .....</b>	<b>100</b>
<b>Chapter C .....</b>	<b>103</b>
<b>Polystyrene supramolecular networks based on DA-AD hydrogen bonds.....</b>	<b>103</b>
Résumé.....	104
Abstract.....	105
C-1. Introduction:.....	106
C-2. Experimental:.....	109
C-2.1. Reagents.....	109
C-2.2. 2-methacrylamidopyridine (MAP) synthesis: monomer with DA moiety..	110
C-2.3. Copolymerization of P(MAAM-co-St) and P(MAP-co-St).....	110
MAAM and styrene copolymerization in THF.....	110
MAP and styrene Bulk copolymerization.....	111
C-2.4. Characterizations.....	111
Fourier transform infrared (FTIR) spectroscopy .....	111
Nuclear magnetic resonance (NMR) spectroscopy.....	111
Size-exclusion chromatography (SEC).....	112
Thermal analysis .....	112

Dynamic mechanical spectroscopy in the molten state .....	112
C-3. Results and discussion .....	113
C-3.1. Dimerization of self-assemblies.....	113
C-3.2. Calculation of association constants $K_{\text{ass}}$ .....	114
C-3.3. Characterization of hydrogen bonds in P(MAAM-co-St) and P(MAP-co-St) by FTIR.....	117
Effect of MAAM concentration to P(MAAM-co-St) in FTIR spectra .....	117
Effect of MAP concentration to P(MAP-co-St) in FTIR spectra.....	119
C-3.4. Solubility of P(MAAM-co-St) and P(MAP-co-St) with various DA moiety concentrations .....	121
C-3.5. Thermal properties of P(MAAM-co-St) and P(MAP-co-St) .....	123
C-3.6. Structure analyses by dynamic rheology in the molten state .....	125
P(MAAM-co-St) copolymers dynamic rheology .....	126
P(MAP -co-St) copolymers dynamic rheology.....	128
C-4. Conclusion .....	132
REFERENCES .....	134
Chapter D.....	138
Polyurea-urethane supramolecular thermo-reversible networks .....	138
Résumé.....	139
Abstract.....	140
D-1.Introduction.....	141
D-2. Experimental Section.....	143
D-3. Results and discussion .....	147
D-4. Conclusion .....	161
REFERENCES .....	163
Annexe .....	166
Annexe 1. $M_c$ calculation of P(MAP-co-St) .....	166
Annexe 3. Network model through hydrogen bonds in the PUU .....	168
Annexe 3. Temperature dependent $^1\text{H}$ NMR in PU Bi F=1 .....	169
Annexe 2. PUU system reinforced with PVA.....	170
General Conclusion.....	172
Conclusion Générale.....	174
Abstract.....	176
Résumé.....	177

## Abbreviations

AcAP	2-acetamidopyridine
AIBN	2-azobis(2-methyl-propionitrile)
AP	2-aminopyridine
BMA	Butyl methacrylate
DMSO	Dimethyl sulfoxide
$K_{\text{ass}}$	Association constant
MA	Methacrylic acid
MAAM	Methacrylamide
MAP	2-methacrylamidopyridine
MC	Methacryloyl chloride
$M_c$	Molecular weight between crosslinks
PCC	Precipitated calcium carbonate
PUU	Polyurea-urethane
St	Styrene
TEA	Triethylamine
$T_g$	Glass transition temperature
THF	Tetrahydrofuran
UPy	Ureidopyrimidone

## General Introduction

The purpose of this study is to introduce the the supramolecular moieties on amorphous polymer chains. Generated supramolecular interactions are expected to improve the mechanical and rheological properties of the materials. By the formation of supramolecular interactions, physically crosslinked materials are considered to result to the appearance of rubbery plateau above the glass transition temperature, and most of all, the thermo reversibility at high temperature.

Three different strategies are applied to generate supramolecular interactions as they are presented in the different chapters of this thesis. All these approaches have some parts in common: monomers that commercially available or easily prepared are used, and polymerizations or assembling to obtain the material are also simply achieved. These common points improve the interests and potentials of polymers in further applications.

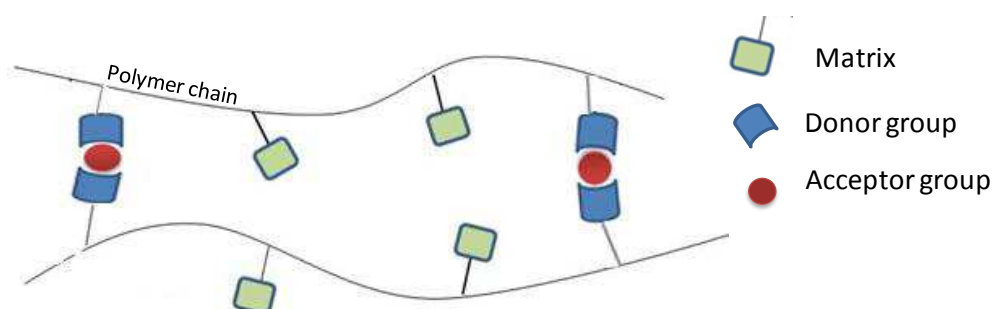


**Figure 1. Illustration of network formation by supramolecular interaction between donor and acceptor groups**

Two kinds of the supramolecular interactions are investigated in this work. One is ionic interaction between metal cations and organic acid anions; this type of interaction was proved as the strongest interaction in supramolecular chemistry. The other one is the based on multiple hydrogen bonding pairs which were the most extensively studied supramolecular interactions.

The first chapter (A) of the thesis is a bibliographic research devoted to supramolecular chemistry applid to polymers. Different types of supramolecular interactions are presented. Among which, the ionic attraction and hydrogen bonds self-assembling, are emphasized and presented in details. The methods that applied in association constant calculation due to the supramolecular interactions are also investigated.

The second chapter (B) presents the supramolecular polymer network synthesis based on ionic interactions. The chosen matrix is PBMA, which is amorphous with a low glass temperature. Organic acid pendant groups are introduced by copolymerization of MAA and BMA, while calcium carbonate is introduced as ionic fillers. Therefore ionic interactions are formed between  $\text{COO}^-$  and  $\text{Ca}^{2+}$  since  $\text{CaCO}_3$  reacts with acids to generate ionic  $\text{Ca}^{2+}$ . From this reaction,  $\text{CaCO}_3$  act as both a filler and a ionic crosslinking agent. Eisenberg well described that ionomers tend to form ion rich aggregates in multiplets. When these regions become sufficiently large, they exhibit phase-separated behavior with a second  $T_g$ , at a higher temperature than the matrix  $T_g$ , associated to the glass transition of the ion-rich cluster phase. The clusters behave as crosslink points, and consequently reinforce the PBMA. The attribution of  $\text{CaCO}_3$  to the system is studied morphologically and rheologically.

Chapter (C) and Chapter (D) are focused on the supramolecular polymer networks through hydrogen bonds interactions, but by two different approaches.

The third chapter (C) presents the synthesis of supramolecular materials by polyaddition. In this approach, a functional monomer containing DA moieties (D for hydrogen donor and A for hydrogen acceptor) is chosen and copolymerized with styrene (St) as co-monomer. Thus the PS as the main chain with DA moiety as pendent groups is obtained. Two functional monomers are MAAM which is commercial available, and MAP which is synthesized in laboratory conditions. The homodimerizations of DA moiety to DA-AD dimers act as crosslinks in the matrix. Their influence to the material rheological properties is investigated.

The last chapter (D) presents the synthesis of supramolecular polymer by polycondensation. In this approach, the functional urea or biuret is reacted with isocyanate to obtain the tri-uret or tetra-uret blocks monomer respectively. Thus multi-uret segments containing DDDD-AAA and DDDDD-AAAA moieties are distributed in a multi-functional branched structure. The conformations and associations of these two types of multi-uret segments are compared, resulting in the distinctive performances in network properties.

Chapter (B), chapter (C) and chapter (D) are written respecting the publication forms of different journals.

## Introduction générale

L'objectif de ce travail de thèse est d'introduire des motifs (ionique ou liaison hydrogène) sur des chaînes macromoléculaires amorphes, susceptibles de générer des interactions supramoléculaires afin d'en améliorer les propriétés mécaniques et rhéologiques. Par la formation d'interactions supramoléculaires, il est envisagé la réticulation physique du matériau accompagnée de la création d'un plateau caoutchoutique au-delà de la température de transition vitreuse et surtout la réversibilité de ces interactions à haute température.

Trois stratégies différentes ont été abordées pour générer de telles interactions et sont présentées dans les différentes parties de cette thèse. Toutes les approches utilisées ont pour point commun d'une part, d'utiliser des réactifs commercialement disponibles ou simples à synthétiser et d'autre part de proposer des procédés de synthèse des matériaux également simples à mettre en œuvre ce qui augmente leur attractivité et leur potentiel d'applications futures.

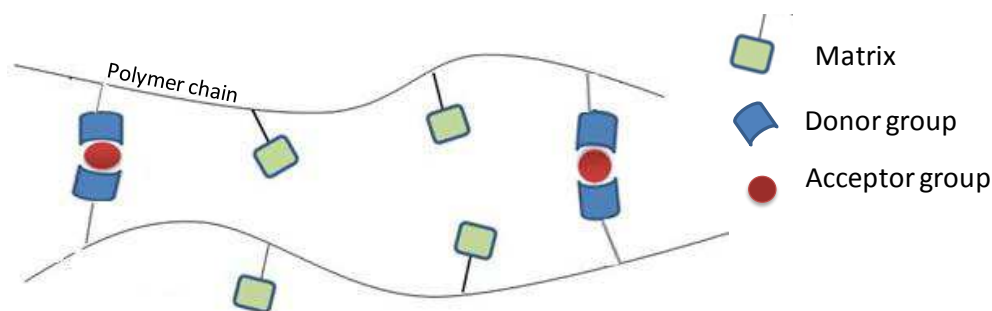


**Figure 1. Illustration of network formation by supramolecular interaction between donor and acceptor groups**

Deux types d'interaction supramoléculaire ont été abordés dans ce travail. Le premier concerne des interactions de type ioniques entre cations métalliques libres et anions provenant de fonctions acide carboxylique. Il a déjà été montré que ce type d'interaction est le plus fort en chimie supramoléculaire. Le second type d'interaction porte sur des motifs à liaisons hydrogène multiples capables d'interagir entre eux. Ce dernier type est certainement celui qui a été le plus développé dans la littérature scientifique ces quarante dernières années.

Le premier chapitre de cette thèse est une présentation bibliographique de la chimie supramoléculaire appliquée aux polymères. Différents types d'interactions supramoléculaires

sont présentés en détail parmi lesquels les interactions ioniques et les liaisons hydrogène. En particulier, les méthodes et modèles de calcul existants des constantes d'association qui permettent d'avoir une quantification des forces d'interaction supramoléculaires sont abordés.

Le second chapitre présente la synthèse de réseaux polymères supramoléculaires par des interactions ioniques. La matrice choisie est un polyméthacrylate de butyle qui est à la base amorphe et possédant une température de transition vitreuse basse. Des fonctions acides carboxyliques ont été introduites sur ce polymère en copolymérisant du méthacrylate de butyle et de l'acide méthacrylique en présence de carbonate de calcium. Ce dernier est présent en tant que charge mais génère aussi des cations métalliques  $\text{Ca}^{2+}$  et des fonctions carboxylates  $-\text{COO}^-$  permettant ainsi la formation des interactions ciblées. Eisenberg décrit très bien la tendance des ionomères à former des agrégats ioniquement riches en multiplets. Lorsque ces multiplets sont suffisamment nombreux, ils tendent à coalescer pour former une seconde phase physiquement liée, en clusters, avec sa propre température de transition vitreuse, supérieure à celle de la matrice. Ces clusters se comportent comme des points de réticulation et sont donc susceptibles de renforcer le matériau. La contribution du carbonate de calcium est étudiée morphologiquement et par rhéologie.

Les deux derniers chapitres sont dédiés à la synthèse des matériaux supramoléculaires pouvant former des réseaux physiques par liaisons hydrogène. Deux approches distinctes ont été utilisées.

Le troisième chapitre traite la synthèse de matériaux polymères supramoléculaires par copolymérisation radicalaire du styrène où un co-monomère est porteur d'un motif difonctionnel donneur-accepteur (DA) pendant. Deux co-monomères supramoléculaires ont été testés. L'un, la méthacrylamide (MAAM) est disponible commercialement et l'autre, la 2-méthacrylamidopyridine (MAP) a été synthétisée au laboratoire pour un protocole mis au point. L'homodimerisation des motifs DA en assemblages DA-AD s'est effectué comme attendu dans les deux cas avec l'obtention de matériaux réticulés physiquement mis en évidence par des études rhéologiques,

Le dernier chapitre présente la synthèse de matériaux supramoléculaires par polycondensation. Cette approche originale a consisté à générer des motifs supramoléculaires par réactions entre l'urée ou le biruet avec des isocyanates. Les motifs générés sont multifonctionnels DDDD-AAA ou DDDDD-AAAA. L'étude va montrer qu'il existe manifestement deux conformations possibles en zig-zag ou repliée qui influent sur la force

des associations de ces motifs et donc sur les propriétés des matériaux obtenus. Ces motifs ont été introduits dans des structures branchées ensuite synthétisées, ayant de un à cinq motifs supramoléculaires. L'impact de la fonctionnalité de ces motifs sur les propriétés des matériaux obtenus est présenté.

Les trois derniers chapitres sont présentés sous la forme de publications telles qu'elles ont été soumises aux éditeurs.

**Chapter A**  
**Bibliography**

# 1. Introduction of supramolecular polymer

## 1.1 What is supramolecular chemistry?

Supramolecular is the chemistry which studies the molecular assemblies and bonds between molecular. It was first mentioned by Jean-Marie Lehn, one of forerunners of supramolecular chemistry and also the winner of 1987 Nobel chemical prize. It can be described as “the chemistry of the intermolecular bond, covering the structures and functions of the entities formed by association of two or more chemical species”<sup>[1]</sup>. The targets of supramolecular research are the molecular assemblies based on the weak intermolecular effect such as noncovalent bonds. These noncovalent bonds include hydrogen bonds, static charge electricity, van de waals, and so on. Even their strength is much weaker than covalent interaction, it endows the materials with reversible properties to exterior environment like temperature, solvent, pH value.(Figure 1.1)<sup>[2]</sup>

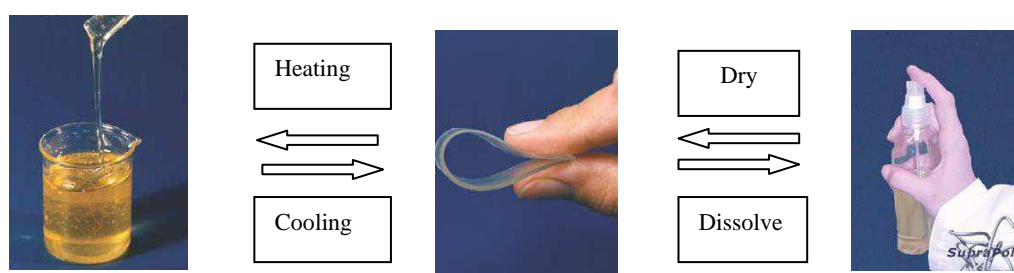


**Figure 1.1 Supramolecular polymer reversible properties, based on poly(ethylene-co-butylene), modified with UPy** <sup>[2]</sup>

Reversibility makes supramolecular materials competent in the most advanced area such as biologic sensor, drug slow release, cell recognition, etc <sup>[3, 4]</sup>. This property could be controlled by introducing different functional group of different quantities in the materials. In 1998, Beijer and Sejbasma group <sup>[5]</sup> succeed in preparing UPy moieties and improved the hydrogen-bonding supramolecular interaction into quadruple hydrogen bond moieties.

In recent years, a large number of concepts have been disclosed based on different noncovalent interactions. After the delicate structure design of supramolecular polymers which are assembled through these non-covalent interactions, materials with reversible properties are obtained while they have polymer-like performance in solution or in bulk.

## 1.2 What is supramolecular polymer?

According to the earliest conception of supramolecular chemistry, supramolecular polymer is a molecular aggregate which is self-assembled by non-covalent interactions between monomeric units <sup>[6]</sup>. To generalize, “monomers”, the repeating units with functional supramolecular group, are combined by noncovalent interaction instead of covalent one as in figure 1.2 A. In other cases, this step could be changed by graft the supramolecular moieties on polymer chains as the pendant groups in figure 1.2 B.

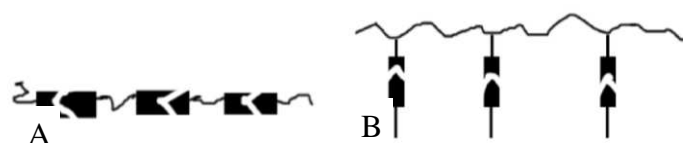


**Figure 1.2 Two different conformation of supramolecular polymer**

The impressive progress in supramolecular chemistry improved the methods to prepare polymers without macromolecular structure. Instead, the secondary interactions are used to assemble the repeating units into a polymer chain. The reasons why these polymers are called as supramolecular polymers, could be explained in two aspects. On one hand, the long chains or further network structures after self-assembling have the chemical structures like polymer chains. On the other hand, the physical performances due to the weak secondary interaction in these materials, such as softness, are also like those in polymers.

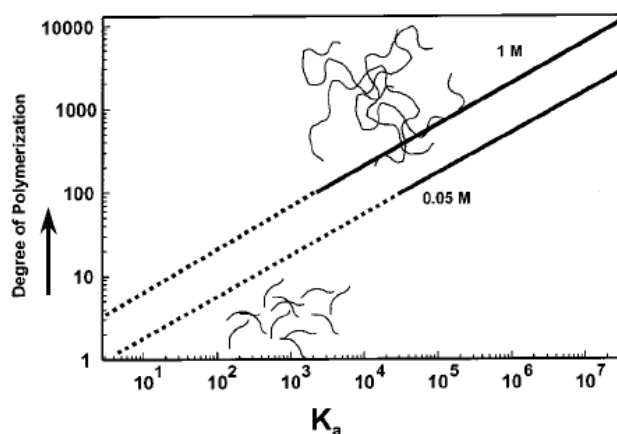


**Figure 1.3 Theoretical relationship between the association constant  $K_a$  and DP (degree of polymerization)**

[7]

Using a directional complementary couple (A-B) or a self-complementary couple (A-A), it is possible to form all known structures of polymers, including linear homo- and copolymers,

cross-linked networks, and even (hyper)branched structures. In supramolecular polymers, which are formed by the reversible association of bifunctional monomers, the average degree of polymerization (DP) is determined by the strength of the end group interaction. The degree of polymerization is obviously dependent on the concentration of the solution and the association constant, and a theoretical relationship is given in Figure 1.3 [7].

Typical supramolecular polymers are reversible aggregates that can break and recombine on experimental time scales. It is shown by the work on ureidopyrimidone-based supramolecular polymers that the model also describes in detail the viscosity behavior of reversible supramolecular polymers [8]. Many of the materials properties of supramolecular polymers are those well-known for traditional polymers, although the reversibility will lead to an unconventional temperature dependence of the materials' properties.

### 1.3 Different categories of supramolecular interaction

Supramolecular polymers can be classified by their different secondary interaction as hydrogen bonds interaction, ionic charges interaction, metal-coordinate interaction and  $\pi$  conjugated interaction. Their binding energy is listed in table 1.1.

**Table 1.1 Binding energy of non-covalent bonds and covalent bonds**

Non-covalent bonds		Covalent bonds	
Ionic interaction	100-350 kJ/mol	C-O bond	340 kJ / mol
Hydrogen bond interaction	~120 kJ/mol	C-C bond	360 kJ / mol
Electrostatic interaction	~20 kJ/mol	C-H bond	430 kJ / mol
Van der Waals interaction	0.4-4 kJ/mol	C=C bond	600 kJ / mol
Cation $-\pi$ interaction	5-80 kJ/mol	C=O bond	690 kJ / mol
$\pi-\pi$ stacking	0-50 kJ/mol		

#### 1.3.1 Hydrogen bonds interaction

A hydrogen bond is composed by a polarizable hydrogen acceptor atom linked to an electronegative atom (A, also known as hydrogen acceptor) that interacts with another nucleophilic donor (D, also known as hydrogen donor). This form could be symbolized as D-H $\cdots$ A [9].

The strength of hydrogen bonds can be characterized by association constant ( $K_a$ ). The bond energy of single hydrogen bonds can reach to  $120 \text{ kJ}\cdot\text{mol}^{-1}$  maximum, almost the half of a  $\sigma$  carbon-carbon bond close to  $348 \text{ kJ}\cdot\text{mol}^{-1}$  [10]. Although hydrogen bonds are not the strongest non-covalent interactions, they are prominent in supramolecular chemistry due to their versatility and directionality.

Structure of a hydrogen bonding supramolecular polymer can be efficiently controlled by calculating and designing the monomeric units [11]. Intermolecular hydrogen bonds at defined positions of these building blocks as well as their respective starting geometry and the initial size determine the mode of assembly into supramolecular polymers in different types in figure 1.4. In all cases, weak-to-strong hydrogen-bonding interactions can act as the central structure-directing force for the organization of polymer chains and thus the final materials properties.

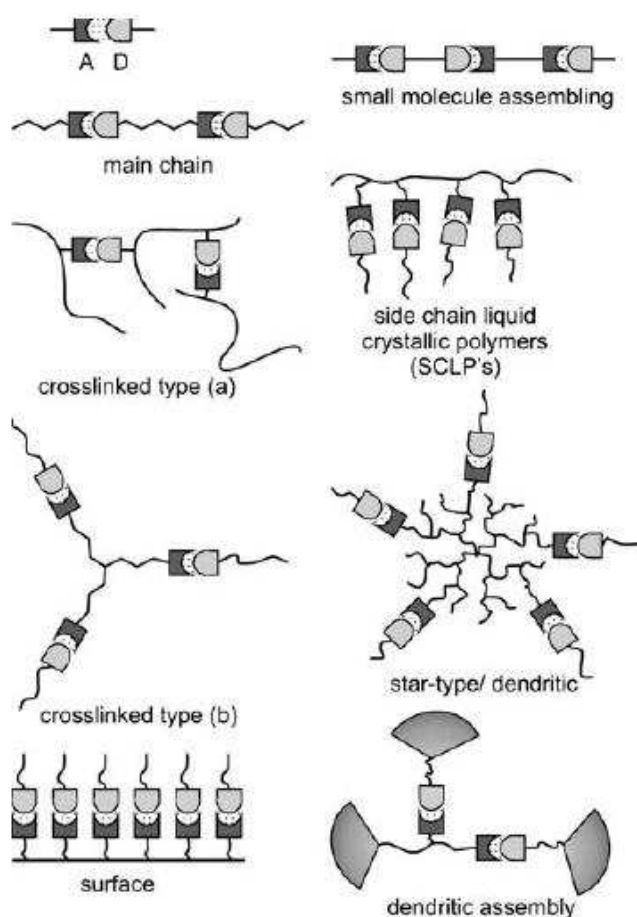


**Figure 1.4 Architectures of different hydrogen bonded supramolecular polymers** [11]

Strength of a single hydrogen bond depends on the nature of D atom and A atom, such as atom radius or electron-withdrawing ability as well as the external environment as solvent

effect. For multiple hydrogen bonds, the influential factors also include the numbers of hydrogen bonds, the serial arrangement of donor and acceptor in one moiety.

Pranata<sup>[12]</sup> is the first deeply studied the influence of different structures of multi-hydrogen-bonding moieties in triple hydrogen bonds system. The structure is shown in Figure 1.5. In a DAD-ADA array, all the four repulsive secondary interactions reduced the  $K_{\text{ass}}$  to  $10^2 \text{ M}^{-1}$  in chloroform solvent, while this value was over  $10^5 \text{ M}^{-1}$  in AAA-DDD array with all four attractive secondary interactions. In DAA-ADD array which is middle case with two repulsive secondary interactions and two attractive interactions,  $K_a$  is around  $10^2\text{-}10^4 \text{ M}^{-1}$ .

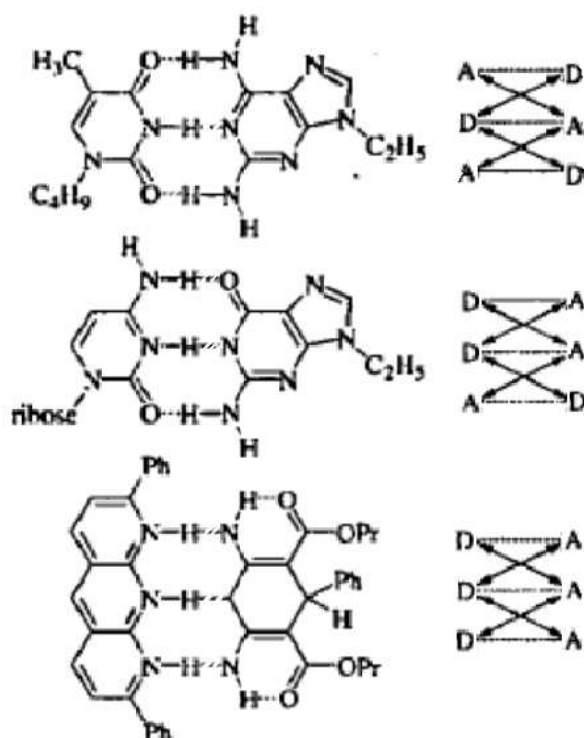


**Figure 1.5 Stability of complex due to different hydrogen bond arrays<sup>[12]</sup>**

Since a strong enough interaction is essential to formation of polymer, scientists are always pursuing the preparation of moiety with higher hydrogen bonds numbers. However, there is also an intrinsic contradiction between the binding strength and the synthetic accessibility of multiple hydrogen-bonding units. Whereas recent years have seen the development of building blocks association via five to ten hydrogen bonds, and with association constant in excess of  $10^9 \text{ M}^{-1}$ , these building blocks are often obtained via complicated synthesizing procedures, and are not available on a large scale.<sup>[13]</sup>

In recent years, Ureidopyrimidinone (UPy) is a popular quadruple hydrogen-bonding unit with high binding strength and synthetic accessibility<sup>[14]</sup>. Meijer, Zimmerman, Sijbesma did

a lot of work concerning supramolecular polymers bearing UPy <sup>[15]</sup>. Beijer <sup>[5]</sup> studied different constant depending on quadruple hydrogen-bonding structures. The two tautomers of UPy have DADA and DDAA conformations, both of which are capable of self-association. However, DADA dimerization has six repulsive secondary interactions, whereas the DDAA dimer has only two shown in Figure 1.6. This leads DADA forms to have lower  $K_{\text{ass}}$  than that in DDAA forms.

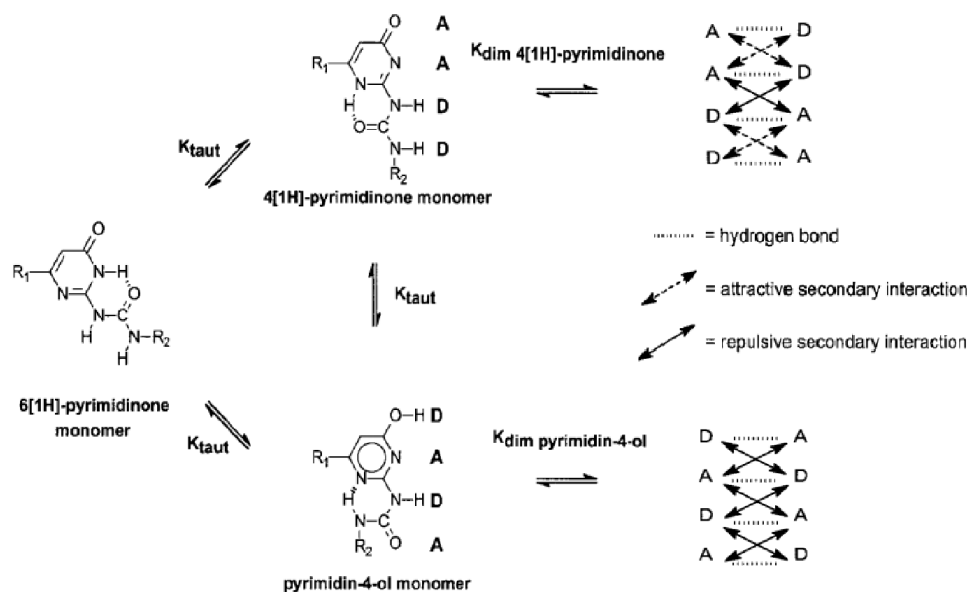


**Figure 1.6 Interactions in UPy (Ureidopyrimidinone) DADA and DDAA dimers**

At first, the procedure to synthesize UPy was complicated and with low yields. Then the synthesis was improved by using more suitable reagents to obtain good to excellent yields till 98% <sup>[16]</sup>, or by simplifying the procedures into one step <sup>[17]</sup>. Furthermore, introducing pendent supramolecular moieties as UPy onto polymer chains yields to reversible and physical networks which is necessarily crosslinked <sup>[18]</sup>.

### 1.3.2 Ionic interaction

The strength between ionic charges has somehow the most similar property to covalent bonds. The strength can exceed to hydrogen bonds and reach 350 kJ/mol. Regarding the supramolecular polymer networks based on ionic interaction, conventional ionomers and polyion complexes are well known. However, little is known about the supramolecular polymer networks based on the ionic interaction between multifunctional low-molecular weight organic compound and polymer.

Mitsuhiro <sup>[19]</sup> worked on the intermolecular interaction and thermal properties of supramolecular polymer networks based on P4VP and organic disulfonic acids (NDS and PDS) as shown in figure 1.7. When the T<sub>g</sub> of P4VP and P4VP/bifunctional proton donor (1/1) complexes are compared, the higher order of T<sub>g</sub> was P4VP/NDS>P4VP/PDS>P4VP in agreement with a higher degree of ionic interaction.

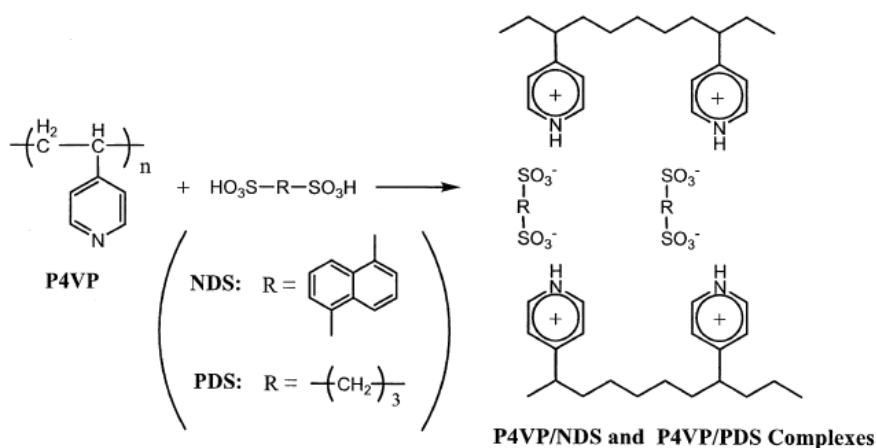


**Figure 1.7 Formation of the supramolecular polymer networks based on P4VP/NDS and P4VP/PDS complexes <sup>[19]</sup> : P4VP=poly(4-vinylpyridine), NDS= 1,5-naphthalenedisulfonic acid, PDS=propanedisulfonic acid, AA=adipic acid**

Supramolecular polymers with ionic interaction are more easily to perform liquid-crystal phase in solvent state. Nadia Canilho <sup>[20]</sup> assembled the branch supramolecular PG2 as in figure 1.8. Product performed the liquid-crystal state due to heating. Different structures were obtained with 3-5 nm scale dependent on different alkyl chain length. Another example to synthesize complicate ionic supramolecular assemblies based on branch shape goes to Raffaele <sup>[21]</sup>.

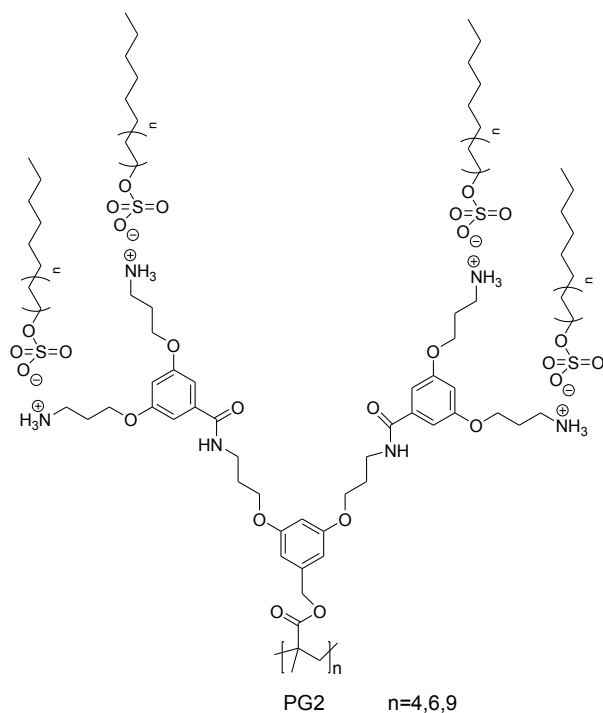


**Figure 1.8** Liquid crystalline from dendronized supramolecular complexes with sulfate alkyl tails <sup>[20]</sup>

### 1.3.3 Coordinate interaction

In a metal-coordination supramolecular polymer, monomeric unit is consisted by a metal ion and an organic or inorganic ligand. A spacer group is also important. Normal metal ions for supramolecular polymer are Ni, Fe, Cu, Co, Cd, Zn cations etc. The organic ligand is normally a pyridine or heterocyclic derivative. Materials realized more specific properties in photoelectricity and electromagnetism since the metal's presence in a metal-coordinate complex.

Two synthesis methods are used to prepare metal-coordination supramolecular polymer. One is first synthesize a organic monomeric unit with spacer group, then it is assembled with metal ion by coordination as in figure 1.9 <sup>[22]</sup>. Absorption and the electrochemical behavior of these new supramolecular polymers are studied by UV/Vis spectroscopy and differential pulse voltammetry (DPV) respectively. The results showed that the introduction of electron donating groups at the pyridine ring affects remarkably the charge transfer and electrochemical properties of the coordination polymers. Significant color change and high reversibility were observed from these polymers.

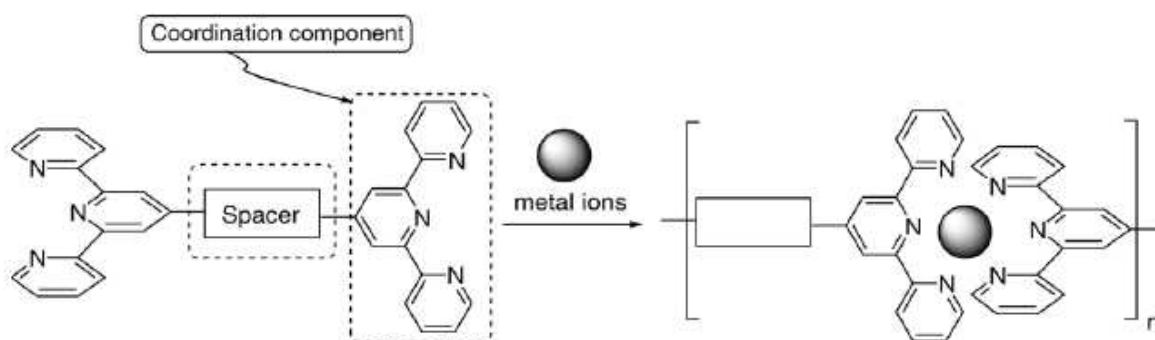


**Figure 1.9 Organic parts as monomers to figure supramolecular complex by metal-coordinate interaction** <sup>[22]</sup>

Another extensively used method is first synthesize the monomeric unit by metal ion and organic ligand, then the hydrogen bonds between monomeric unit are used to assemble the single or multi layer supramolecular polymer. This method combined metal-coordination and other supramolecular interaction was also often used in supramolecular synthesis.

#### 1.3.4 $\pi$ -conjugated interaction

$\pi$ - $\pi$  conjugation is also called  $\pi$ - $\pi$  stacking. It happens when two aromatic ring are ranging parallel or approximately parallel. This phenomenon can be described as following: the practical distance is less than van-de-waals thickness due to repulsive effect by  $\pi$  electron cloud between interfacing aromatic rings. Two forms of  $\pi$ -conjugated interaction, face to face or edge to face, will result in different structures. The strength of  $\pi$ -conjugation depends on the number of aromatic rings. More aromatic rings it has, stronger the  $\pi$ -conjugation effect is.

$\pi$ - $\pi$  interaction is not very strong (less than 50 kJ/mol), so it is always combined with other supramolecular interactions, such as hydrogen-bonding or metal-coordination. This method is also applied in the case that only one type of secondary interaction is too weak to form a network. Zhang <sup>[23]</sup> prepared two novel photoluminescent compounds of the formula  $[\text{Cd}(\text{atpt})\text{phen}(\text{H}_2\text{O})] \cdot \text{H}_2\text{O}$  (1) and  $[\text{Zn}_2(\text{atpt})_2(\text{bipy})_2(\text{H}_2\text{O})_2]$  (2) ( $\text{H}_2\text{atpt}$ = 2-aminoterephthalic acid,  $\text{bipy}$ =2,2'-bipyridine and  $\text{phen}$ =1,10-phenanthroline). The monomeric units were connected respectively by coordination effect before  $\pi$ - $\pi$  stacking. Compound 1 showed 1D architecture and further assembled into a 3D supramolecular network via interchain hydrogen bonds and  $\pi$ - $\pi$  stacking interactions as in Figure 1.10. Compound 2 exhibited a binuclear structure with intramolecular  $\pi$ - $\pi$  stacking interactions and further extended into a 3D

supramolecular framework via intermolecular hydrogen bonds and edge to face  $\pi$ - $\pi$  interactions.

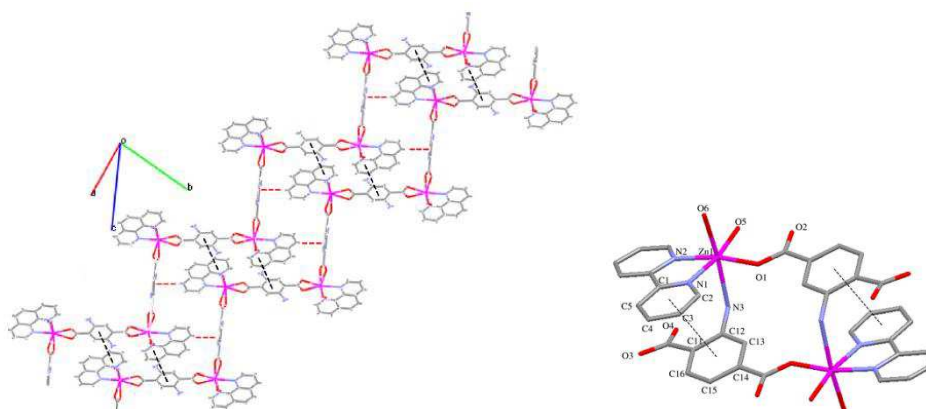


**Figure 1.10 View of the different  $\pi$ - $\pi$  stacking schemes between the nearest chains in compound 1 and 2: edge to face (red dashed line in the left figure compound 1) and face to face (black dashed line in the right figure compound 2) [23].**

## 1.4 Conclusion

In this section, the interactions in the supramolecular polymers are discussed. Common used supramolecular interactions are hydrogen-bonding interaction, ionic interaction, metal-coordination interaction and  $\pi$ -conjugated interaction. The last two interactions, metal coordination and  $\pi$ - $\pi$  conjugation, are not very strong compared with former ones, so they are always used with other interactions to form a stable structure. Several examples are listed for each category to compare the present status and the prospect of its field.

Two interactions are chosen as research aspect in my doctoral study: ionic interaction and hydrogen bonds interaction. The former has the highest bonding energy in supramolecular chemistry. And the latter, hydrogen-bonding interaction is predominant in different supramolecular interactions despite of its comparatively lower binding strength. It is highly directional, i.e.  $D-H \cdots A$  is found to be linear in most cases. Although secondary interactions in a system could force  $D-H \cdots A$  away from linearity, it is the directionality in hydrogen bonding resulting in an anisotropic intermolecular potential that separates it from other isotropic interactions.

## 2. Determination of supramolecular bonding

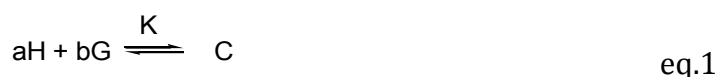
### 2.1 Binding constant determination by NMR titration <sup>[24]</sup>

#### 2.1.1 Host-guest 1:1 complex (heterodimers) system with fast exchange kinetics

##### General view of binding constant calculation

A general way to determine the binding constant is based on a simple binding equilibrium model, i.e. Eq.1. The terms binding constant, equilibrium constant, and stability constant are synonymous with each other. The activity coefficients are generally unknown and the stability constant  $K$ , based on the concentrations, is usually employed. Judging from this situation, the question of the activity coefficients of the solutes is disregarded here in order to simplify the discussion. Nevertheless, it should be remembered that this point is not always insignificant <sup>[24]</sup>.

The basic equations for the host-guest complexation are the following four Eqs.1-4.



$$K = \frac{[C]}{[H]^a \times [G]^b} \quad \text{eq.2}$$

$$[H] = [H]_0 - a \times [C] \quad \text{eq.3}$$

$$[G] = [G]_0 - b \times [C] \quad \text{eq.4}$$

With H: host; G: guest; C: complex( $H_a \cdot G_b$ )

a,b: stoichiometry as shown in Eq.1

$[H]_0$ : initial(total) concentration of host molecule

$[G]_0$ : initial(total) concentration of guest molecule

$[H]$ ,  $[G]$ ,  $[C]$ : equilibrium concentrations of host, guest, and complex, respectively

Equation 5 is derived from Eqs. 2-4.

$$K = \frac{[C]}{([H]_0 - [C])([G]_0 - [C])}$$

$$\frac{1}{K} = [C] - ([H]_0 + [G]_0) + \frac{[H]_0[G]_0}{[C]} \quad \text{eq. 5}$$

The parameters can be classified as follows:

K, a, b: Constants (a and b are integers larger than or equal to 1)

[H]<sub>0</sub>, [G]<sub>0</sub>: Variables which can be set up as experimental conditions

[H], [G], [C]: Variables dependent on the equilibrium

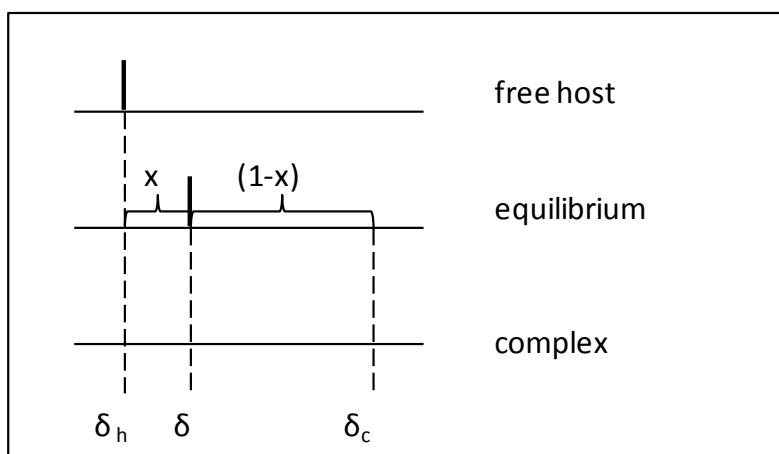


**Figure 2.1 Representative NMR spectra for the correlation of complexation ratio  $x$  and chemical shifts** <sup>[24]</sup>

A typical NMR spectrum for 1:1 host-guest complexation system is shown in figure 2.1.  $x$  is induced as a correlation of complexation, it is the ratio of complexed host at equilibrium over total host.  $\delta$  is the observed chemical shift;  $\delta_h, \delta_c$  are chemical shifts of the free and complexed host, respectively. If the solvent contains only the host, then  $x=0$ ; if all the host groups in the system are complexed, then  $x=1$ .

So we can define:

$$\delta = \delta_h(1 - x) + \delta_c x$$

$$x = \frac{[C]}{H_0}$$

$$\rightarrow [C] = \frac{\delta - \delta_h}{\delta_c - \delta_h} [H]_0 \quad \text{Eq. 6}$$

Back in equation 5, in order to simplify this equation, we set:

$$y = \frac{1}{K}$$

$$x = [C]$$

$$a = [H]_0[G]_0$$

$$b = [H]_0 + [G]_0$$

The equation 5 is expressed as followed:

$$y = x + \frac{a}{x} - b \quad \text{Eq. 7}$$

This is just a quadratic equation with one variable that can be easily solved:

$$[C] = \frac{\left([H]_0 + [G]_0 + \frac{1}{K}\right) \pm \sqrt{\left([H]_0 + [G]_0 + \frac{1}{K}\right)^2 - 4[G]_0[H]_0}}{2} \quad \text{Eq. 8}$$

Using eq. 6 in eq. 8, then K in relation with  $\delta_h$ ,  $\delta_c$  and host/guest concentration is solved as in equation 9.

$$\delta = \delta_h + \frac{(\delta_c - \delta_h) \left([H]_0 + [G]_0 + \frac{1}{K}\right) - \sqrt{\left([H]_0 + [G]_0 + \frac{1}{K}\right)^2 - 4[G]_0[H]_0}}{2[H]_0} \quad \text{Eq. 9}$$

### Determination of stoichiometry and $\delta_c$

In order to obtain the K from previous calculations, it is essential to design the stoichiometry of host-guest complexation system. The method involves preparing a series of solutions with different molar ratios of host and guest. The proportion of host  $\frac{[H]_0}{[H]_0 + [G]_0}$  is between 0 and 1 as in table 2.1, and the total concentration  $[H]_0 + [G]_0$  is constant for each solution.

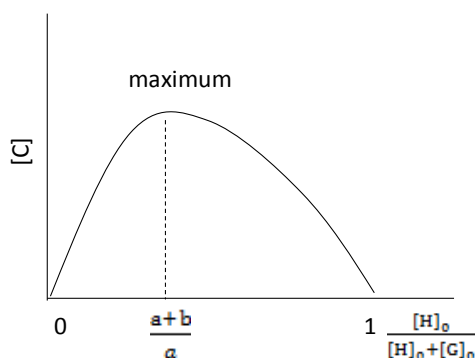


**Figure 2.2 Determination of stoichiometry(a,b) from the x-cooriate at the maximum of the curve iin Job's Plot <sup>[24]</sup>**

In order to study the stoichiometry by the continuous variation method, the following for points have to be considered and carried out.

\*keeping the sum of  $[H]_0$  and  $[G]_0$  constant ( $\alpha$ )

\*changing  $[H]_0$  from 0 to  $\alpha$

\*measuring  $[C]$

\*data treatment(Job's plot)

In equation 9,  $[H]_0$  and  $[G]_0$  are known from the experiment condition.  $\delta$  is the observed chemical shift which is obtained directly from NMR spectrum of host/guest system.  $\delta_h$  is the chemical shift of the free host, this can be obtained by running a sample that only contain the host.  $\delta_c$  is the chemical shift of complexed host that is the only variable that can't be observed directly. But it could be available by running NMR samples be the method mentioned above and in table 2.1:

**Table 2.1 The  $\delta_c$  derived from NMR titration**

host/guest mol equivalency	Chemical shift
1/1	$\delta_1$
1/2	$\delta_2$
1/4	$\delta_3$
1/8	$\delta_4$
.....	.....
1/ $\infty$	$\delta_c$

By elongating the curve of chemical shift-host concentration,  $\delta_c$  value could be obtained when host concentration approach to infinitesimal.

**Data treatments for NMR method** <sup>[25]</sup>

Graphical (or linearization) methods are applied to produce the linear relationship between  $\delta_{\text{obs}}$  and K, from which the NMR data are treated graphically. There are three mostly used treatments as follows:

**Benesi-Hildebrand(Hanna-Ashbaugh) treatment** <sup>[25]</sup>

$$\frac{1}{\Delta\delta} = \frac{1}{K\Delta\delta_{\text{max}}[H]_0} + \frac{1}{\Delta\delta_{\text{max}}}$$

in which:

$[H]_0$  and  $[G]_0$  are known total concentration of host and guest;  $\Delta\delta$  is measured change in chemical shift (upon addition of host species) referenced to that of the uncomplexed guest;  $\Delta\delta_{\text{max}}$  is the difference in chemical shifts between that observed in the guest molecule and that observed in the host-guest complex.

This method allows the linear relationship of  $1/\Delta\delta$  against  $1/[H]_0$ , producing the  $1/K\Delta\delta_{\text{max}}$  as a slope and  $1/\Delta\delta_{\text{max}}$  as a intercept.

The key feature of this method is that the observing species G is in the presence of a large excess (minimum 10X) of species H when 1:1 complex is formed. Then concentration of H can be set equal to the initial concentration,  $[H]=[H]_0$ .

**Scatchard (Foster-Fyfe) method** <sup>[25]</sup>

$$\frac{\Delta\delta}{[H]_0} = -K\Delta\delta + K\Delta\delta_{\text{max}}$$

This method could obtain the linear relationship of  $\Delta\delta/[H]_0$  against  $\Delta\delta$ , producing the -K as a slope coefficient and  $\Delta\delta_{\text{max}}$  as a intercept. But it requires an extrapolation of infinitely dilute solution and the  $K_{\text{ass}}$  is not dependent on the extrapolation.

**Rose-Drago Method** <sup>[25]</sup>

$$(\Delta\delta_{\text{max}} - \Delta\delta)K = \frac{\Delta\delta\Delta\delta_{\text{max}}}{\Delta\delta_{\text{max}} - \Delta\delta[G]_0}$$

For each  $[H]_0$ , K is calculated from a series of assumed  $\Delta\delta_{\text{max}}$  value. A graph of  $K^{-1}$  against  $\Delta\delta_{\text{max}}$  is constructed. The intercept of these lines gives  $1/K$  and  $1/\Delta\delta_{\text{max}}$ . This method does

not require the condition  $[H]=[H]_0$ , and it is not currently used because it has been made obsolete by the curve fitting methods.

### 2.1.2 Self-dimerization (homodimer) systems with fast exchange kinetics

#### General view of binding constant calculation

In the case of self-complementary supramolecular moieties such as DA or DDAA, they can dimerize with themselves and produce  $(DA)_2$  or  $(DDAA)_2$ . Thus the equations summarized above are no longer suitable.

Horman was the first person that deduced the equations based on self-dimerization progress in caffeine <sup>[26]</sup>.



$$K = \frac{[C_2]}{[C]^2} \quad \text{eq. 11}$$

$$[C]_0 = [C] + 2[C_2] \quad \text{eq. 12}$$

$$[C] = [C]_0 - 2[C_2] \quad \text{eq. 13}$$

With  $[C_2]$  is the dimer concentration,  $[C]_0$  is the nominal concentration of C in solution. K is the dimerization constant.

Using eq. 13 in eq.11, we have:

$$K = \frac{[C_2]}{([C]_0 - 2[C_2])^2} \quad \text{eq. 14}$$

Rearrangement of eq.14 gives:

$$\frac{1}{2K[C]_0} = \frac{2[C_2]}{[C]_0} + \frac{[C]_0}{2[C_2]} - 2 \quad \text{eq. 15}$$

By the similar simplification in host-guest system, we let:

$$y = \frac{1}{2K[C]_0}$$

$$x = \frac{2[C_2]}{[C]_0}$$

Eq. 15 is simplified as:

$$y = x + \frac{1}{x} - 2 \quad \text{Eq. 16}$$

For a given value of  $y_i$ ,  $x_i$  is calculated as:

$$x_i = \left(1 + \frac{y_i}{2}\right) - \sqrt{\left(1 + \frac{y_i}{2}\right)^2 - 1} \quad \text{Eq. 17}$$

In which

$$x_i = \frac{\delta_m - \delta_i}{\delta_m - \delta_d}$$

$$\delta_i = \delta_0 - x_i(\delta_0 - \delta_\infty) \quad \text{eq. 18}$$

Here  $\delta_m$  is the chemical shift of the monomer and  $\delta_d$  is the chemical shift of dimer.  $\delta_i$  is the observed chemical shift with certain  $[C]_0$ .

### Data treatment by Chen's equation <sup>[27]</sup>

Chen found that the displacement of chemical shifts with concentration is usually steep and nonlinear at high dilutions. Furthermore, errors in monomer's chemical shift in Horman's model influence the accuracy when constant of dimerization is calculated. Thus it leads to the further determination of enthalpy and entropy based on the Van't Hoff's equation unreliable. So a new equation which is extensively used in recent self-association systems is introduced:

$$\delta_{obs} = \delta_m + (\delta_d - \delta_m) \frac{\sqrt{1 + 8KC} - 1}{\sqrt{1 + 8KC} + 1} \quad \text{Eq. 19}$$

In which:

$\delta_m$  is the chemical shift of the monomer;

$\delta_d$  is the chemical shift of dimer;

$\delta_{\text{obs}}$  is the chemical shift observed;

$K$  and  $C$  are association constant and concentration of monomer respectively. This equation is applied in systems with monomer-dimer fast exchange kinetics when  $\delta_{\text{d}} > \delta_{\text{m}}$ .

Since the  $\delta_{\text{m}}$ ,  $\delta_{\text{d}}$ , and  $K$  are constants, the monomer concentration  $C$  is the only independent variable, while the  $\delta_{\text{obs}}$  is the dependent variable. Therefore,  $\delta_{\text{m}}$ ,  $\delta_{\text{d}}$ , and most importantly,  $K_{\text{ass}}$ , will be derived by fitting the experimental data with this equation on typical data-processing software.

### 2.1.3 Examples of curve fitting by using NMR methods

In Bertrand's <sup>[28]</sup> work, he used 1:1 host-guest model to treat the  $K_{\text{a}}$  calculation in a pair of triple hydrogen bonds DAD-ADA. ADA moiety is based on thymine and DAD moiety is based on diaminopyridine as in figure 2.3.

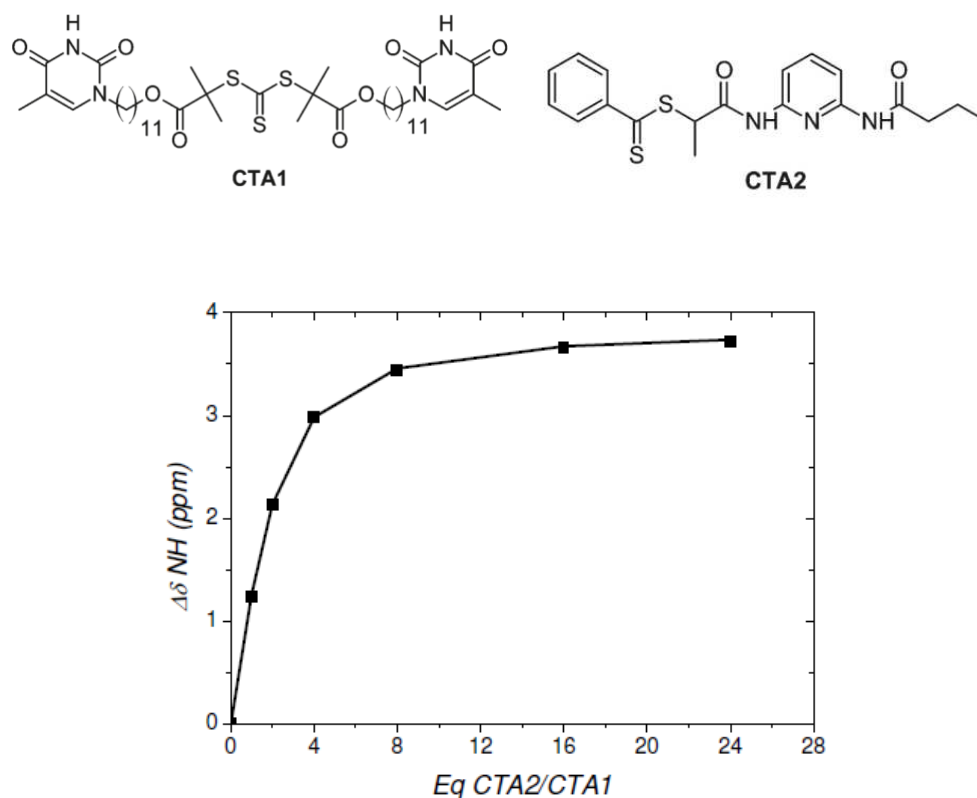


**Figure 2.3** NMR titration of motif CTA1 (with ADA array) and motif CTA2 (with DAD array)

For the data treatment, different solutions with mol ratio CTA2/CTA1 from 24 to infinity in  $\text{CDCl}_3$  are prepared with fixed concentration of CTA1 at  $1.26 \times 10^{-2} \text{ mol.L}^{-1}$ . Data related to the concentration-dependence of the chemical shift of thymine NH proton for a mixture of a

thymine-functionalized CTA2 and DAP-functionalized CTA1 were fitted according to the following equation 9 to provide K:

$$\delta_{\text{mixt}} = \delta_{\text{CTA1}} + \frac{(\delta_{\infty} - \delta_{\text{CTA1}}) \left( [\text{CTA1}]_0 + [\text{CTA2}]_0 + \frac{1}{K} \right) - \sqrt{\left( [\text{CTA1}]_0 + [\text{CTA2}]_0 + \frac{1}{K} \right)^2 - 4[\text{CTA1}]_0[\text{CTA2}]_0}}{2[\text{CTA1}]_0}$$

where the experimental parameters are : [CTA1] and [CTA2], the respective molar concentrations of the thymine-functionalized polymer and DAP-functionalized polymer;  $\delta_{\text{mixt}}$ , the measured NH chemical shift for CTA1 and CTA2 mixture;  $\delta_{\text{CTA1}}$ , the measured NH chemical shift for CTA1 solution. The fitted parameters are: K, the association constant and  $\delta_{\infty}$ , the NH chemical shift of the fully associated system.

Curve fitting gives the intercept of y axis when CTA2/CTA1=0, and  $\delta_{\infty}$  was equal to 12.6 ppm when CTA2 is diluted to infinity, and  $K_{\text{ass}}$  as  $110 \text{ M}^{-1}$ .

Other example of self-association is based on a series of acylaminopyridine as in figure 2.4. The nitrogen on the pyridine ring and neighboring N-H form the DA moiety which has the capacity of self-association as DA-AD pairs.

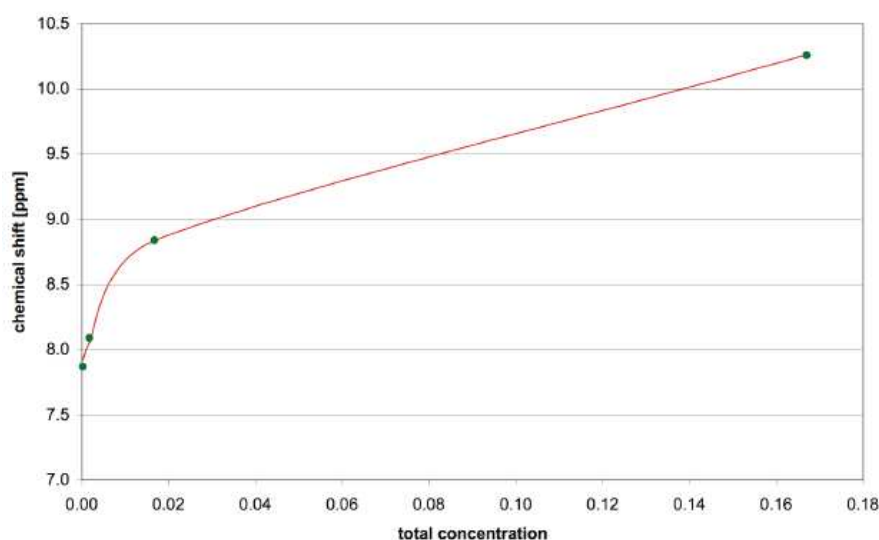
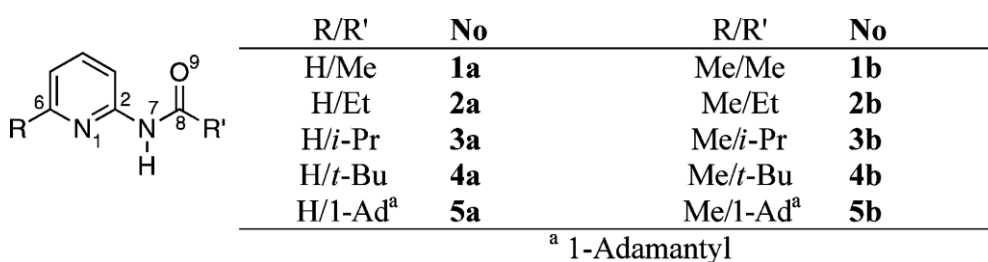
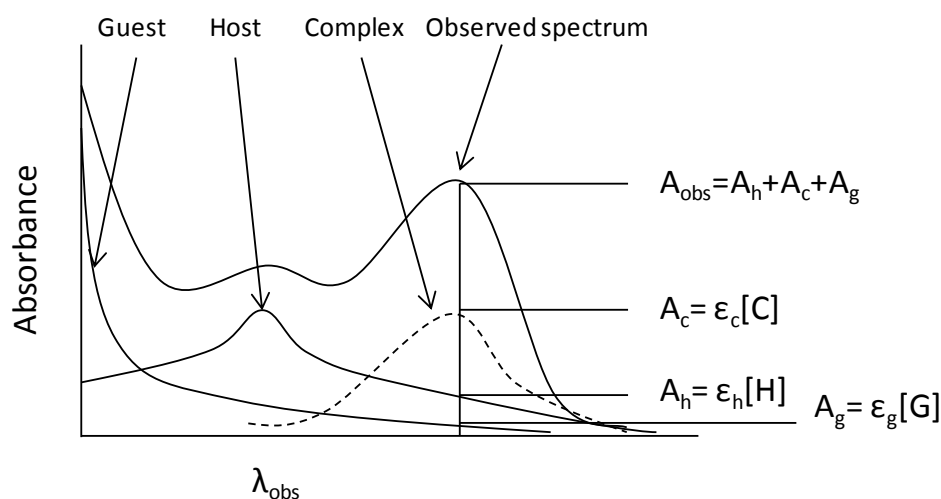


Figure 2.4 Dilution curve fit  $\delta(\text{NH})$  for compound 1a and corresponding structures <sup>[29]</sup>

As compound 1a as an example, the N-H proton has a magnificent shift from 10.5 to 7.7 ppm when its concentration in CDCl<sub>3</sub> is diluted. The fitted parameters gives the intercept of y axis equal to 7.7 ppm, and K<sub>a</sub> from curve fitting is derived as 13 M<sup>-1</sup>.

## 2.2 Binding constant by UV-vis titration <sup>[24]</sup>

### 2.2.1 General view of binding constant calculation



**Figure 2.54 Representative UV-vis spectra to show correlation of observed spectra and each component <sup>[24]</sup>**

The UV-vis method is applied in systems concerning organic conjugation and complexes with metals, by which way the electron transfer occurs. The relationship of spectra and component in 1:1 host-guest system is similar as in NMR method, except here the absorbance is observed.

The concentrations and absorbance of each species are related as the following equations.

$$A_h = \epsilon_h[H] = \epsilon_h([H]_0 - [C]) \quad \text{eq. 20}$$

$$A_g = \epsilon_g[G] = \epsilon_g([G]_0 - [C]) \quad \text{eq. 21}$$

$$A_c = \epsilon_c[C] \quad \text{eq. 22}$$

$$A_{\text{obs}} = A_h + A_g + A_c \quad \text{eq. 23}$$

A<sub>obs</sub>: observed absorbance

A<sub>h</sub>, A<sub>g</sub>, A<sub>c</sub>: absorbances of host, guest, and complex respectively

$\epsilon_h, \epsilon_g, \epsilon_c$ : molar absorptivities of host, guest, and complex respectively

Using equations 20-23 in equation 5, we have:

$$\frac{1}{K} = \frac{A_{\text{obs}} - \epsilon_h[H]_0 - \epsilon_g[G]_0}{\epsilon_c - \epsilon_h - \epsilon_g} - ([H]_0 + [G]_0) + \frac{\epsilon_c - \epsilon_h - \epsilon_g}{A_{\text{obs}} - \epsilon_h[H]_0 - \epsilon_g[G]_0} [H]_0[G]_0 \quad \text{Eq. 24}$$

We let:

$$Y = \frac{1}{K}$$

$$X = \epsilon_c - \epsilon_h - \epsilon_g$$

$$a_n = A_{\text{obsn}} - \epsilon_h[H]_{0n} - \epsilon_g[G]_{0n}$$

$$b_n = [H]_{0n} + [G]_{0n}$$

$$c_n = \frac{[H]_{0n}[G]_{0n}}{A_{\text{obsn}} - \epsilon_h[H]_{0n} - \epsilon_g[G]_{0n}}$$

$A_{\text{obsn}}$ : observed absorbance of n-th measurement

$[H]_{0n}$ : concentration of host molecule at initial stage for n-th measurement

$[G]_{0n}$ : concentration of guest molecule at initial stage for n-th measurement

Then Eq. 24 can be rearranged as:

$$y = \frac{a_n}{x} - b_n + c_n x$$

As an example, one combination of data where n=1 and n=2 (e.g. {  $A_{\text{obs1}}, [H]_{01}, [G]_{01}$  } and {  $A_{\text{obs2}}, [H]_{02}, [G]_{02}$  } is used here)

$$x = \frac{-(b_1 - b_2) \pm \sqrt{(b_1 - b_2)^2 - 4(c_1 - c_2)(a_1 - a_2)}}{2(c_1 - c_2)}$$

The maximum number of obtainable answer pairs {x, y} is  ${}_n C_2$  pairs for n combinations of concentration conditions. For example, 5 pairs of {  $[H]_{0n}, [G]_{0n}$  } give  $10(=5C_2)$  pairs of {x, y}. These {x, y} are obtained under premise where 1 to 1 complexation. NO approximation is

introduced into this solution. This reciprocal of the obtained Y's is the binding constant K. The number of obtained K at this stage might be  $nC_2$ .

### 2.2.1 Examples of data treatments by using UV-Vis titration

The restriction for UV-vis method is that it is only applied to organic/metal conjugated systems when electron transfers occur. A typical process of UV-Vis titration is applied as below in figure 2.6 <sup>[30]</sup>. The terpyridine derivative functionalizing as supramolecular monomer was dissolved in chloroform, iron chloride in solution is added generally. After each addition, a UV-vis spectrum was recorded after 5 min. The 318 nm absorption band attributed to the ligand-centered absorption and 558 nm absorption attributed to metal-to-ligand charge-transfer band (MLCT). Then the  $K_{ass}$  was calculated by statistical method.

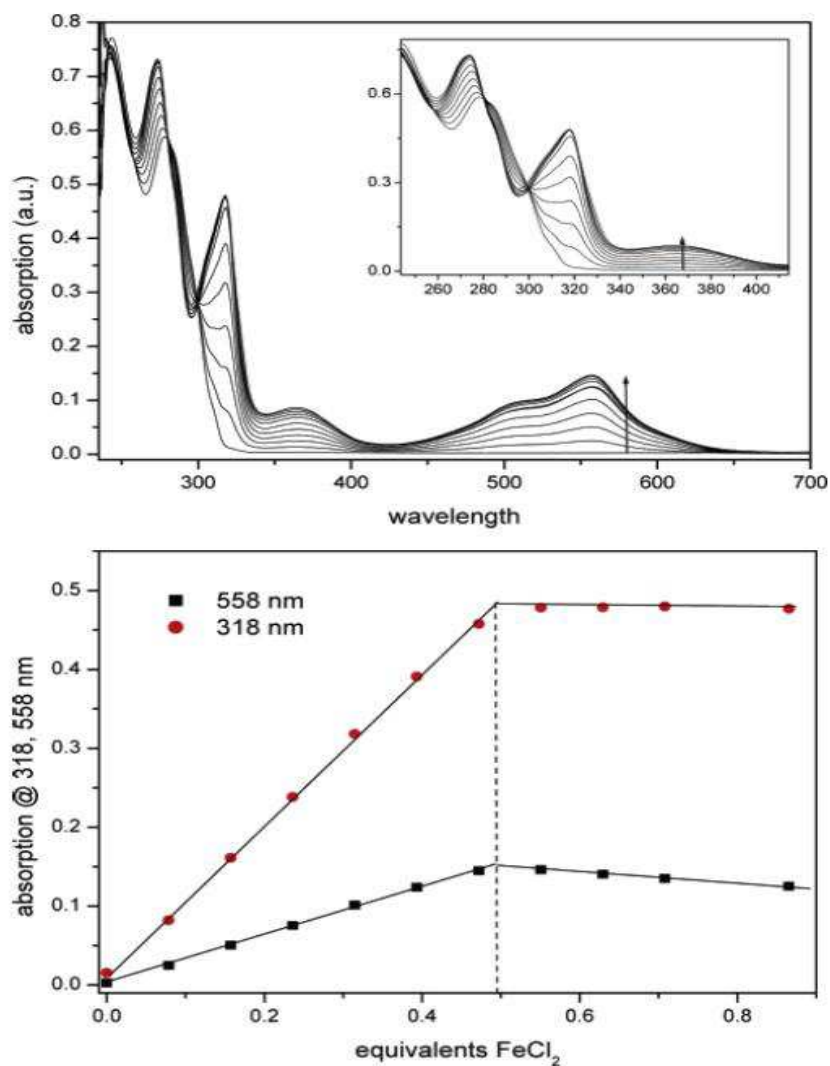


Figure 2.6 The UV-vis titration of a terpyridine derivative with FeCl<sub>2</sub> (in chloroform) <sup>[30]</sup>

### 2.3 Alternative spectroscopic methods

Although NMR and UV-vis titration are extensively used for calculating the binding constant  $K_{\text{ass}}$  other common spectroscopic techniques, such as UV <sup>[31]</sup>, IR <sup>[32]</sup>, ITC (isothermal titration calorimetry) <sup>[33]</sup> or unfrequently, VPO (vapour pressure osmometry) <sup>[34]</sup> are also used to determine association constants.

## 2.4 Conclusion

This section describes in details the theoretical principles of binding constant calculations based on the two most extensively used methods, NMR and UV-vis titration. As a concrete example, practical measurements and practical data treatments of an UV/vis and NMR titration experiment are discussed. These methods should be functioned with commonly available spreadsheet software on personal computers and provide another way to understand the contents described in this chapter. In addition, other alternative methods, such as IR, ITC and VPO, are also mentioned.

It should be mentioned that in these typical K calculation methods, NMR and UV-vis, the samples are diluted in solutions in order to fit the experimental requirements and be controlled with accurate stoichiometry. However, the binding strength, represented by K, is influenced by external environments, including solvents. As a result, although the parameter K was widely calculated and compared association strength in different supramolecular motifs, it only represent the constant in certain solvent at certain temperature. With the development of characterization methods, the new method, such as ITC and VPO, still couldn't be used to calculate the K in bult state.

### 3. Ionic supramolecular interaction: application of $\text{CaCO}_3$ in polymer materials

#### 3.1 Introduction of nano inorganic fillers

Polymer-matrix composites containing inorganic fillers (filler/polymer composites) have been receiving significant attention lately because of their interesting and useful characteristics, such as good mechanical properties, thermal resistance and chemical reagent resistance<sup>[35]</sup>. Due to recent developments in the field of nanotechnology, there has been growing interest in polymer-matrix composites in which nano-sized fillers are distributed homogeneously (known as filler/polymer nanocomposites), due to their unique optical, electric and magnetic properties, as well as their dimensional and thermal stability. The nanocomposite materials are also potential candidates for catalysts, gas-separation membranes, contact lenses and bioactive implant materials<sup>[36]</sup>. The traditional practical method for dispersing inorganic nanofillers in polymer matrices is direct melt-compounding of the polymer with the fillers<sup>[37-39]</sup>. However, the surface activity of the nanofillers is extremely high, and the particles consequently have a tendency to aggregate tightly, creating micron-sized filler-clusters. This is one of the major problems in the fabrication of filler/polymer nanocomposites. In view of this issue, there have been a number of attempts to disperse nanofillers uniformly in polymer matrices by using methods with organic modification of the surface or interlayer of nanofillers and a variety of sol-gel and/or polymerization reactions. However, these technologies require complicated chemical reactions making them unsuitable for industrial-scale production of nanocomposites with a wide volume fraction range of nanofillers and various combinations of filler and polymer material species. From the viewpoint of the fabrication of high performance particle/polymer nanocomposites on an industrial scale, the author and coworkers have developed a simple method for dispersing inorganic nanoparticles into various polymers by direct melt-compounding, without requiring any surface modification of the nanoparticles or complicated reactions.

### 3.2 Use calcium carbonate: advantage and disadvantage

Calcium carbonate is one of the most frequently used additives. The size of nano calcium carbonate is between 10nm and 100nm. It had different crystallization shape such as spindle, cube, needle and global shape. Nano calcium carbonate was the earliest developed inorganic nano fillers. Nowadays, for the overall weight of all kinds of inorganic powder additives being used, over 70% attributes to calcium carbonate. It is the cheapest commercially available inorganic material and is extensively used as a particulate filler in the manufacture of paint, paper, rubber, plastics, and so forth<sup>[40]</sup>.

Precipitated calcium carbonate (PCC) or nano calcium carbonate is an inodorous, innocuity white powder which relative density is 2.7-2.9. Although the characteristics of PCC, including regular shape and small grain diameters, are positive, they also have disadvantages:

\*. The smaller the  $\text{CaCO}_3$  particles are, the higher the surface energy is. The absorption effect of the particle becomes stronger, and lead to an unstable thermodynamic state. According to the minimum energy principle, particles tend to aggregate into agglomerates. As a result,  $\text{CaCO}_3$  particles couldn't be well dispersed into isolated grains in the matrix, which decrease the practical improvement by adding  $\text{CaCO}_3$ .

\*. The surface of calcium carbonate is hydrophilic and oleophobic, with strong polarity. So it is difficult to uniformly disperse them in the organic matrix. The poor adhesion between the base material (polymer) and  $\text{CaCO}_3$  particles is easy to cause interfacial defects, resulting in the decline of material properties. Therefore, surface modification must be conducted in order to eliminate the high potential energy and adjust the hydrophobicity. Only by improving the adhesion between the organic base materials and  $\text{CaCO}_3$ , can the performance of the filler as well as materials be maximized, and thereby reduce the cost of raw materials.

### 3.3 Modifications of precipitated calcium carbonate (PCC)

Surface modification of calcium carbonate is to absorb the surface modifier on the surface of calcium carbonate by physical or chemical methods. Since the membranes formed on the particles reduces the viscosity, surface properties would be further improved. In the manufacture of some kinds of polymer materials, calcium carbonate could be used without any modifications, such as PVC. However, the plasticizer added already acts as a modifier more or less. As filler in rubber or plastic products, calcium carbonate could enhance the heat resistance, wear resistance, size stability and reduce the cost in the meantime. But it has the

surface effect that makes it easy for aggregation and instability in the high temperature. Furthermore, the hydrophilic properties of the calcium carbonate reduce the interface miscibility with organic polymers.

In fact, if nano calcium carbonate is used without any modification, the homogeneous in the organic phase would lead to the poor mechanical properties of the final manufactures.

Mechanism of PCC surface modification includes two aspects, one is the interaction mechanism between modifier and PCC surface, the other one is the interaction between the modified PCC and polymer matrix. And the modification methods could be physical, chemical and mechanical.

### **3.3.1 Physical modifications of PCC**

All the ways to modify calcium carbonate without a modifier could be attributed a physical way, such as surface coating. Different from chemical one, a chemical reaction doesn't occur between modifier and calcium carbonate particles in this kind of coating. Instead, it relies on the physical interaction or van de waals force. For example, adding surfactant into a solvent in which calcium carbonate is preparing, the size of the resulting nano calcium carbonate particles will be uniformed. This way could improve dispersion of nano calcium carbonate particles.

### **3.3.2 Micro-emulsion modification of PCC**

This method changes the particle surface property by coating a membrane of other materials. The difference from physical coating or chemical coating is that the membrane is homogenous. A W/O emulsion will be first prepared containing  $\text{CO}_3^{2-}$ , then  $\text{Ca}^{2+}$  solvent is added with acute agitation.<sup>[41, 42]</sup>

### **3.3.3 High-energy surface modification of PCC**

High-energy surface modification is using high-energy radiation, such as x ray,  $\gamma$  ray or plasma, to impact the calcium carbonate particles in the electric accelerator. The impaction gives the surface effective point which makes the particle possible to react with another monomer added in like ethylene, thus forming a organic membrane. This method has some

disadvantages like high cost, modification unsteadiness, low manufactory efficiency, so it is not widely used.

### 3.3.4 Mechanical force modification of PCC

It uses the ultrafine grinding or other strong mechanical power to triturate calcium carbonate particles. This method is useful to the calcium carbonate with big size. For nano calcium carbonate, its size has already reached a good fineness. It is not effectual by mechanical crushing and grinding. But it can multiply the interaction of surface modifier by activating the active points and active groups on particles surface. So this method could help to improve the surface of calcium carbonate in some cases if it combines with other modification methods to process modification and treatment.

### 3.3.5 Chemical modifications of PCC

It is the designation for all the modifications of calcium carbonate in which chemical reaction happens between modifier and calcium carbonate particles. It is the most widely used and most efficient method. A modifier usually has a polar group at one end and a lipophilic group at the other end. The polar group could graft on the surface of calcium carbonate physically or chemically while the lipophilic group is to twist physically or react chemically with the matrix. This makes a “bridge” between the calcium carbonate fillers and organic polymers to connect two materials with different polarities. Chemical modification could be in a dry mode or wet mode. In dry mode, the calcium carbonate powder is directly put in a modification machine, and then a modifier is poured in to be well mixed. This way is industrial and convenient for the packing and transportation. In wet mode, all the modifications are done in the calcium carbonate solution and it covers the particle surface most efficiently. In the laboratories, the wet chemical methods are much more common.

Lots of researches made efforts to the modifications of calcium carbonate. Organic acids were the classical and principal modifier since 1980s<sup>[43]</sup>. Many works proved that the function of carboxyl group can efficiently react with calcium carbonate to form strong combination between  $\text{CaCO}_3$  and polymer matrix. Ma<sup>[44]</sup> et al. used oleic acid to treat  $\text{CaCO}_3$  nanoparticles, which improved the compatibility between  $\text{CaCO}_3$  and the monomers. Scanning electron microscopy (SEM) and transmission electron microscopy (TEM) were used to prove the dispersion of  $\text{CaCO}_3$  is effectively enhanced. Stearic acid is chosen to play

a similar role in linear low-density polyethylene (LLDPE) system in Bellayer's study<sup>[45]</sup>. Using coupling agent to react with the hydroxyl group on  $\text{CaCO}_3$ 's surface is another kind of modification. Both of these treatments were usually considered as coating methods<sup>[42, 46-49]</sup>. And they needed to separate the synthesis to two step, modification and polymerization, which reduced the yield and also the efficiency.

### 3.4 Surface modifier

Here the surface modifier in chemical modification is only discussed. There are a lot of categories of surface modifier which usually used are aliphatic acid, titanate coupling agent, aluminate coupling agent, silicone coupling agent and phosphate modifier.

The modifiers could be classified as follows.

#### 3.4.1 Organic acids

Abundant hydrophilic hydroxyl groups on the surface of calcium carbonate make it strongly alkaline. And the carboxyl group of the aliphatic acid could react with  $\text{Ca}^{2+}/\text{CaHCO}_3^{3+}/\text{CaOH}^+$  in the calcium carbonate slurry and generate calcium tallate. This dregginess covers on the calcium carbonate particles to make the surface hydrophobic.

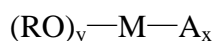
Aliphatic acid containing hydroxyl group or amino group is widely used due to its functional group Ma<sup>[44]</sup> et al chose the oleic acid as the modifier to synthesis . OA was dissolved in ethanol to be well dispersed in water and was added dropwise into the calcium carbonate aqueous solution. OA-modified nanometer  $\text{CaCO}_3$  latex is then react with MMA in  $60^\circ\text{C}$ . X-ray diffraction and Fourier transform infrared were applied to investigate the chemical and physical properties of the composite microspheres, and the results proved that the composites were composed of  $\text{CaCO}_3$  and PMMA. Oleic acid improved the compatibility between  $\text{CaCO}_3$  and the monomer MMA efficiently.

Stearic acid and stearate acid modifier is the most common used modifier to calcium carbonate fillers because it is cheap and efficient. The earliest publication is the Papirer's work<sup>[43]</sup> about the surface properties of calcium carbonate treated with stearic acid in 1984. This kind of modifier is still used in other plastics in recent years, such as LLDPE<sup>[45]</sup>.

CHEN studied the dispersion of nano calcium carbonate modified with different unsaturated acid, concluding acrylic acid, methacrylic acid, maleic acid(maleic anhydride) in poly(n-butyl methacrylate)<sup>[50]</sup>polystyrene<sup>[51]</sup>. Calcium carbonate is put into the other reactants in different ways. In the PBMA/MA/CaCO<sub>3</sub> system, precipitated calcium is directly used without any solvent while it is used with the ethanol as a solvent in PS/MA/CaCO<sub>3</sub>.

### 3.4.2 Coupling agents

This kind of modifier, including titanate coupling agent, aluminate coupling agent, silane coupling agent and phosphate coupling agent. The molecular structure of coupling agents is as followed:



M stands for central atoms such as Al, Ti, Si, Zr etc. A<sub>x</sub> stands for long chain with carbons and oxygen, (RO)<sub>y</sub> stands for short chain with carbons and oxygen. Polar group (RO)<sub>y</sub> at one end could react with functional group on the calcium carbonate to make a stable chemical connection while a lipophilic group A<sub>x</sub> at the other end could twist with the matrix physically or chemically. The tight combination of calcium carbonate and polymer matrix makes composite better properties.

Xu<sup>[52]</sup>used titanate coupling agent to modify the nano calcium carbonate in polystyrene. The results indicated that adsorption free energy and dispersive component of the surface free energy of nano calcium carbonate were decreased with adsorbing titanate coupling agent (NDZ-101) on the surface of nano calcium carbonate, the adsorption free energy and dispersive component of the surface free energy of nano calcium carbonate treated with about 3%(by weight of nano calcium carbonate) titanate coupling agent (NDZ-101) were lowest.

### 3.4.3 Phosphate modifier

Phosphate modifier effected as a surfactant. The modifier covered over the surface of nano calcium carbonate particles by reacting with calcium carbonate surface to produce calcium phosphate. It can change the surface property from hydrophilic to lyophobic.

This modifier is also widely used like organic acid modifier. Nakatsuka used phosphate-modified calcium carbonate copolymerized with styrene<sup>[53]</sup>.

### 3.5 The ionic state ( $\text{Ca}^{2+}$ ) dispersion based from $\text{CaCO}_3$

From the reaction of acid and  $\text{CaCO}_3$ , the calcium transforms to its ionic form,  $\text{Ca}^{2+}$ , and have a strong interaction with the  $\text{COO}^-$  which produce the assemblies<sup>[54]</sup>. If the acid is from an organic acid and connected to the polymer backbone, crosslinked polymer networks are prepared by the ionic associations. These crosslinked ionic polymers, which are also called ionomers, have been studied in recent decades.

#### 3.5.1 Morphology: Eisenberg model

The model developed by Eisenberg is generally admitted<sup>[55]</sup>. Shown in figure 3.1, the ionic pairs in the ionomers are called as multiplets<sup>[56]</sup>. One multiplet contains the several metal cations and organic acid anions instead of one cation and one anion pair whose electric charges are equal and maintain electrical neutrality in multiplets (figure 3.1 a). And the aggregates composed by several multiplets are called clusters. With the concentration and dispersion of clusters and multiplets, the polymer chain movements are restricted to various degrees that perform distinctive mechanical properties (figure 3.1 b).

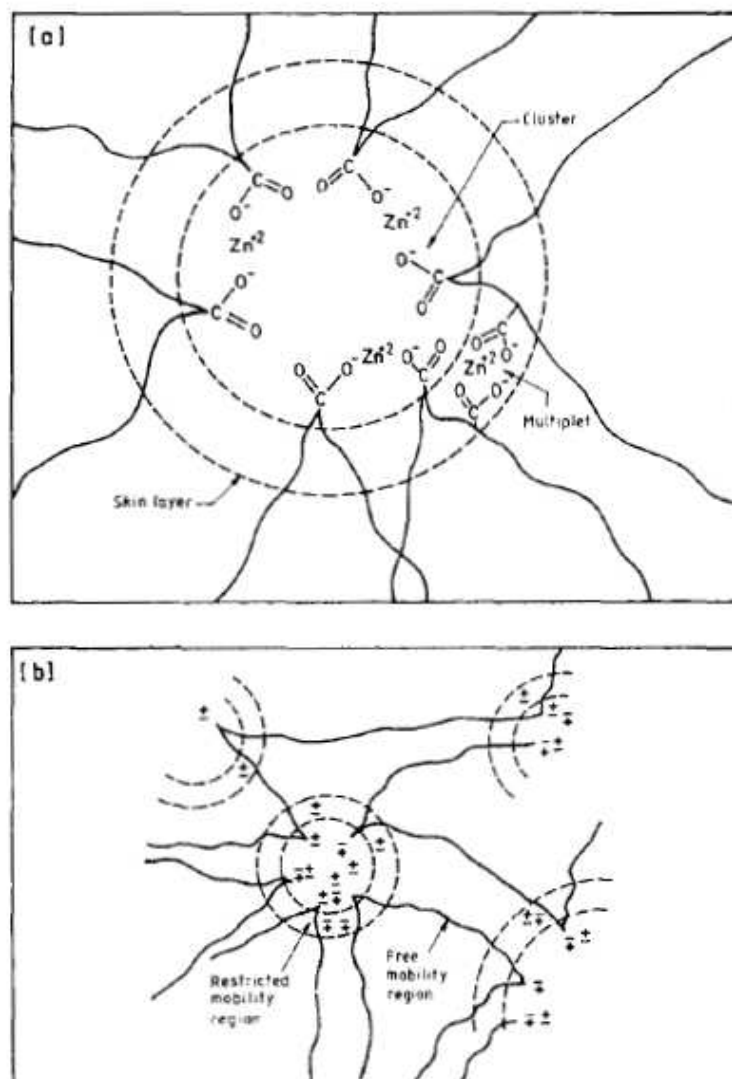


Figure 3.1 The multiplets and cluster model in ionomer <sup>[56]</sup>

Sizes of multiplets are not affected by the extents of metal and carboxylated / sulfonated groups in the polymer chains, SAXS analyzes determine their size from Bragg-spacing around 2-5 nm, depending on the polymer considered <sup>[55]</sup>. The position of the ion pairs relative to the backbone may also influence this size <sup>[57]</sup>. Eisenberg determined that the multiplets are surrounded by amorphous regions of restricted mobility of polymer chains<sup>[55, 58]</sup>. At very low ion content, isolated multiplets are dispersed acting as physical cross-links, in the polymer matrix, just increasing the glass transition temperature (T<sub>g</sub>) by increasing their concentration and reducing the polymer chains mobility. As the ion concentration increases, the regions of restricted mobility surrounding each multiplet overlap to form larger contiguous regions of restricted mobility, which are the clusters <sup>[55, 59, 60]</sup>. The presence of clusters can be proved by SAXS with ionic peaks since it is attributed to the intermultiplet

distance within the cluster phase <sup>[55]</sup>. With further increment of ion content, concentration of clusters is increased and phase separation is favored together with the intensifying of ionic peak. The height of this peak increases approximately linearly with ion content.

### 3.5.2 Influence of ionic interactions to the mechanical properties of polymers

#### Determination of cluster phase by SAXS

The ionic molar content from which clusters are observed, depends on the types of repeat units and can vary from 1 to 12% <sup>[61]</sup>. If multiplets exist, the distance between them has to be determined from the “ionic peak” determined by X diffraction. The Bragg spacing of intermediate ion contents (5-10 mol %) is around 23 Å with Bragg spacing comprised between 300 and 20 Å <sup>[55]</sup>. In general, the Bragg distance has to be a function of the concentration (c) of the ionic sites, following  $c^{-1/3}$  scaling law. This model is not applied in ionomers since the Bragg distance is attributed to the intermultiplet distance, which is indirectly in relation with their concentration. The intermultiplet spacing is believed to be related to the loopback distance, which is a function of the nature of the polymer chain and the ion pair rather than simply ion concentration <sup>[58]</sup>.

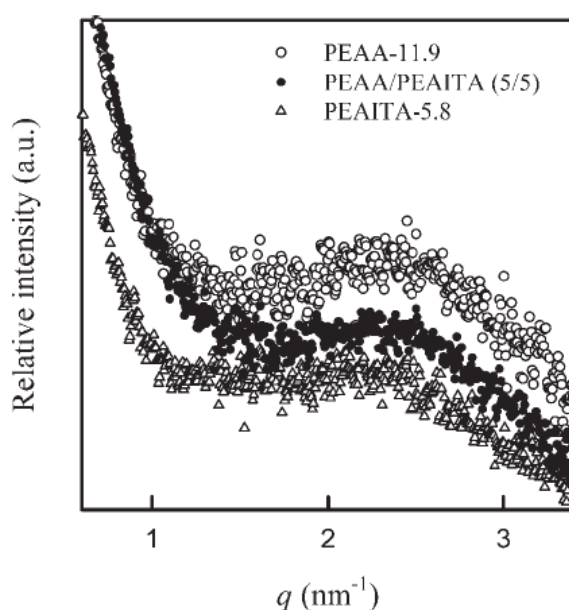


Figure 3.2 SAXS profiles for PEAITA(poly(ethyl acrylate-co-itaconate))-5.8 and PEAA(poly(ethyl acrylate-co-acrylate)) -11.9 ionomers and PEAA-11.9/PEAITA-5.8 ionomer homoblends. <sup>[62]</sup>

In Na<sup>+</sup>/COO<sup>-</sup> ionomers based on PEAA (poly(ethyl acrylate-co-acrylic acid)) and PEAITA (poly(ethyl acrylate-co-itaconic acid)) shown in figure 3.2 <sup>[62]</sup>, the ionic peaks represented by q value are found at around 2.2 nm<sup>-1</sup> which are corresponding to the Bragg spacing between scattering centers of around 2.7 nm.

### **Influence to glass transition of polymers**

The transition from glassy state to rubbery state is the the feature in many polymer solids. It depends on the thermal energy of the molecules. When temperature increased to some extent, the segmental mobility also increases until the rubbery-like deformation upon a small applied stress becomes possible. The segmental mobility is expected to be depended on the inter-chain forces, which in ionomers they are the degree of ionization and the concentration of ionic bonds. With high multiplets concentration in the ionomer, the chain mobility is restricted and T<sub>g</sub> is increased.

Since the ionic peaks observed by SAXS represent the cluster phase which means that phase separation occurs, two glass transitions are consequently derived. The first T<sub>g</sub> relates to the T<sub>g</sub> of matrix, and the second T<sub>g</sub> at a higher temperature than the matrix T<sub>g</sub>, is associated to the glass transition of the ion-rich cluster phase <sup>[63, 64]</sup>..

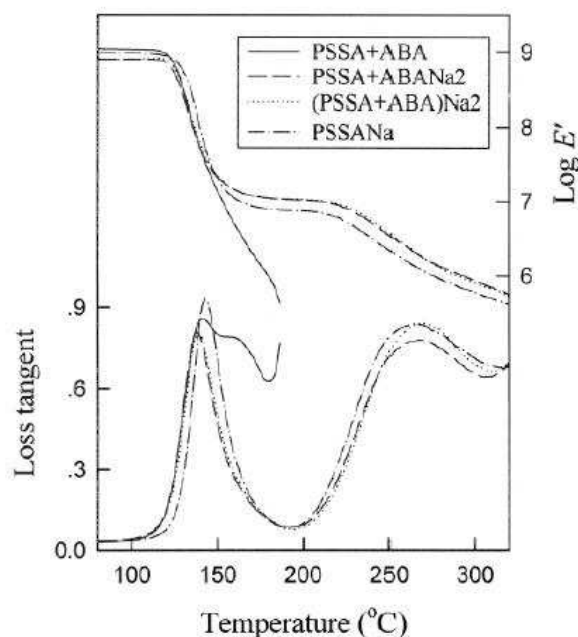


Figure 3.3 Storage moduli and loss tangents against temperature graph in a  $\text{Na}^+$  introduced ionomer blends (PSSA= polystyrene sulphonic acid and ABA= p-aminobenzoic acid) <sup>[65]</sup>

Kim established a relation between the nature of the metallic cation nature (size and charge) and both the matrix  $T_g$  and Cluster  $T_g$  shown in figure 3.3 <sup>[65]</sup>. The peak of  $\tan \delta$  from temperature sweep tests by dynamic rheology at 250 °C is referring to the  $T_g$  of ionic cluster phase. From specific mixing conditions, a third peak is observed <sup>[66]</sup>. Extensive studies based on this model have revealed that the formation of multiplets and clusters in ionomers are linked to the ionic species <sup>[67]</sup>, the nature of the polymer and their concentration, types and sizes. Eisenberg mentions that the most important ionic parameter that affects multiplets formation is the strength of the electrostatic interactions between the ion pairs. This is determined by the sizes of the ions and the partial covalent character of the ionic bond <sup>[55, 57]</sup>. Furthermore, a relationship between two  $T_g$ s and the functionality of ionic group ratio  $R$  is given <sup>[54]</sup>: the first  $T_g$  is independent to  $R$  value which means the matrix  $T_g$  is not influenced by the content of ionic groups, while the second  $T_g$  decreases significantly with increasing diacid salt content.

### Influence to viscoelasticity of polymers

Capek <sup>[54]</sup> reviewed all the parameter affecting the morphologies and consequently the properties. This model is different from the previous one by the absence of electrostatic forces between multiplets within a cluster. Because the multiplets effect as multifunctional cross-links, a rubbery plateau, called ionic-plateau, is observed at temperatures between the polymer matrix and a temperature higher than the cluster phase. Actually, the multiplets remain stable over this temperature range. As in figure 3.4<sup>[54]</sup>, sulfonated ionomer have a higher rubbery plateau than the copolymer. And it is stable with no indication of changes in  $E'$  at 100 °C as is observed for the non-modified copolymer.

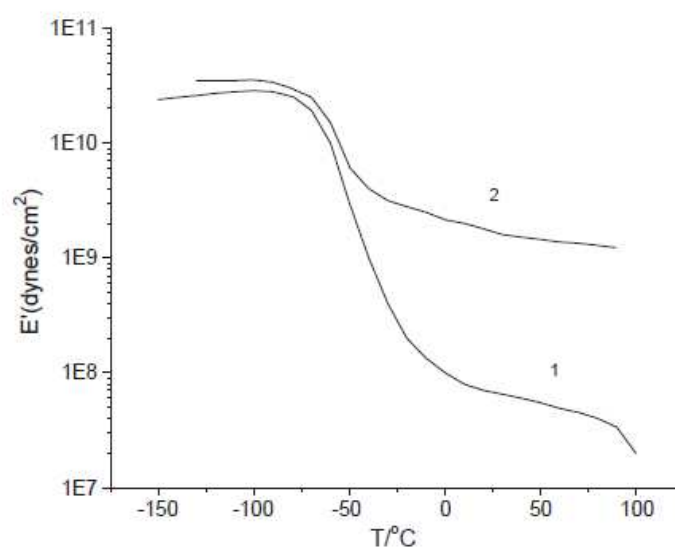


Figure 3.4 The tensile storage modulus  $E'$  of unmodified PSt-PIB-PSt copolymer and its ionomer

1—poly(styrene-*b*-isobutylene-*b*-styrene), 2—sulfonated poly(styrene-*b*-isobutylene-*b*-styrene) <sup>[54]</sup>

If the multiplets act as independent multifunctional cross-links, the value of this rubbery modulus is expected to be in keeping with the modulus predicted by the classical theory of rubber elasticity  $E = 3\rho RT/Mc$ <sup>[68]</sup>. When the requirements for phase-separated behavior are fulfilled <sup>[57]</sup>, ionomers may be melt-processable despite the fact that multiplets still exist at elevated temperatures over  $T_g$  <sup>[57, 69, 70]</sup> and ionic species migrate from one multiple to another by ion hopping or act as a filler <sup>[57, 71]</sup>. The temperature at which melt flow begins, can be controlled to a large extent through the choice of the neutralizing cation. Divalent cations such as  $Ca^{2+}$  or  $Zn^{2+}$  can have extreme impacts on the processability. Calcium maintains generally the rubbery plateau <sup>[68]</sup> to high temperature and  $Zn^{2+}$  is often observed to begin the

material to flow at lower temperatures compared to monovalent cations <sup>[61]</sup>. In polystyrene matrix, the counterion type modifies the deformation modes in strained thin films of rigid ionomers <sup>[68]</sup>.

### **3.6 CaCO<sub>3</sub> / acid / polybutyl methacrylate composite**

#### **3.6.1 Why PBMA?**

Poly(alkyl methacrylate)s are well-known for their diversified applications because of their mechanical and electrical properties, optical clarity, and high chemical and thermal stability. Alkyl methacrylates have the ability to form copolymers with the other monomers. The properties of the polymers depend on the length of the ester side chain and the monomer ratios in the copolymer. Though methyl methacrylate has advantage in copolymerization, methyl group makes it irritative to human body.

The monomer of PBMA, butyl methacrylate, containing n-butyl group is less toxic and has fine adaptability to the living animals which makes PBMA develop rapidly as biomedical polymer. Low glass transition temperature makes it easy for recycling. And if the correspondingly poor mechanical properties become stubborn for processing, PBMA can be modified using inorganic additives, such as carbon black <sup>[72]</sup>, montmorillonite <sup>[73, 74]</sup>, calcium carbonate <sup>[50]</sup>. They can impressively increase mechanical modulus of materials, thus make up for PBMA's disadvantages.

#### **3.6.2 CaCO<sub>3</sub> influence to polymer**

As inorganic filler, CaCO<sub>3</sub> is usually used to increase the glass transition temperature and improve materials' toughness, young's modulus and other mechanical properties <sup>[42]</sup>. The network mobility decreased with increasing CaCO<sub>3</sub> particle concentration, particle size, and aspect ratio, and contributed to form a cohesive network during burning when the thermal stress is high enough <sup>[75-77]</sup>.

Jin <sup>[78]</sup> synthesized a composite materials by copolymerization of styrene, acrylic acid and CaCO<sub>3</sub>. Acrylic acid worked as a modifier. The result found that the CaCO<sub>3</sub> Composite exhibits good performances in wear and friction reduction. The anti-wear improvement capability of the machine oil turn up to be the most efficient when 5 wt% CaCO<sub>3</sub> composite was added.

One shortcoming of using calcium carbonate to reinforce materials is that the tensile stress decreases with increasing filler content and the impact stress increases with increasing filler content <sup>[79]</sup> if the modification is not well processed.

As a previous work, Chen <sup>[80]</sup> studies the viscosity and some rheological modulus of PBMA/MA/CaCO<sub>3</sub>. The storage modulus and viscosity are shown in Figure 3.5.

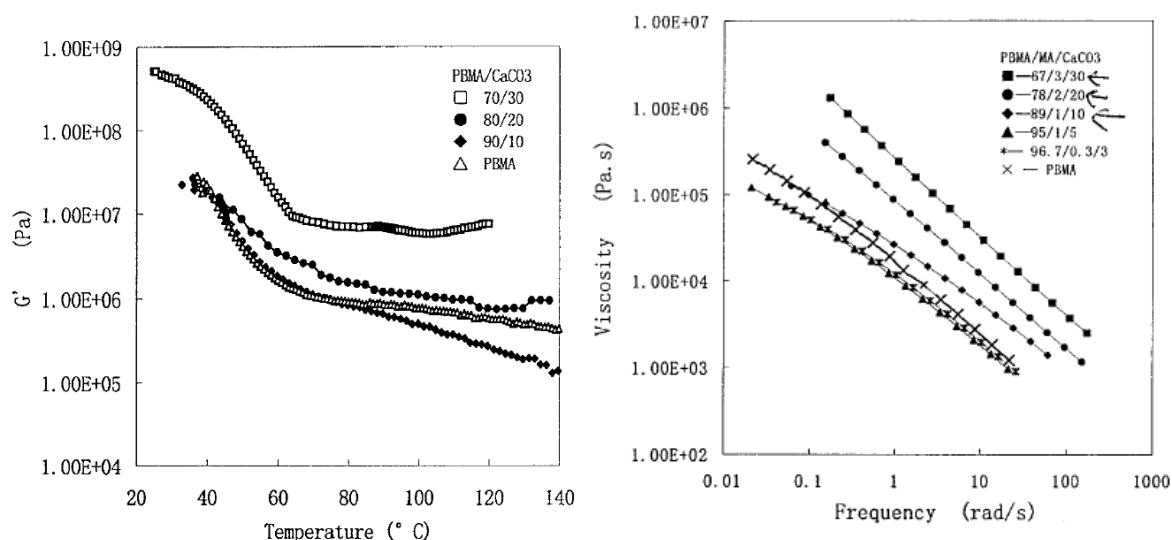


**Figure 3.5 Comparison of  $G'$  and viscosity of composites PBMA/MA/CaCO<sub>3</sub> with PBMA at 160°C for the same molar mass,  $M_w = 360,000$  g/mol. <sup>[80]</sup>**

It is not surprising that the  $G'$  and viscosity increased with CaCO<sub>3</sub> portion increasing. However, when CaCO<sub>3</sub> is in low concentration in the materials, we can see the data from sample PBMA/CaCO<sub>3</sub>=90/10 (in the left graph), and sample PBMA/MA/CaCO<sub>3</sub>=94/1/5, sample PBMA/MA/CaCO<sub>3</sub>=96.7/0.3/3 (in the right graph). Their moduli are lower than pure PBMA. This is not the only example. Li <sup>[81]</sup> found nano-CaCO<sub>3</sub> performed as plasticizer to PS when added in low concentration. In his system, poly(styrene-butadiene-styrene) triblock copolymer (SBS), a poly(styreneisoprene-styrene) triblock copolymer (SIS), SBS-grafted maleic anhydride (SBS-MAH), and SIS-grafted maleic anhydride were used as modifiers or compatibilizers. The results showed that CaCO<sub>3</sub> had some effects on the compatibility of PS/SBS (or SBS-MAH)/CaCO<sub>3</sub> composites, in which SBS could effectively retard the movement of PS chain segments.

The reason that why CaCO<sub>3</sub> can improve the compatibility was explained attributing to the chemical interaction between CaCO<sub>3</sub> and the grafted maleic anhydride had obvious effects on

the rheological behavior of the composites. The results showed that nano- $\text{CaCO}_3$  could plasticize the PS matrix to some extent when the  $\text{CaCO}_3$  concentration is low in the matrix.

There are not many publications which had clearly defined the interaction between  $\text{CaCO}_3$  and organic acid as an ionic interaction. Most researcher considered it's only a partly ionic interaction on the surface of  $\text{CaCO}_3$  aggregation because the organic acid is not strong as inorganic one such as  $\text{HCl}$  or  $\text{H}_2\text{SO}_4$ . The space configuration is like figure 3.6<sup>[51, 82]</sup>. Nano  $\text{CaCO}_3$  particles were aggregated into different scales due to different modification methods. The aggregation connected to the voluble polymer chain by ionic or covalent interaction due to different modifiers.

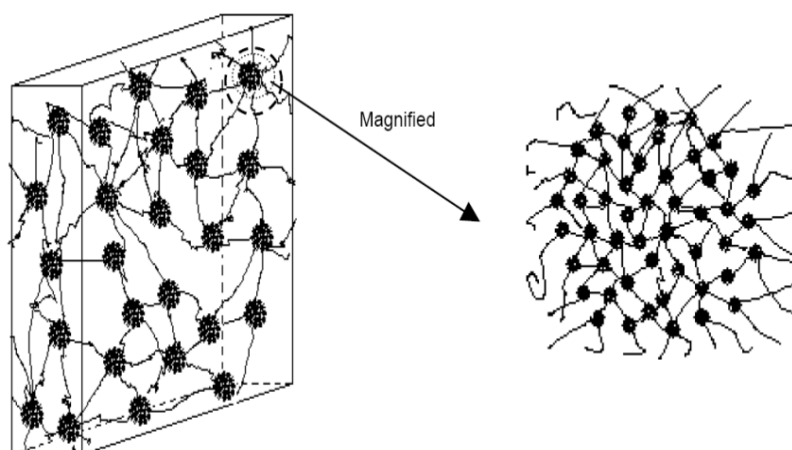


**Figure 3.6** Schematic demonstration of the *in-situ* nano- $\text{CaCO}_3$ /PS composite structure<sup>[51]</sup>

Karlsson<sup>[83]</sup> used a methacrylic acid containing copolymer together with calcium carbonate and silicone elastomer (CaSiEMAA) compared to a butyl acrylate containing copolymer (CaSiEBA). The structure was shown in Figure 3.7. High temperature was considered as a positive aspect since the methacrylic acid initially provides the material with carboxylic acid groups that interact with calcium ions from the calcium carbonate starting at a temperature  $300^\circ\text{C}$ . The degradation of polymer actually produced the more and more  $\text{COO}^-$  and  $\text{Ca}^{2+}$  ionic interaction. So  $\text{CaCO}_3$  containing composite was also used as flame retardancy materials<sup>[84]</sup>.

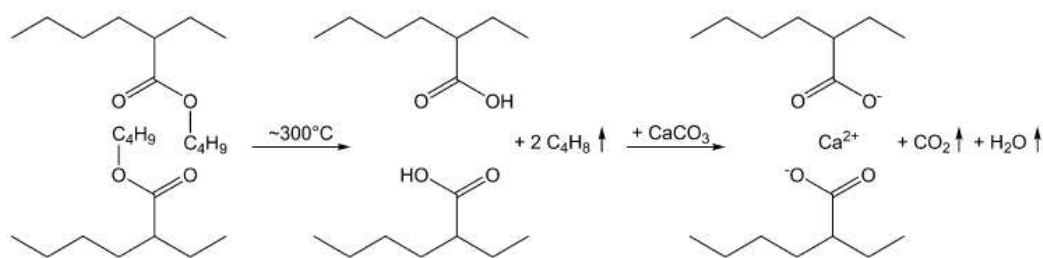


Figure 3.3 Ester pyrolysis of EBA followed by ionomer formation with calcium carbonate <sup>[83]</sup>.

### 3.7 Conclusion

In this section, advantages and disadvantages of using CaCO<sub>3</sub> as inorganic filler are discussed. In order to take full use of CaCO<sub>3</sub>, different modification methods and modifiers are classified. In our case, organic acid is the most efficient and accessible modifier. Reason for PBMA chosen as a polymer matrix is elaborated. The dispersion of CaCO<sub>3</sub> both in particle states as well as in ionic states is demonstrated in details. It results in the reinforcement of mechanical properties of polymers and the viscoelasticity is ameliorated. Although the fact that calcium carbonate used as additive in nanocomposite or ionomers has been reported for decades, few emphasized on the supramolecular interaction. Prospect of CaCO<sub>3</sub> composite is still developable.

## 4. Nonionic supramolecular interaction: hydrogen bonding polymer

The basic conception and conformation have already been discussed in the section 1. In this section, more specific functional group of hydrogen bonds applied in this study will be discussed and described.

### 4.1 Why double hydrogen bonding moiety?

Although single hydrogen bond can be used in self-association interaction, two or more complimentary hydrogen bond pairs are required in the same moiety if more stable assemblies are to be designed. Moiety with even six hydrogen bonds is achievable<sup>[85]</sup>. However these moieties are always complicated to synthesize despite their high  $K_{\text{ass}}$ . Furthermore, such strong interactions are not indispensable to prepare correct cross-linked materials with good properties. Chen<sup>[86]</sup> studied the single hydrogen bonds between  $N_{\text{pyridine}}$  and  $N_{\text{amide-H}}$  in polymer chains. Great reinforcement and reversible properties are observed although the  $K_{\text{ass}}$  value was not specifically calculated.

The double hydrogen bonding could be divided as DD, AA, and DA moieties due to their atom arrangement. A DD agent must be mixed with a AA agent to combine the assembly which is called heterodimer. The heterodimer is also the typical host-guest system in which the supramolecular moiety associates with a countering part from another entity. In the other side, DA is more easy and satisfying to get a supramolecular interaction than the other two kinds of moieties since it could self-assemble with itself which is known as homodimer. A homodimer is a dimer that composed by two identical moieties with same chemical structure. The advantage of homodimer is that only one molecule needed to be synthesized and problems of exact stoichiometry of heterodimers are avoided.

Double hydrogen bonding agents are not very complicate to be obtained from synthesis. If moiety can be chosen as a simple double hydrogen bond moiety which is easy to prepare or even commercially available, materials with desired properties as well as the potentials in industrial application could be prepared.

## 4.2 The motifs based on aminopyridine derivatives

Aminopyridine derivative is chosen as an important product in our study. The N-H connected on ortho position of pyridine ring gives an array of AD moiety from mono-substituted aminopyridine, or DAD moiety from di-substituted diaminopyridine.

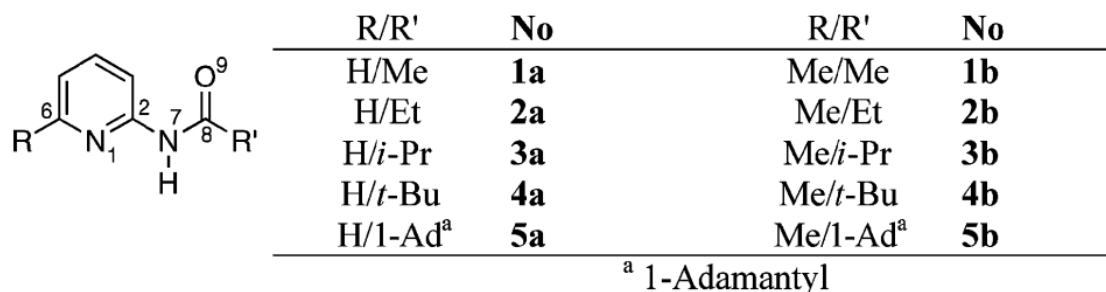


**Figure 4.1** 2-acylamino pyridine derivatives studied by Osmialowski <sup>[29]</sup>

Osmialowski <sup>[29]</sup> studied the 2-acylamino pyridine with different substitutes in figure 4.1. NMR and IR methods were used to study the dimerizations in solid and solution states. The substituent R connecting with the amide group influences the binding constants from 1.5 to 17 M<sup>-1</sup> in CDCl<sub>3</sub>. The DA conformation could be -N<sub>amide</sub>H-CO- or -N<sub>pyridine</sub>-NH-. The X-ray results showed that both N<sub>amide</sub>-H...O=C and both N<sub>pyridine</sub>...H-N took place in some derivatives, but the latter was more predominantly detected in solid state which was also confirmed by IR.

The simple small molecules concerning 2-acrylamidopyridine are approachable by chemical synthesis or even commercial available, but few references discussed about how to introduce the moiety into the polymer chains. Coskun and Temuz <sup>[87, 88]</sup> was the first to prepare the monomer 2-methacrylamidopyridine based on the former work about acrylamidopyridine <sup>[89]</sup>. The aminopyridine derivatives containing the unsaturated double bonds could enable the monomer to copolymerize with other co-monomer such as methyl methacrylate, or graft on the cellulose <sup>[90]</sup> in his work. But only the thermo-properties were focused and no relationship between the hydrogen bond moiety and materials physical properties.

Di-substituted diaminopyridine derivatives with DAD moiety could form a supramolecular association with ADA moiety in heterodimer conformation<sup>[91, 92]</sup>. Patra <sup>[93]</sup> grafted a diaminopyridine derivative as DAD moiety on the polymer main chains as in figure 4.2. The crosslinker C and F were designed with a ADA~ADA sequence. Supramolecular networks after crosslinking had impressive enhancement of photophysical, electrochemical, and

photovoltaic properties. However, the important parameter,  $K_{\text{ass}}$ , was not calculated in his work.

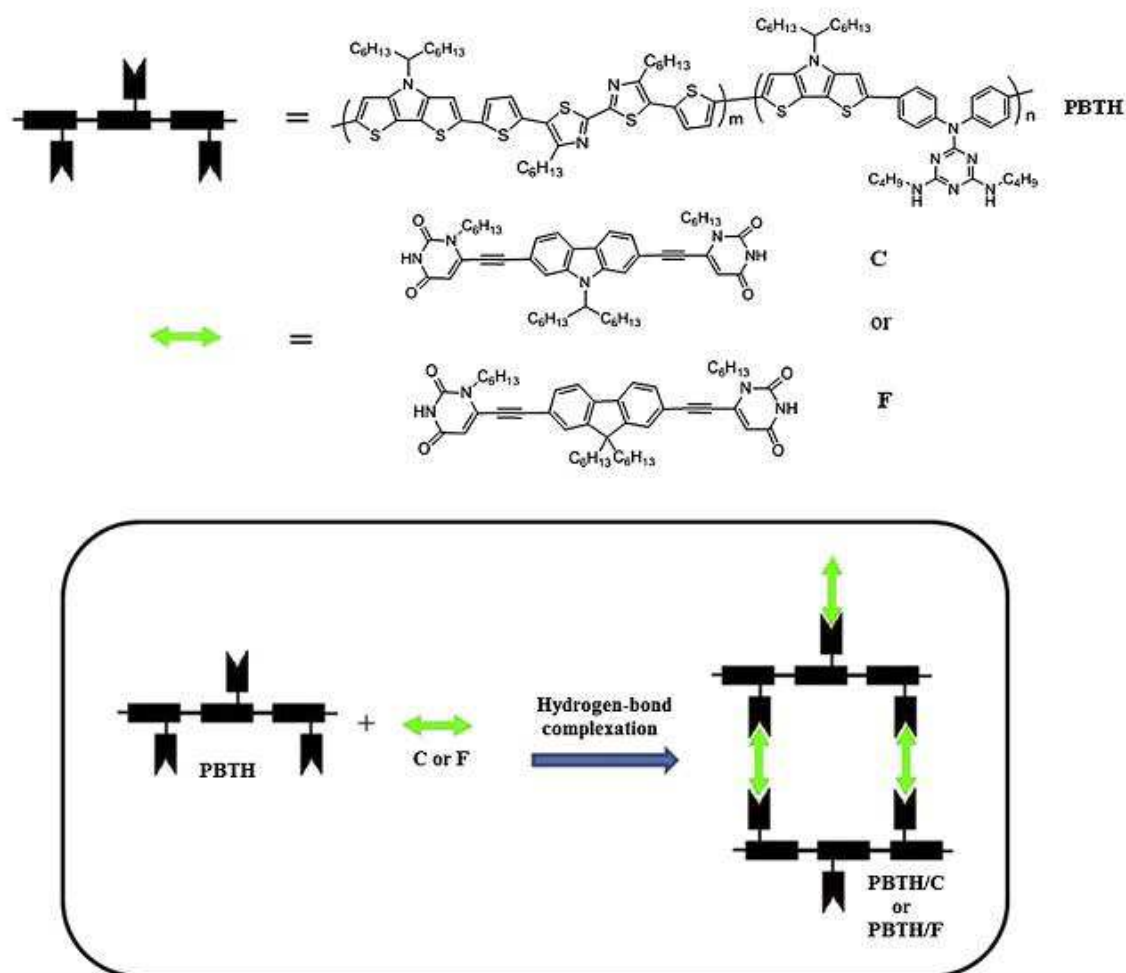


**Figure 4.2 Schematic illustration of conjugated main-chain polymer (PBTH) and supramolecular polymer networks (PBTH/C, and PBTH/F).**

Chen and Bertrand<sup>[28, 94]</sup> used same moieties, and calculated the  $K_{\text{ass}}$  around  $100 \text{ M}^{-1}$ . This is a little pity since although the experimental synthesis of both DAD and ADA moiety was with low yields after complicated multi-steps procedures, the association constant doesn't increased a lot compared to the DA-AD associations.

### 4.3 The moieties based on amide blocks

An amide block has a hydrogen donor N-H and an acceptor C=O that endows it the capacity to self-assemble in homodimers. Assembling patterns could be cyclic or catenary (ribbon)

hydrogen bonded structures in figure 4.3. Poly amides are not novel materials. Many scientists worked on them since they had great water soluble property which made them outstanding in polymers <sup>[95, 96]</sup>. However, their advantages are not only water solubility, but also the reversibility which is given by the DA-AD association.

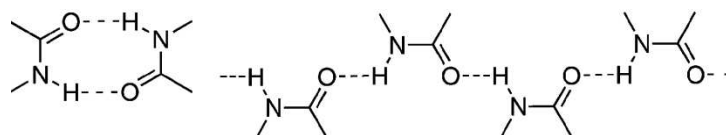


Figure 4.3 Associations between amide groups

Oishi <sup>[97]</sup> synthesized poly(acrylamide) macromonomers by 2-methacryloyloxyethyl isocyanate and prepolymers (Figure 4.3). The chiroptical properties of the copolymers obtained from poly(acrylamide) macromonomers with ST and MMA were slightly influenced by comonomer units. A strong temperature dependence on the specific optical rotation was observed. This phenomenon and the chiral discrimination could attribute to the conformation caused by hydrogen bonds between polymer-graft branches in the polymacromonomer. The chemical shift of N-H bonds in the amide group was also observed moving depending on temperature which is always connected to a supramolecular interaction.

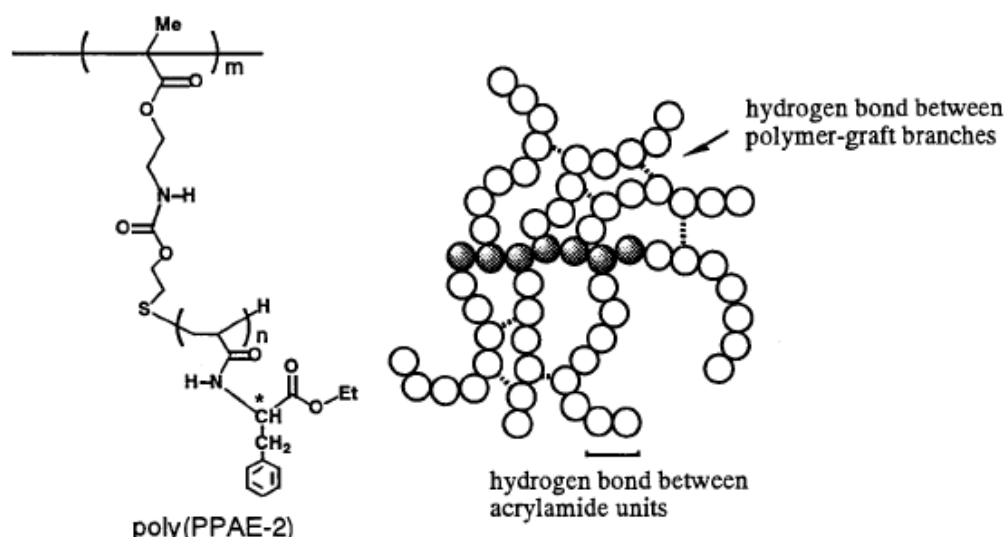


Figure 4.4 Hydrogen bonds between amide groups <sup>[97]</sup>

In another work of Woodward <sup>[98]</sup>, the amide groups were prepared by the reaction of isocyanate and amine. The binding constant varied from 7~45 M<sup>-1</sup> as in table 4.1. Although K<sub>ass</sub> values were not very high, the polymer rheological properties were magnificently

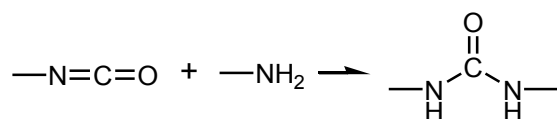
improved after these supramolecular groups were grafted on poly(ethylene-co-butylene). They exhibited the drops in storage modulus due to the phase transition in the soft P(E-co-B) segments. After that, the rubbery plateau was appeared and the end of which depended on the association strength. Copolymer containing supramolecular end group with higher  $K_{ass}$  was more resistant to the heat, and plateau was insistent until high temperature at 125 °C.

**Table 4.1 Structures and Binding Constants (CDCl<sub>3</sub>, 25 °C) for the model Compounds 7-12** <sup>[98]</sup>

Compound	$K_d/M^{-1}$		$R_1$
	X = O	X = NH	
	<b>7</b> 1.4 ± 0.4	<b>10</b> 6.9 ± 1.7	<b>7</b> = undecane <b>10</b> = 2-ethylhexane
	<b>8</b> 1.5 ± 0.3	<b>11</b> 9.7 ± 4.5	<b>8</b> = undecane <b>11</b> = 2-ethylhexane
	<b>9</b> 15 <sup>17</sup>	<b>12</b> 45 ± 11	<b>9</b> = decane <b>12</b> = 2-ethylhexane

#### 4.4 The moieties based on urea blocks

The preparation of polyurea is derived from the reaction of isocyanate and amine in scheme 4.1. The chemical structure of polyurea is controllable with designed ratios and structures of amine and isocyanate derivatives.



**Scheme 4.1 Reaction to synthesize polyurea**

Hydrogen bonds interactions are expected due to the two hydrogen donors and one acceptor in the urea. On one hand, it is capable to associate with other DA moieties to form DA-AD dimers. It is reported that when reacted with carboxylic acid which was a DA moiety, the dimerizations could take place not only through the DA-AD double hydrogen bonds in figure

4.5a<sup>[99]</sup>, but also as through ionic interaction in figure 4.5b<sup>[100]</sup> when the acid was a strong organic acid with high  $pK_a$ .

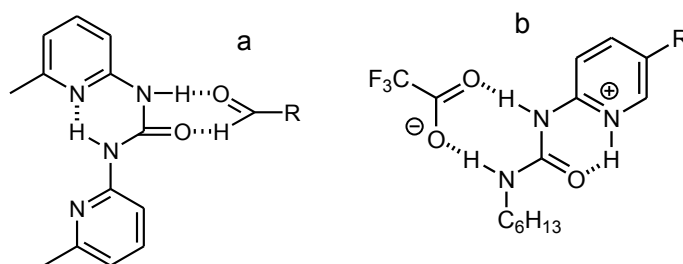


**Figure 4.5 Binding of carboxylic acids with ureas: a) with double hydrogen bonds<sup>[99]</sup>; b) with ionic interaction<sup>[100]</sup>**

On the other hand, the self-association among urea blocks is also possible, leading to the reversible cross-linking between linear polyurea chains.

Van Esch<sup>[101]</sup> prepared low molecular weight gelators based on the structure R-NHCONH-X-NHCONH-R, which are tested for their ability to cause gelation of organic solvents. These urea compounds spontaneously form highly ordered fibers when absorbed on graphite and fibers from cooled homogeneous solution through the formation of multiple intermolecular hydrogen bonds. The overall result is a long-term thermal stability of the structures. The gels formed by these urea compounds are stable but irreversibly disrupted by mechanical agitation. However, they can be restored by heating above the melting temperature, followed by cooling to room temperature, indicating that the gel formation is thermo reversible.

Moreover, the molecular features of fatty acids based self crosslinking polyurethane urea that influence the micro phase morphology and dynamic mechanical behavior of polymers, were exploited by Patel<sup>[102]</sup>. With higher urea contents, higher strength of hydrogen-bonding among urea linkages results in improved inter connectivity of hard segments.

Although the hydrogen bonds were generally admitted between urea blocks, it is until recent years that polyurea was reported as “supramolecular” fillers. As in figure 4.6<sup>[103, 104]</sup>, the small molecular bi-urea segments were prepared and mixed with long chain polyureas. This resulted in stiffer materials by doubled Young’s modulus with 23 mol % of filler content, while the no decrease in tensile strength or elongation at break were observed. In another work<sup>[105]</sup>, similar reinforcement of mechanical properties was observed. Furthermore, the reversibility dependent on the temperature was also obtained by IR spectroscopy with repetitive heating and cooling ramps.

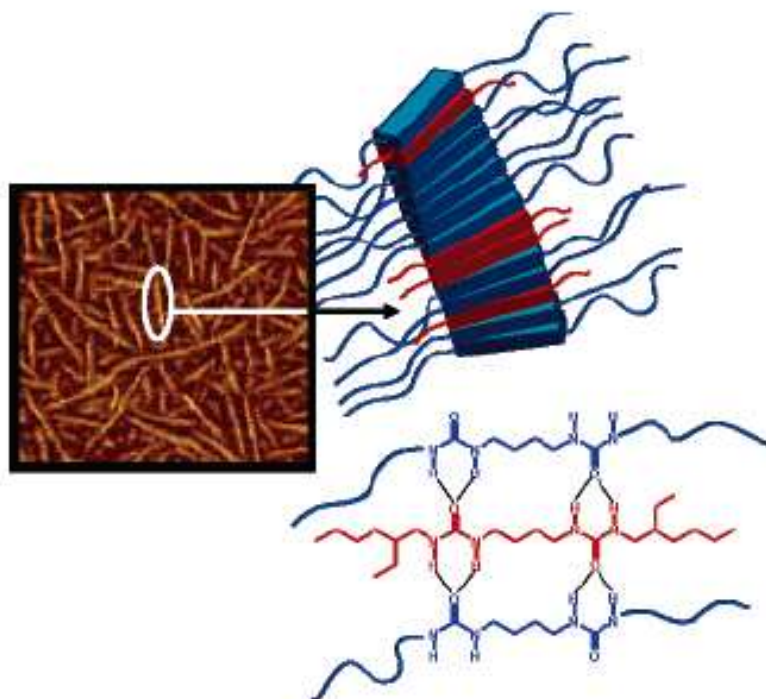


**Figure 4.6** supramolecular filler (red) is incorporated into the PCLU4U hard domains (blue) via bifurcated hydrogen bonds. <sup>[104]</sup>

The supramolecular interactions also endow polyurea with ordered structure. Kim<sup>[106]</sup> prepared bis-acylureas bearing different end groups which could assemble to biaxial intermolecular hydrogen bonding networks in two directions (figure 4.7). Furthermore, thin nanosheets and cocoon- or sponge-like micro-spheres could be assemble due to the strong intermolecular interactions among bis-acylureas.

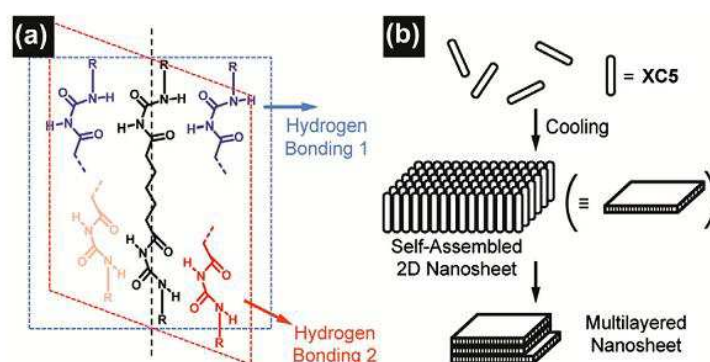


**Figure 4.7** Schematic illustration of bis-acylureas. (a) Biaxial hydrogen bondings of bis-acylurea. (b) Formation of multilayered nanosheets via two dimensional self-assembly <sup>[106]</sup>

#### 4.5 Conclusion

In this section, multiple hydrogen bonds based on aminopyridine derivatives, amide, urea are discussed in details since they are the applied moieties in this study. The association strengths in these systems are compared, and they are reflected in the physical and thermo properties in polymers. For polyaddition, the difficulty of supramolecular polymer preparation is to design the supramolecular monomer with both functional moiety and polymerisable double bond. For polycondensation such as polyurea synthesis, although the strategy was already proved achievable and successful, the study concerning  $K_{\text{ass}}$  calculation based on urea association<sup>[107]</sup> were rarely reported.

## References

- [1] Lehn, J. M. *Angew. Chem.-Int. Edit. Engl.* **1988**, 27, (1), 89-112.
- [2] BOSMAN A W, S. R. P., Meijer E W. *Materials Today* **2004**, 7, (4), 34-39.
- [3] Lin, M.; Xu, P.; Zhong, W. *J. Biomed. Mater. Res. Part B* **2012**, 100B, (4), 1114-1120.
- [4] Zhou, D. X.; Sun, T.; Deng, W. *Chinese Journal of Organic Chemistry* **2012**, 32, (2), 239-253.
- [5] Beijer, F. H.; Sijbesma, R. P.; Kooijman, H.; Spek, A. L.; Meijer, E. W. *Journal of the American Chemical Society* **1998**, 120, (27), 6761-6769.
- [6] De Greef, T. F. A.; Smulders, M. M. J.; Wolffs, M.; Schenning, A.; Sijbesma, R. P.; Meijer, E. W. *Chem. Rev.* **2009**, 109, (11), 5687-5754.
- [7] Brunsveld, L.; Folmer, B. J. B.; Meijer, E. W.; Sijbesma, R. P. *Chemical Reviews* **2001**, 101, (12), 4071-4097.
- [8] Hirschberg, J.; Beijer, F. H.; van Aert, H. A.; Magusim, P.; Sijbesma, R. P.; Meijer, E. W. *Macromolecules* **1999**, 32, (8), 2696-2705.
- [9] Aakeröy, C.; Epa, K. *Topics in Current Chemistry* **2012**, 1-23.
- [10] Adamson, A. W., *A textbook of physical chemistry*. Academic Press: 1986.
- [11] Binder, W. H.; Zirbs, R., Supramolecular polymers and networks with hydrogen bonds in the main- and side-chain. In *Hydrogen Bonded Polymers*, 2007; Vol. 207, pp 1-78.
- [12] Pranata, J.; S.G.Wierschke; W.L.Jorgenson. *J. Am. Chem. Soc* **1991**, 113, (8), 2810-2819.
- [13] Philippova, O. E.; Hourdet, D.; Audebert, R.; Khokhlov, A. R. *Macromolecules* **1996**, 29, (8), 2822-2830.
- [14] Wang, S. M.; Yu, M. L.; Ding, J.; Tung, C. H.; Wu, L. Z. *J. Phys. Chem. A* **2008**, 112, (17), 3865-3869.
- [15] Cifeffi, A., *Supramolecular Polymers*. Second ed.; CRC Press: 2004.

- [16] Keizer, H. M.; Sijbesma, R. P.; Meijer, E. M. *European Journal of Organic Chemistry* **2004**, (12), 2553-2555.
- [17] Lee, K. J.; Lee, D. K.; Kim, Y. W.; Kim, J. H. *European Polymer Journal* **2007**, 43, (10), 4460-4465.
- [18] Rieth, L. R.; Eaton, R. F.; Coates, G. W. *Angewandte Chemie-International Edition* **2001**, 40, (11), 2153-2156.
- [19] Mitsuhiro Shibata, Y. K., Daisuke Yaginuma. *Polymer* **2004**, 45, 7571-7577.
- [20] Canilho, N.; Kasëmi, E. *Macromolecular Symposia* **2008**, 270, (1), 58-64.
- [21] Raffaele, M.; Janne, R.; Nadia, C. *Soft Matter* **2008**, 5, (1), 92-97.
- [22] HAN, F.; HIGUCHI, M.; AKASAKA, Y. *Thin Solid Films* **2008**, 516, (9), 2469-2473.
- [23] Zhang, K.; Gao, H.; Pan, Z. *Polyhedron* **2007**, 26, (17), 5177-5184.
- [24] Schalley, C., *analytical methods in supramolecular chemistry*. wiley-vch Verlag GmbH &Co. KGaA, Weinheim: 2007.
- [25] Fielding, L. *Tetrahedron* **2000**, 56, (34), 6151-6170.
- [26] Horman, I.; Dreux, B. *Helvetica chimica acta* **1984**, 67, (3), 754-764.
- [27] Chen, J. S.; Rosenberger, F. *Tetrahedron Letters* **1990**, 31, (28), 3975-3978.
- [28] Bertrand, A.; Chen, S. B.; Souharce, G.; Ladaviere, C.; Fleury, E.; Bernard, J. *Macromolecules* **2011**, 44, (10), 3694-3704.
- [29] Osmialowski, B.; Kolehmainen, E.; Dobosz, R.; Gawinecki, R.; Kauppinen, R.; Valkonen, A.; Koivukorpi, J.; Rissanen, K. *J. Phys. Chem. A* **2010**, 114, (38), 10421-10426.
- [30] Hofmeier, H.; Hoogenboom, R.; Wouters, M. E. L.; Schubert, U. S. *Journal of the American Chemical Society* **2005**, 127, (9), 2913-2921.
- [31] Bocian, W.; Kawecki, R.; Bednarek, E.; Sitkowski, J.; Pietrzyk, A.; Williamson, M. P.; Hansen, P. E.; Kozerski, L. *Chemistry-a European Journal* **2004**, 10, (22), 5776-5787.
- [32] Kao, D. Y.; Shu, W. T.; Chen, J. S. *J. Chin. Chem. Soc.* **2005**, 52, (6), 1171-1178.

- [33] Dethlefs, C.; Eckelmann, J.; Kobarg, H.; Weyrich, T.; Brammer, S.; Nather, C.; Luning, U. *European Journal of Organic Chemistry* **2011**, (11), 2066-2074.
- [34] Brammer, S.; Luning, U.; Kuhl, C. *European Journal of Organic Chemistry* **2002**, (23), 4054-4062.
- [35] Tanahashi, M. *Materials* **2010**, 3, 1593-1619.
- [36] Hashimoto, M. T., H.; Mizuno, M.; Kokubo, T. *Mater. Res. Bul* **2006**, 41, 515-524.
- [37] Yang, F. N., G.L. *Polym. Adv. Technol.* **2006**, 17, 320-326.
- [38] Kalaitzidou, K. F., H.; Drzal, L.T. *Compos. Sci. Technol.* **2007**, 67, 2045-2051.
- [39] Jankong, S. S., K. *J. Met. Mater. Mine* **2008**, 18, 143-146.
- [40] Leong, Y. W.; Abu Bakar, M. B.; Ishak, Z. A. M.; Ariffin, A.; Pukanszky, B. *J. Appl. Polym. Sci.* **2004**, 91, (5), 3315-3326.
- [41] Davery, R. J.; Hirai, T. *Journal of Crystal Growth* **1997**, 171, 318–320.
- [42] Wang, N. Y.; She, Q. Y.; Xu, H. P.; Yao, Y. M.; Zhang, L. Q.; Qu, X. W.; Zhang, L. C. *J. Appl. Polym. Sci.* **2010**, 115, (3), 1336-1346.
- [43] Papirer, E.; Schultz, J.; Turchi, C. *European Polymer Journal* **1984**, 20, (12), 1155-1158.
- [44] Ma, X. K.; Zhou, B.; Sheng, Y.; Wang, C. Y.; Pan, Y.; Ma, S. S.; Gao, Y.; Wang, Z. C. *J. Appl. Polym. Sci.* **2007**, 105, (5), 2925-2929.
- [45] Bellayer, S.; Tavard, E.; Duquesne, S.; Piechaczyk, A.; Bourbigot, S. *Polymer Degradation and Stability* **2009**, 94, (5), 797-803.
- [46] Kato, T.; Suzuki, T.; Irie, T. *Chemistry Letters* **2000**, (2), 186-187.
- [47] Shi, J.-m.; Bao, Y.-z.; Huang, Z.-m.; Weng, Z.-x. *J Zhejiang Univ Sci* **2004**, 5, (6), 709-13.
- [48] Sasaki, T.; Shimizu, M.; Wu, Y. S.; Sakurai, K. *Journal of Nanomaterials* **2008**.
- [49] Deshmukh, G. S.; Pathak, S. U.; Peshwe, D. R.; Ekhe, J. D. *Bull. Mat. Sci.* **2010**, 33, (3), 277-284.

- [50] Chen, J. D.; Carrot, C.; Chalamet, Y.; Majeste, J. C.; Taha, M. *Journal of Applied Polymer Science* **2003**, 88, (5), 1376-1383.
- [51] Shengguang, W.; Jianding, C.; Zhean, X.; Shengmiao, Z.; Qiufang, W. *The Chinese Journal of Process Engineering* **2007**, 7, (4), 790-795.
- [52] Xu, W.; Jian, S.; Rui, H. *Icemi'2003: Proceedings of the Sixth International Conference on Electronic Measurement & Instruments, Vols 1-3* **2003**, 2533-2537.
- [53] Nakatsuka, T.; Kawasaki, H.; Yamashita, S.; Kohjiya, S. *J. Colloid Interface Sci.* **1983**, 93, (1), 277-280.
- [54] Capek, I. *Advances in Colloid and Interface Science* **2005**, 118, (1-3), 73-112.
- [55] Eisenberg, A.; Hird, B.; Moore, R. B. *Macromolecules* **1990**, 23, (18), 4098-4107.
- [56] Eisenberg, A. *Macromolecules* **1970**, 3, (2), 147-154.
- [57] Hird, B.; Eisenberg, A. *Abstracts of Papers of the American Chemical Society* **1992**, 204, 40-PMSE.
- [58] Eisenberg, A.; Kim, J.-S., *Introduction to ionomers*. 1998; p 327.
- [59] Tsou, L.; Ma, X.; Sauer, J. A.; Hara, M. *Journal of Polymer Science Part B-Polymer Physics* **1998**, 36, (7), 1235-1245.
- [60] Kim, H. S.; Nah, Y. H.; Kim, J. S.; Yu, J. A.; Lee, Y. *Polymer Bulletin* **1998**, 41, (5), 569-575.
- [61] Tant, M. R.; Wilkes, G. L. *Journal of Macromolecular Science-Reviews in Macromolecular Chemistry and Physics* **1988**, C28, (1), 1-63.
- [62] Song, J. M.; Luqman, M.; Kim, J. S.; Shin, K. *Journal of Polymer Science Part B-Polymer Physics* **2007**, 45, (9), 1045-1052.
- [63] Kurian, T.; Datta, S.; Khastgir, D.; De, P. P.; Tripathy, D. K.; De, S. K.; Peiffer, D. G. *Polymer* **1996**, 37, (21), 4787-4793.
- [64] Datta, S.; De, P. P.; De, S. K. *Journal of Applied Polymer Science* **1996**, 61, (10), 1839-1846.

- [65] Kim, S. H.; Kim, J. S. *Macromolecules* **2003**, 36, (7), 2382-2386.
- [66] Song, J. M.; Oh, S. H.; Kim, J. S.; Kim, W. G. *Polymer* **2005**, 46, (26), 12393-12400.
- [67] Castagna, A. M.; Wang, W.; Winey, K. I.; Runt, J. *Macromolecules* **2011**, 44, (13), 5420-5426.
- [68] Hara, M.; Sauer, J. A. *Journal of Macromolecular Science-Reviews in Macromolecular Chemistry and Physics* **1994**, C34, (3), 325-373.
- [69] Chu, B.; Wu, D. Q.; Macknight, W. J.; Wu, C.; Phillips, J. C.; Legrand, A.; Lantman, C. W.; Lundberg, R. D. *Macromolecules* **1988**, 21, (2), 523-525.
- [70] Galambos, A. F.; Stockton, W. B.; Koberstein, J. T.; Sen, A.; Weiss, R. A.; Russell, T. P. *Macromolecules* **1987**, 20, (12), 3091-3094.
- [71] Page, K. A.; Park, J. K.; Moore, R. B.; Sakai, V. G. *Macromolecules* **2009**, 42, (7), 2729-2736.
- [72] Moon, J.; Park, M. *Polym.-Korea* **2009**, 33, (5), 477-484.
- [73] Yang, I. K.; Hu, C. C. *Eur. Polym. J.* **2006**, 42, (2), 402-409.
- [74] Sedlakova, Z.; Plestil, J.; Baldrian, J.; Slouf, M.; Holub, P. *Polym. Bull.* **2009**, 63, (3), 365-384.
- [75] Guvendiren, M.; Heiney, P. A.; Yang, S. *Macromolecules* **2009**, 42, (17), 6606-6613.
- [76] Quan, Y.; Yang, M. S.; Liang, T. X.; Yan, Q.; Liu, D. S.; Jin, R. G. *J. Appl. Polym. Sci.* **2007**, 103, (6), 3940-3949.
- [77] Pai, R. K.; Ng, J. B. S.; Pillai, S.; Bergstrom, L.; Hedin, N. *Journal of Colloid and Interface Science* **2009**, 337, (1), 46-53.
- [78] Jin, D. L.; Yue, L. H. *Materials Letters* **2008**, 62, (10-11), 1565-1568.
- [79] Wang, Q.; Qu, J. P. *Polym. Int.* **2006**, 55, (11), 1330-1335.
- [80] Chen, J. D.; Chalamet, Y.; Taha, M. *Macromolecular Materials and Engineering* **2003**, 288, (4), 357-364.
- [81] Li, G.; Mai, K. C.; Feng, K. C. *J. Appl. Polym. Sci.* **2006**, 99, (5), 2138-2143.

- [82] Yue, L. H.; Jin, D. L.; Shui, M.; Xu, Z. D. *Solid State Sciences* **2004**, 6, (9), 1007-1012.
- [83] Karlsson, L.; Lundgren, A.; Jungqvist, J.; Hjertberg, T. *Polymer Degradation and Stability* **2009**, 94, (4), 527-532.
- [84] Lundgren, A.; Hjertberg, T.; Sultan, B. A. *J. Fire Sci.* **2007**, 25, (4), 287-319.
- [85] Corbin, P. S.; Zimmerman, S. C.; Thiessen, P. A.; Hawryluk, N. A.; Murray, T. J. *Journal of the American Chemical Society* **2001**, 123, (43), 10475-10488.
- [86] Chen, S. J.; Hu, J. L.; Zhuo, H. T.; Yuen, C. W. M.; Chan, L. K. *Polymer* **2010**, 51, (1), 240-248.
- [87] Coskun, M.; Temüz, M. M.; Demirelli, K. *Polymer degradation and stability* **2002**, 77, (3), 371-376.
- [88] Coskun, M.; Barim, G.; Temuz, M. M.; Demirelli, K. *Polymer-Plastic Technology and Engineering* **2005**, 44, (4), 677-686.
- [89] Diab, M. A.; Elsonbati, A. Z.; Elsanabari, A. A.; Taha, F. I. *Polymer degradation and stability* **1989**, 24, (1), 51-58.
- [90] Temüz, M. M.; Coşkun, M.; Ölçücü, A. *Journal of Macromolecular Science, Part A: Pure and Applied Chemistry* **2007**, 44, (9), 947-952.
- [91] Lee, S. H.; Ouchi, M.; Sawamoto, M. *Macromolecules* **2012**, 45, (9), 3702-3710.
- [92] Thalacker, C.; Miura, A.; De Feyter, S.; De Schryver, F. C.; Wurthner, F. *Organic & Biomolecular Chemistry* **2005**, 3, (3), 414-422.
- [93] Patra, D.; Ramesh, M.; Sahu, D.; Padhy, H.; Chu, C. W.; Wei, K. H.; Lin, H. C. *Polymer* **2012**, 53, (6), 1219-1228.
- [94] Chen, S. B.; Bertrand, A.; Chang, X. J.; Alcouffe, P.; Ladaviere, C.; Gerard, J. F.; Lortie, F.; Bernard, J. *Macromolecules* **2010**, 43, (14), 5981-5988.
- [95] Kao, H. C.; Kuo, S. W.; Chang, F. C. *J. Polym. Res.-Taiwan* **2003**, 10, (2), 111-117.
- [96] Qiu, F. R.; Chen, S. M.; Ping, Z. H.; Yin, G. M. *Magnetic Resonance in Chemistry* **2005**, 43, (11), 918-925.

- [97] Oishi, T.; Lee, Y. K.; Nakagawa, A.; Onimura, K.; Tsutsumi, H. *Journal of Polymer Science Part a-Polymer Chemistry* **2002**, 40, (11), 1726-1741.
- [98] Woodward, P. J.; Merino, D. H.; Greenland, B. W.; Hamley, I. W.; Light, Z.; Slark, A. T.; Hayes, W. *Macromolecules* **2010**, 43, (5), 2512-2517.
- [99] Goswami, S.; Jana, S.; Dey, S.; Sen, D.; Fun, H. K.; Chantrapromma, S. *Tetrahedron* **2008**, 64, (27), 6426-6433.
- [100] Jordan, L. M.; Boyle, P. D.; Sargent, A. L.; Allen, W. E. *J. Org. Chem.* **2010**, 75, (24), 8450-8456.
- [101] VanEsch, J.; DeFeyter, S.; Kellogg, R. M.; DeSchryver, F.; Feringa, B. L. *Chemistry-a European Journal* **1997**, 3, (8), 1238-1243.
- [102] Patel, A. N.; Patel, M. M.; Dighe, A. *Progress in organic coatings* **2012**, 74, (3), 443-452.
- [103] Wisse, E.; Govaert, L. E.; Meijer, H. E. H.; Meijer, E. W. *Macromolecules* **2006**, 39, (21), 7425-7432.
- [104] Wisse, E.; Spiering, A. J. H.; van Leeuwen, E. N. M.; Renken, R. A. E.; Dankers, P. Y. W.; Brouwer, L. A.; van Luyn, M. J. A.; Harmsen, M. C.; Sommerdijk, N.; Meijer, E. W. *Biomacromolecules* **2006**, 7, (12), 3385-3395.
- [105] Kuo, M. C.; Jeng, R. J.; Su, W. C.; Dai, S. A. *Macromolecules* **2008**, 41, (3), 682-690.
- [106] Kim, J. U.; Davis, R.; Zentel, R. *J. Colloid Interface Sci.* **2011**, 359, (2), 428-435.
- [107] Barboiu, M.; van der Lee, A. *Acta Crystallogr. Sect. C-Cryst. Struct. Commun.* **2003**, 59, M366-M368.

## Chapter B

# Poly(butyl methacrylate-co-methacrylic acid) copolymers with calcium carbonate supramolecular networks

Yiping NI<sup>1,2,3</sup>, Frédéric BECQUART\*<sup>1,2,3</sup>, Mohamed TAHA<sup>1,2,3</sup>, Jean-Charles  
MAJESTE<sup>1,2,3</sup>, Jianding CHEN<sup>4</sup>

<sup>1</sup> Université de Lyon, F-42023, Saint-Etienne, France;

<sup>2</sup> CNRS UMR 5223, Ingénierie des Matériaux Polymères, F-42023, Saint-Etienne, France

<sup>3</sup> Université de Saint-Etienne, Jean Monnet, F-42023, Saint-Etienne, France;

<sup>4</sup> Laboratory of Advanced Materials Processing, East China University of Science and  
Technology, 200237 Shanghai, China

Corresponding author: Frederic.Becquart@univ-st-etienne.fr

## Résumé

Des copolymères, Poly(méthacrylate de butyle-co-acide méthacrylique), ont été synthétisés par polymérisation radicalaire avec du carbonate de calcium dispersé ( $\text{CaCO}_3$ ) comme charge. Le  $\text{CaCO}_3$  est capable de réagir partiellement avec les fonctions acides du co-monomère pour produire des sites cationiques  $\text{Ca}^{2+}$  en interaction avec deux groupes carboxylate de chaînes polymères. Ces espèces ioniques ont été envisagées pour améliorer le matériau en particulier au-dessus de la température de transition vitreuse ( $T_g$ ) avec en plus le reste de  $\text{CaCO}_3$ . Ces charges solides étaient structurées en grappes reliées par des chaînes de copolymères ioniques, l'existence des sites ioniques à la surface des grains ont été supposés pour compléter la description structurale des matériaux. La microscopie électronique par transmission a montré la dispersion de la charge et l'analyse rhéologique décrit le comportement du matériau au-dessus de  $T_g$ . Il est contrôlée par le taux d'acide méthacrylique (MA) dans la chaîne copolymère lorsque le rapport  $\text{CaCO}_3/\text{MA} > 1$  (mol / mol). La diffraction de rayons X a d'abord prouvé l'existence de multiplets et clusters comme l'avait décrit Eisenberg pour les matériaux polymères avec des charges ioniques. Les Multiplets, composés par des associations ioniques locales riches, se comportent comme des charges polymères ioniques qui renforcent le matériau alors que les clusters, composés par la percolation de multiplets lorsque leur concentration est suffisamment élevée, produisent un réseau physique au-dessus de  $T_g$ . Cette étude a démontré clairement que l'augmentation de la concentration de  $\text{CaCO}_3$  permet d'atteindre un comportement réticulé avec une relation entre la concentration de charge et le module de conservation au-dessus de  $T_g$ . Néanmoins, ces réseaux forts de clusters sont brisés plus facilement lorsque la teneur en  $\text{CaCO}_3$  est élevée, car la charge solide restante les fragilise.

## Abstract

Poly(butyl methacrylate-co-methacrylic acid) copolymers were synthesized by radical polymerization with dispersed calcium carbonate ( $\text{CaCO}_3$ ) fillers.  $\text{CaCO}_3$  is able to partially react with the acid functions from the co-monomer to produce  $\text{Ca}^{2+}$  cationic sites in interaction with two carboxylate groups from polymer chains. These ionic species were expected to structure the material particularly above the glass transition temperature ( $T_g$ ) with the rest of  $\text{CaCO}_3$  solid filler. These solid fillers are structured in grapes with ionic copolymer chains sandwiched between them, assuming ionic sites existence at the grains surface. Transmission Electron Microscopy showed the filler dispersion and rheological analysis described the material behavior above  $T_g$ . It is controlled by the methacrylic acid (MA) content in the copolymer chain when  $\text{CaCO}_3/\text{MA} > 1$  (mol/mol). X-Ray diffraction first proved the existence of multiplets and clusters as Eisenberg described them first in polymer materials with ionic fillers. Multiplets, composed by local rich ionic associations, behave like ionic polymer fillers which reinforce the material whereas clusters, composed by the percolation of multiplets when their concentration is high enough, produce a strong network above  $T_g$ . This study clearly demonstrates that increasing the  $\text{CaCO}_3$  concentration allows to reach the cross-linked behavior with a relation between their concentration and the storage modulus above  $T_g$ . Nevertheless these strong cluster networks are broken more easily when the  $\text{CaCO}_3$  content is high since the remaining solid filler obstructs the cluster percolation.

**Keywords:** supramolecular, ionomer, calcium carbonate, network, exfoliation, methacrylic acid

## B-1. INTRODUCTION

Eco-conception of new polymer materials takes into consideration the reuse and recycling with the possibility to transform materials for several life cycles. This challenge is relatively easy with thermoplastic polymer materials in case that thermomechanical and ageing degradations are reduced. It is more complicated when recycling concerns covalent cross-linked polymers. An alternative is the preparation of physically crosslinked materials. Ideally, in this case, the no-covalent bonds between the polymer chains can be destroyed at high temperatures leading a thermoplastic backbone that can be processed using classical techniques. In addition, the thermal, rheological and mechanical properties of the materials should be controlled above the glass transition temperature ( $T_g$ ) of the polymer matrix with often a persistence of the rubbery plateau in the dynamic tensile modulus. Supramolecular chemistry offers one possible and an original way to build such physically and reversibly crosslinked polymers<sup>[1]</sup>. Interactions by hydrogen bonds are very attractive<sup>[2-4]</sup>. On the Importance of the nature of hydrogen bond donors in multiple hydrogen bond systems, the AAAA center dot DDDD hydrogen bond dimer associations between donor and acceptor sites can be efficient with possible conformational effects limiting the expected associations. A second possibility is to develop interchain interactions between an organic moiety with a negative charge, generally from a carboxylate or a sulfonate group, and a filler, generally a cationic metal<sup>[5-7]</sup>. These polymers, accurately ionomers<sup>[8]</sup>, have unique properties owing to ionic interactions and were actively studied three decades ago till nowadays. Different models were developed to describe the multiplet-cluster morphology of random ionomers<sup>[9, 10]</sup>. The model developed by Eisenberg is now admitted<sup>[11]</sup>. Eisenberg showed that ionic pairs aggregate to form collectively multiplets<sup>[12]</sup>. Their size are not affected by the extents of metal and carboxylated / sulfonated groups in the polymer chains, SAXS analyzes determine their size from Bragg-spacing around 2-5 nm, depending on the polymer considered<sup>[11]</sup>. The position of the ion pairs relative to the backbone may also influence this size<sup>[13]</sup>. Eisenberg determined that the multiplets are surrounded by amorphous regions of restricted mobility of polymer chains<sup>[8, 11]</sup>. At very low ion content, isolated multiplets are dispersed acting as physical cross-links, in the polymer

matrix, just increasing the glass transition temperature ( $T_g$ ) by increasing their concentration and reducing the polymer chains mobility. As the ion concentration increases, the regions of restricted mobility surrounding each multiplet overlap to form larger contiguous regions of restricted mobility, called clusters<sup>[11, 14, 15]</sup>. In these structures, the ionic peaks observed by SAXS always exist since it is attributed to all the aggregates' distance within the cluster phase<sup>[11]</sup>. With further increment of ion content, phase separation is favored and the ionic peak grows in intensity. The height of this peak increases approximately linearly. The peak height is only appropriate for estimating the fraction of each phase if the loss peak shapes do not change with composition. The expression is indeed from the classic first approximation to the description of rubber elasticity. The ionic molar content from which clusters are observed, depends on the types of repeat units and can vary from 1 to 12%<sup>[9]</sup>. When these regions become sufficiently large, they exhibit phase-separated behavior with a second  $T_g$ , at a higher temperature than the matrix  $T_g$ , associated to the glass transition of the ion-rich cluster phase<sup>[16, 17]</sup>. This interpretation matches with the observation of "ionic" peak observed by SAXS<sup>[9, 18]</sup> analyses and two maximum peaks on  $\tan\delta$  from temperature sweep tests by dynamic rheology. The ratio between each phase may be determined from the area of  $\tan\delta$  peak. Kim established a relation between the nature of the metallic cation nature (size and charge) and both the matrix  $T_g$  and Cluster  $T_g$ <sup>[19]</sup>. From specific mixing conditions, a third peak is observed<sup>[18]</sup>. Extensive studies based on this model have revealed that the formation of multiplets and clusters in ionomers are linked to the ionic species<sup>[20]</sup>, the nature of the polymer and their concentration, types and sizes. Eisenberg mentions that the most important ionic parameter that affects multiplets formation is the strength of the electrostatic interactions between the ion pairs. This is determined by the sizes of the ions and the partial covalent character of the ionic bond<sup>[11, 13]</sup>. Capek<sup>[21]</sup> reviewed all the parameter affecting the morphologies and consequently the properties. This model is different from the previous one by the absence of electrostatic forces between multiplets within a cluster. Because the multiplets effect as multifunctional cross-links, a rubbery plateau, called ionic-plateau, is observed at temperatures between the polymer matrix and a temperature higher than the cluster phase. Actually, the multiplets remain stable over this temperature range. When the requirements for phase-separated behavior are fulfilled<sup>[13]</sup>, ionomers may be melt-processable despite the fact that multiplets still exist at elevated temperatures over  $T_g$ <sup>[13, 22, 23]</sup> and ionic

species migrate from one multiple to another by ion hopping or act as a filler [13, 24]. The temperature at which melt flow begins, can be controlled to a large extent through the choice of the neutralizing cation. Divalent cations such as  $\text{Ca}^{2+}$  or  $\text{Zn}^{2+}$  can have extreme impacts on the processability. Calcium maintains generally the rubbery plateau [25] to high temperature and Zinc is often observed to begin the material to flow at lower temperatures compared to monovalent cations<sup>[9]</sup>. In polystyrene matrix, the counterion type modifies the deformation modes in strained thin films of rigid ionomers [25].

In the present study, thermoreversible networks by ionomers formation are expected from calcium carbonate addition. This additive is a good candidate to strongly interact with carboxylic acid functions from copolymers copolymerized, for example, with acrylic acid or methacrylic acid.  $\text{CaCO}_3$  is frequently used because it is efficient, abundant and cheap. It is extensively employed in the manufacture of rubbers, plastics, and so forth [26] as a filler to improve hardness and higher material modulus<sup>[27]</sup>. Since it may agglomerate and is hydrophilic, chemical modification of calcium carbonate is a solution to improve its compatibility or dispersion. Organic acids, such as succinic acid, acrylic acid or methacrylic acid, are the classical and main modifiers [28, 29]. The improvement of the mechanical or rheological properties is mostly attributed to a network formation when the  $\text{CaCO}_3$  fillers interact with the polymer matrix [27, 30] but very few works really characterize the structures and microstructures of the filled materials.

Poly(*n*-butyl methacrylate) (PBMA) is widely chosen, for biomedical applications [31, 32]. Methacrylate monomers containing *n*-butyl groups are more bio-adaptive and have fine adaptability to living animals. Since the PBMA has a low glass transition temperature at 20°C and correspondingly poor mechanical properties around room temperature, it is often used after its chemical modification or mixed with other additives or fillers. Inorganic additives, such as carbon black [33], montmorillonite [34, 35], calcium carbonate [6], impressively increase its mechanical moduli. Butyl methacrylate (BMA) is here chosen as a co-monomer with methacrylic acid since BMA is not able to interact with the acid functions or calcium carbonate with its possible derivatives.

Literature analysis clearly shows that soluble metal salts are an interesting solution to improve polymer materials properties over the glass transition temperature by the

appearance of an ionic plateau in the molten state if material's structuration in cluster occurs. These materials are commonly synthesized by the introduction of carboxylate or sulfonate functions. At relatively low metal salt concentrations, ionic moieties are organized in multiplets behaving like fillers, which only reinforce mechanical properties below the glass transition. To obtain such reinforcement, metal or inorganic fillers are preferentially chosen and mixed in the molten state with the polymer matrix.

In this work, calcium carbonate is used to behave like dispersed fillers and ionic sites by a partial dissociation/reaction at  $\text{CaCO}_3$  surface. Ionic moieties from  $\text{CaCO}_3$  are also expected to disperse the  $\text{CaCO}_3$  grapes leading to a nanocomposite. These nanofillers, in association with the less dispersed grapes, reinforce the polymer matrix below  $T_g$  and to create a plateau modulus above  $T_g$  which doesn't exist for the original P(BMA-co-MA) matrix. Ionic calcium formation from  $\text{CaCO}_3$  was never envisaged to form ionomers and its reaction was never experimentally proved to produce cationic calcium. The balance between a filler/nanofiller effect and an ionic structuration agent is discussed here.

## **B-2. EXPERIMENTAL**

### **B-2.1. Materials**

Precipitated calcium carbonate (CCP SOCAL® 31) was supplied by Solvay (Brussels, Belgium).

The  $\text{CaCO}_3$  powder size distribution was obtained with a Mastersizer 2000 particle size analyzer from Malvern (dry way with a high air flow, measures were repeated twice on the same sample). The particle sizes were measured from 0.01 to 10000  $\mu\text{m}$  diameter. A main size distribution was observed between 2 and 12  $\mu\text{m}$  and minor size distributions were observed (0.2-2.0, 35-100 and 150-500  $\mu\text{m}$ ). These four size distributions clearly show the heterogeneity of the starting calcium carbonate with different agglomerates sizes.

Butyl methacrylate (BMA), Methacrylic acid (MA), 2-azobis(2-methyl-propionitrile) (AIBN), tetrahydrofuran (THF) were purchased from SIGMA-ALDRICH (France). BMA was purified by distillation under reduced pressure and stored at  $-23^\circ\text{C}$  before use. All the other reagents were used as received without further purifications.

### CO<sub>2</sub> formation and quantification

The reaction between the methacrylic acid and the CaCO<sub>3</sub> was conducted for another five minutes and the gas synthesized as product, carried by an argon flow. This gas was caught and analyzed by GC-MS. One peak with a mass peak at 44 g.mol<sup>-1</sup>, proved the CO<sub>2</sub> formation and then calcium carboxylate salts formation. A quantitative experience to quantify the CO<sub>2</sub> elimination by formation of carboxylate salts from acid/carbonate reaction was made. 60.2 mmol of CaCO<sub>3</sub> and 254 mmol of BMA were mixed in a three neck flask heated at 70 °C with a regulated oil bath. 70°C is the chosen temperature to synthesize the material (3.b) as well as the BMA is used to model the synthesis conditions. A rubbery tube was connected from one neck to a second two neck flask filled with a non-saturated Ba(OH)<sub>2</sub> aqueous solution. A second gas absorption tube was connected to a third two neck flask also filled with the same non-saturated Ba(OH)<sub>2</sub> solution to control if all the CO<sub>2</sub> really react in the first solution. All these three glasses were vigorously mixed by magnetic agitation to disperse correctly the gas bubbles in the Ba(OH)<sub>2</sub> solutions. An argon flow was induced continuously for 5 minutes to purge the air in all the flasks. 42.0 mmol of methacrylic acid was injected in the flask with a syringe with stable and low argon flow. This CO<sub>2</sub> reacted as expected with Ba(OH)<sub>2</sub> to produce a precipitate of barium carbonate BaCO<sub>3</sub>. The suspension was filtered off, dried and weight giving 1.06 mmol that represents 1.76 mol% of the total CaCO<sub>3</sub>. CO<sub>2</sub> formation is either accompanied by ionic Ca<sup>2+</sup> or CaO formation but this CaO formation is not plausible at this temperature<sup>[36, 37]</sup>. In consequence, Ca<sup>2+</sup> formation is really envisaged despite any structural analysis of PBMA based CaCO<sub>3</sub> material doesn't complete this result yet.

### Samples preparation

Two ratios, CaCO<sub>3</sub>/MA mol/mol and MA/BMA mol/mol, were defined to study the final materials properties. Subsequent samples were denominated PBMA(x, y), where x represents CaCO<sub>3</sub>/MA mol/mol, and y represents MA/BMA mol/mol. The initiator AIBN concentration was fixed at 0.5 mol % of the total vinyl monomers. Their compositions are listed in table 1.

*Table 1. Nomenclature and composition of the samples*

PBMA(CaCO <sub>3</sub> /MA, MA/BMA)	BMA mol%	BMA wt%	MAA mol%	MAA wt%	CaCO <sub>3</sub> mol%	CaCO <sub>3</sub> wt%
PBMA(1.43, 0.25)	63.5%	72.4%	15.0%	10.4%	21.5%	17.3%
PBMA(1.43, 0.16)	71.3%	78.9%	11.8%	7.9%	16.9%	13.2%
PBMA(2.5, 0.16)	63.4%	71.9%	10.5%	7.2%	26.2%	20.9%
PBMA(1, 0.16)	75.2%	82.2%	12.4%	8.2%	12.4%	9.6%
PBMA(1.43, 0.06)	88.1%	91.8%	4.9%	3.1%	7.0%	5.2%
PBMA(0, 0.16)	85.8%	90.9%	14.2%	9.1%	0.0%	0.0%

### Preparation in tubes

Tube samples were first prepared to test the solubility in THF of the final material for different compositions. BMA, MA, AIBN and CaCO<sub>3</sub> were introduced in a closed three neck flask with an ULTRA TURRAX mixer (ULTRA TURRAX T25, from IKA) under argon flow (around 100 ml/minute). The mixture was mixed at 11000 rpm for four minutes at room temperature. 5 ml of the blended mixture was poured into a glass tube heated at 70°C in a silicone oil bath for seven hours. After cooling down, 1g of the filled copolymer was mixed with 10 ml of THF for 48hrs to test the solubility. By this polymerization mode, an atactic copolymer should be obtained since the reactivity ratio BMA/MA is given at 2.01<sup>[38]</sup>.

### Plates preparation

Plates were prepared to obtain regular shape specimens for thermal analyses, TEM photographs and mechanical spectroscopy. From the same mixture prepared at room temperature for tube polymerization, the reactive system was transferred in a 250 ml glass reactor with an anchor for mechanical stirring, at 150 rpm. The reactor was placed in a silicon oil bath for pre-polymerization at 70°C for 40-60 min until the blend becomes viscous enough, based on a chosen torque value corresponding to a sufficient viscosity level. The reactive system was finally quickly transferred into a closed mold (2x100x100 mm) and pressed at 200 bars and 70°C for 7 hours. Less

than 1% unpolymerized monomer was residued and eliminated by oven with vacuum (2 mbar) at 150°C for 6 hours.

## **B-2.2 Characterizations**

### **Rheology**

Considering the wide range of temperatures investigated and to prevent from sample slipping and/or transducer overload, rheological measurements have been divided into solid state rheology for the lowest temperatures (below 100 °C) and molten state rheology above this limit.

Solid state rheology was carried out with a strain controlled rheometer ARES from Rheometrics, in the linear viscoelasticity domain of the materials. Dynamic shear was applied using rectangular torsion tool. The ramp temperature was 3°C.min<sup>-1</sup> between -100°C and 100°C. The frequency was fixed at 1 rad.s<sup>-1</sup> and the strain varies from 0.1 % at -100°C to 2% around 100°C. The rectangular bars (length 50 mm, width 4 mm, thickness 2 mm) were prepared using the protocol detailed in previous paragraph.

Molten state rheology has been performed changing the geometry and then using a parallel plate geometry with 25 mm diameter. All experiments were carried out in the same conditions as for the solid state measurements excepted for the strain which was fixed at 5% at 100°C to remain in the transducer sensitivity range.

Both kind of test have been performed taking care to the sample and tools dilation during the temperature ramp. Specific procedure was then activated on the rheometer to ensure the stability of the normal force (~ 20 g) applied on the sample.

### **Thermal analysis**

Thermal transitions were determined by Differential scanning calorimetry (DSC) with a TA Q10 instrument, by heating and cooling ramps from -60 to 250°C at 10°C/min under a nitrogen flow for two circles. The transitions were obtained by the second heating ramp.

### **Thermodegradation analyses**

Thermogravimetric analyses were performed with a Mettler Toledo TGA, STAR<sup>e</sup> system from 30°C to 500°C with ramps at 10°C/min. The gas products extracted during the ramp were analyzed by coupled IR spectrometer.

### **Microscopy analyses**

TEM (Transmission Electron Microscopy) photographs were obtained with a Hitachi H-800-3 electron microscope coupled with a numeric camera AMT XR40 Hamamatsu. Ultrathin sections (ca. 30nm thick) were cut from the samples at room temperature and collected on copper grids.

Average sizes, were obtained from ImageJ software. The average sizes were calculated from particle agglomerates in the picture. Area fraction is the percentage of pixels in the image that have been highlighted.

### **X-ray diffraction**

X-ray Scattering were done with a Bruker D8 Advance. The detector was a PSD (Position Sensitive Detector) VÅNTEC-1 "SUPER SPEED", and the focusing diameter fixed at 500mm. The wavelength was 1.54 Å and the X-Ray ceramic tube was supplied with 33 kV and 45 mA.

## **B-3. RESULTS AND DISCUSSION**

### **B-3.1 Calcium carbonate reactivity and decomposition**

To obtain ionomers and their characteristic behaviors, the calcium carbonate must react to form cationic Ca<sup>2+</sup>. In all cases, this filler must produce carbon dioxide (CO<sub>2</sub>) if Ca<sup>2+</sup> is produced in-situ. Numerous studies discuss thermal CaCO<sub>3</sub> reactivity from different models<sup>[36, 37, 39]</sup> taking into account that such filler is composed by particules and agglomerates. Studied by TGA, all the experiments are analyzed by the carbon dioxide elimination which occurs at higher temperatures than those of the present materials preparation. The thermogravimetric analysis of CCP SOCAL® 31 calcium carbonate in P(BMA-co-MA) matrix, confirms this elimination. CaCO<sub>3</sub> decomposition was followed by CO<sub>2</sub> IR absorbance peak at 2350 cm<sup>-1</sup> (Figure 1). CaCO<sub>3</sub> starts to decompose from 220°C till 570°C. This thermo-degradation shows clearly that the

material is stable until 220°C. This It confirms also that at the reaction temperature, 70°C, there is no reaction between the filler and other components.

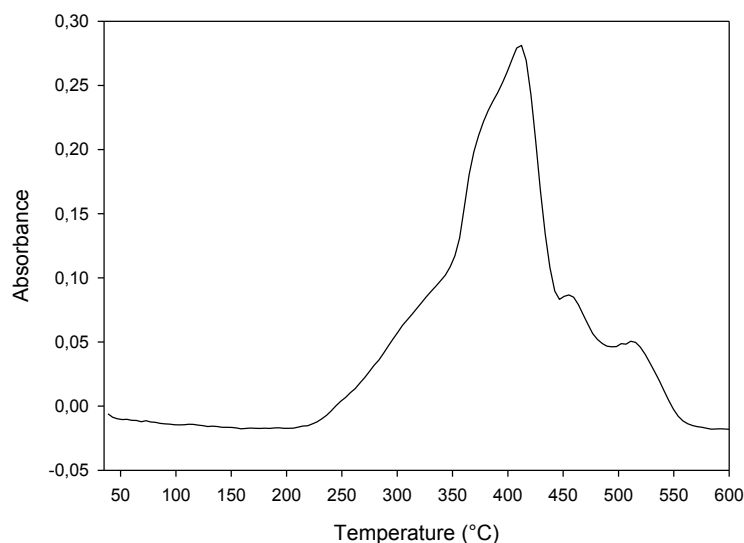


Figure 1: *Thermo-degradation of P(BMA-co-MA) (1.00, 0.16) followed by CO<sub>2</sub> IR absorbance peak at 2350 cm<sup>-1</sup>.*

Thermal CaCO<sub>3</sub> decomposition may also happen if this filler is in contact with carboxylic acids such as tartaric, succinic and citric acid<sup>[36, 37, 40]</sup>. Faster weight losses start at much lower temperatures as compared to neat CaCO<sub>3</sub>, in particular above 220°C where 2.2-2.7 % of weight loss are observed compare to 0.23% when the filler is not treated. The reaction products are not the same. It is well defined that neat CaCO<sub>3</sub> produces CaO calcium oxide at high temperature and calcium carboxylates are formed as a result of interactions between CaCO<sub>3</sub> and acids. The formation of carboxylates have been reported earlier<sup>[36, 37]</sup> and confirmed by the X-ray diffraction technique. Therefore, carboxylates salts, with eventually hydrated forms, as reported, are possibly constituted during the synthesis conditions of the present work.

To determine if such carboxylates salts are formed at 70°C, with small percentages as presented by Kasselouri<sup>[36, 37]</sup>, an experience was created to determine if Ca<sup>2+</sup> formation is plausible from the quantification of CO<sub>2</sub> formation by a reaction between CaCO<sub>3</sub> and carboxylic functions leading to Ca<sup>2+</sup>(RCOO<sup>-</sup>)<sub>2</sub>. This quantitative experiment is presented in detail in the experimental part and showed that only 1.8 mol% of CaCO<sub>3</sub> is decomposed to form ionic calcium. To show that an “ionic” peak is observed by X-ray, diffraction should prove the presence of the ionic calcium in the system

### Cluster structuration from CaCO<sub>3</sub> decomposition

Cluster formation, as described by Eisenberg consequently to CaCO<sub>3</sub> sufficient decomposition in Ca<sup>2+</sup>, can be observed using X-ray diffraction technique. The chosen technique allows screening 2θ angles from 1.5 to 30° (Figure 2).

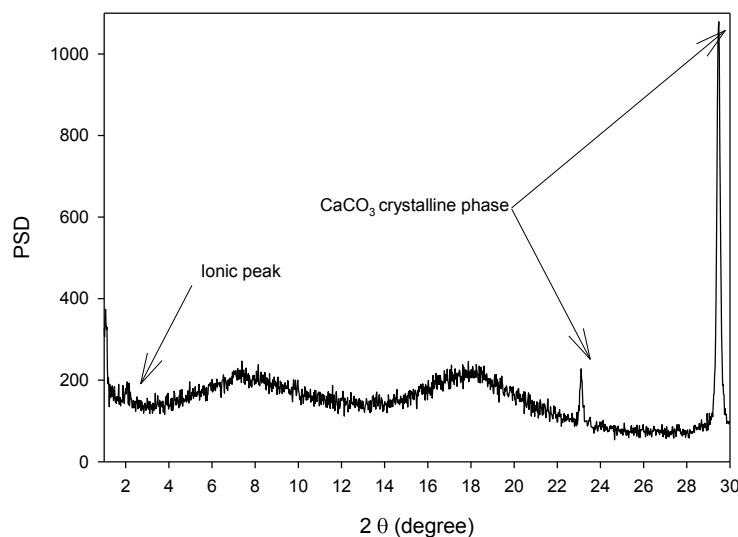


Figure 2: *X-ray diffraction of P(BMA-co-MA) (1.43,0.25) at  $\lambda=1.54$  Å with X-Ray ceramic tube supplied with 33 kV and 45 mA. It is reminded that each sample is named with two indexes successively x and y where x represents CaCO<sub>3</sub>/MA mol/mol, and y represents MA/BMA mol/mol.*

#### Crystalline peaks

This spectrum (Figure 2) showed that the crystalline CaCO<sub>3</sub> is well observed at 23.11 and 29.46° corresponding to a calcite structure<sup>[41]</sup>. These peaks are expected since only a part of the starting CaCO<sub>3</sub> reacts to produce CO<sub>2</sub>. Since there is micron sized CaCO<sub>3</sub> in the system, the scattering could be attributed to these particles and/or to micro sized CaCO<sub>3</sub> with polymer shell.

#### Ionic peak

The “ionic” peak, as described by Eisenberg and Hird<sup>[11, 12]</sup>, is only observed for certain samples (Figure 3) at 2θ = 1.884. These samples are those insoluble in THF: They globally contain the highest fraction in CaCO<sub>3</sub> excepted the (2.5, 0.16) sample which doesn't show an ionic peak and is not soluble in the THF. This last sample is the analyzed sample which has the highest fraction in CaCO<sub>3</sub>. For the (1.43, 0.16)

and (1.43, 0.25) samples, the ionic species formation is sufficiently present to be observed by X-Ray and to have effects on the material properties that are presented further. It was verified that the peaks from SAXS are not noise; these experiments were repeated with other systems. In all cases, the ionic peak at 1.884 was present (figure 3).

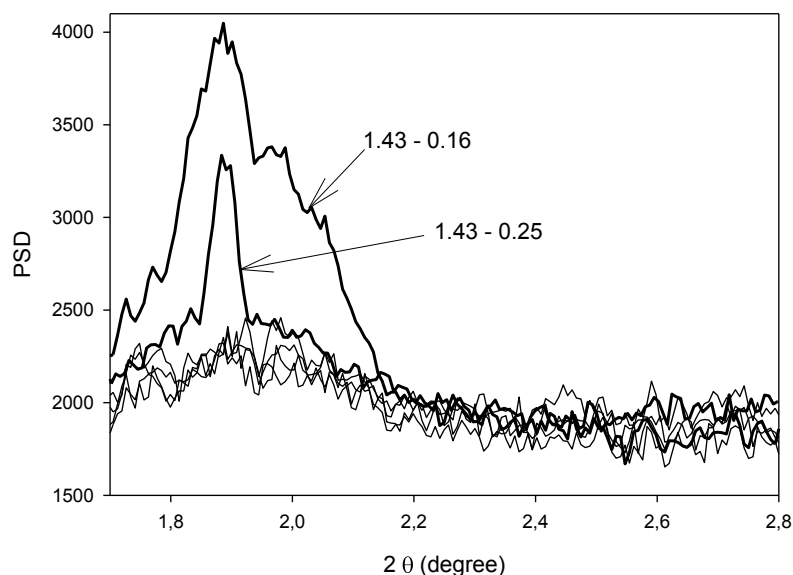


Figure 3: X-ray diffraction of *P(BMA-co-MA)* at  $\lambda=1.54 \text{ \AA}$  with X-Ray ceramic tube supplied with 33 kV and 45 mA. Analyzed samples: (1, 0.16), (1.43, 0.06), (1.43, 0.11), (1.43, 0.16), (1.43, 0.25), (2.5, 0.16).

In materials like *P(S-co-MANa)* ionomers<sup>[11, 42, 43]</sup>, the multiplets size are 6-8 Å and the isolated multiplets, along with their reduced mobility layer, are expected to be too small to manifest their own  $T_g$ . Multiplet is expected to essentially behave as a cross-link. This behavior is indeed observed at low ion contents with most of monomers. When the number of multiplets is high enough with increasing the ion content, overlapping regions of restricted mobility composed by multiplets and near surrounding, become large enough to exceed the threshold size for independent phase behavior called cluster (50-100 Å), they exhibit a second  $T_g$ <sup>[8]</sup>. This expected observation will be analyzed by dynamic rheology and thermal analyses, further in this study.

If multiplets exist, the distance between them has to be determined from the “ionic peak” determined by X diffraction. The Bragg spacing of intermediate ion contents

(5-10 mol %) is around 23 Å with Bragg spacing comprised between 300 and 20 Å<sup>[11]</sup>. In general, the Bragg distance has to be a function of the concentration (c) of the ionic sites, following  $c^{-1/3}$  scaling law. This model is not applied in ionomers since the Bragg distance is attributed to the intermultiplet distance, which is indirectly in relation with their concentration. The intermultiplet spacing is believed to be related to the loopback distance, which is a function of the nature of the polymer chain and the ion pair rather than simply ion concentration<sup>[8]</sup>. Since the CaCO<sub>3</sub> is very partially decomposed in ionic Ca<sup>2+</sup> ( $\xi$  3.1.), the exact ionic moieties concentration remains unknown in these systems and the exact structures of these materials can be only described qualitatively. In this study,  $2\theta = 1.884$ , the Bragg distance d can be calculated from the classical Bragg law  $n\lambda = 2d \sin\theta$ . It corresponds here to  $d = 46.8$  Å and is typically in the range expected by the literature.

This also shows that at least a part of Ca<sup>2+</sup> was formed and separated from CaCO<sub>3</sub> particles leading, in association carboxylic acid to clusters. These clusters are big enough in the material to be observed by RX but complementary analysis, such as thermal or rheological, must complete this result to conclude if a physical network exists to form globally a crosslinked material. A cluster can be considered as local volume of the material but their concentration must high enough to percolate and to finally generate a network. The thermal analysis is generally used to observe a second glass transition temperature attributed to the cluster phase independently of its physical effect: filler effect or network effect. The thermal analysis is also a good technique to show the effect of the interactions between the polymer chains of the matrix, due to presence of the ionic calcium in the system.

### **B-3.2 Thermal properties**

Since the ionic peak was observed by X-ray spectrometry for certain compositions as expected for ionomers, two glass transitions are consequently expected<sup>[8, 11]</sup>. These glass transitions have been studied by two heating and one cooling ramps at 20°C/min. The obtained results are depicted in Table 2.

Table 1: *Thermal analyses by DSC of P(BMA-co-MA) for different formulations determined by a first ramp at 10 K.min<sup>-1</sup>.*

Sample name	T <sub>g</sub> (°C)
PBMA(1.43, 0.06)	55.8
PBMA(1, 0.16)	76.9
PBMA(0, 0.16)	46.6
PBMA(1.43, 0.16)	76.8
PBMA(2.5, 0.16)	77.8
PBMA(1.43, 0.25)	90.2

Without CaCO<sub>3</sub>, one sample with 16 MA units for 100 BMA units was analyzed and presents only and logically one glass transition at 46°C. The same copolymer with in more CaCO<sub>3</sub>/MA = 1 (mol/mol) has its glass transition temperature at 77°C. Added CaCO<sub>3</sub> increases T<sub>g</sub> of 30°C. Then, the CaCO<sub>3</sub> content never influences the glass transition if CaCO<sub>3</sub>/MA ratio is superior to 1 (mol/mol). This T<sub>g</sub> increase is attributed to less motion of the copolymer chains by the presence of ionic moieties that physically link in the matrix, independently of the existence of multiplets or clusters. The CaCO<sub>3</sub> content when CaCO<sub>3</sub>/MA > 1 (mol/mol) doesn't influence the chains motion while the initial CaCO<sub>3</sub> concentration modifies also the ionic calcium concentration and then, possibly both the copolymer chains motion and the T<sub>g</sub>.

As it is well observed on Figure 4, the glass transition temperature is higher than the one predicted by simple additivity law or the Fox law. The theoretical T<sub>g</sub> calculated by the Fox law is represented on the Figure 4 by the black curve. Both the glass transition temperatures of polybutylmethacrylate and polymethacrylic acid homopolymers were reported at respectively 20 and 185°C (polymer Handbook source). The higher observed T<sub>g</sub>s, compared to the expected T<sub>g</sub> by Fox law, may be attributed to weaker mobilities of the copolymer chains due to interchain interactions through ionic moieties reducing their mobility as already discussed.

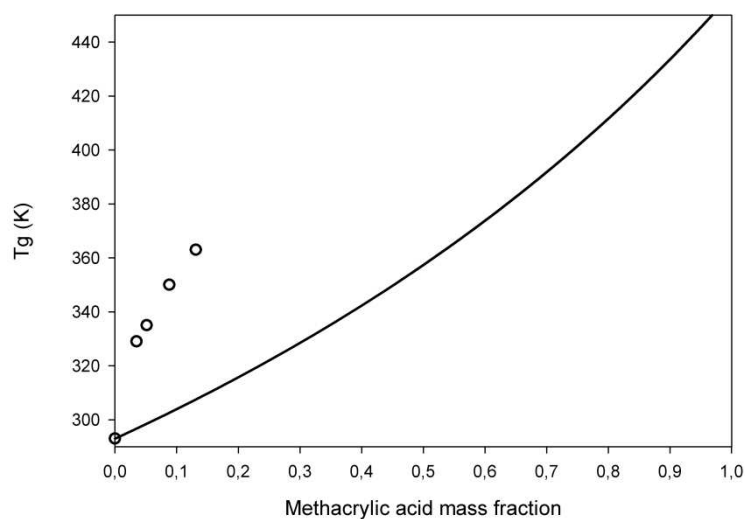


Figure 4: *First glass transition (K) vs methacrylic acid mass fraction in synthesized P(BMA-co-MA) copolymers in presence of CaCO<sub>3</sub>. Black curve fits T<sub>g</sub> respecting Fox law. ○: Experimental points.*

The Figure 5 shows the T<sub>g</sub> dependence, determined by tanδ maximum, for different MA contents in the copolymer chain with CaCO<sub>3</sub>/MA = 1.43 (mol/mol). This T<sub>g</sub>, as observed by DSC, is shifted to the higher temperatures with the MA content increases since the PMA T<sub>g</sub> is higher than the PBMA T<sub>g</sub>.

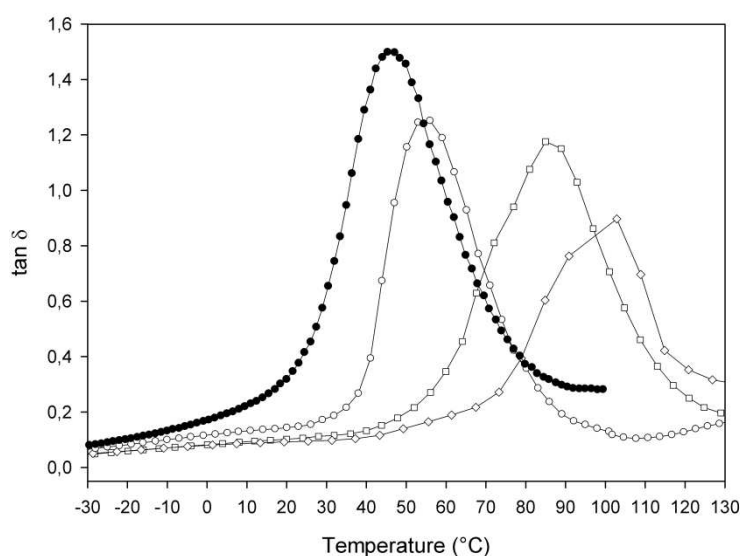


Figure 5: *Tan δ by rectangular torsion and temperature ramps at 3°K.min<sup>-1</sup> and 1 rad/s with CaCO<sub>3</sub>/MA = 1.43 (mol/mol) at different MA contents in the b(MA-co-BMA) : ○ MA/BMA = 6/100 (mol/mol) □ MA/BMA = 16/100 (mol/mol) ◇ MA/BMA = 25/100 (mol/mol) ● Without CaCO<sub>3</sub>*

The thermal analysis by DSC doesn't produce reproducible results above 200°C, since the materials become thermally unstable. The figure 6 clearly shows this instability. At 200°C, the storage modulus increases very slowly with time whereas this effect is effective and faster at 240°C. Indeed, the copolymer chains are thermally degraded and it was proved that CaCO<sub>3</sub> reacts faster with the free carboxylic acid functions when the temperature increases above 200°C. For samples where the ionic peak are obtained in X-ray analysis, the DSC exhibit a second thermal transition above T<sub>g</sub>, around 220-240°C. A difference exists when this second transition is measured by two consecutive heating ramps, with a controlled cooling ramp. A 30 °C shift can be obtained, depending of the used formulation. This increase is not aberrant since, during the first heating, the high temperatures initiates again the reaction between the CaCO<sub>3</sub> and the methacrylic function. This generates more ionic moieties that form more multiplets and clusters having their own T<sub>g</sub>'s.

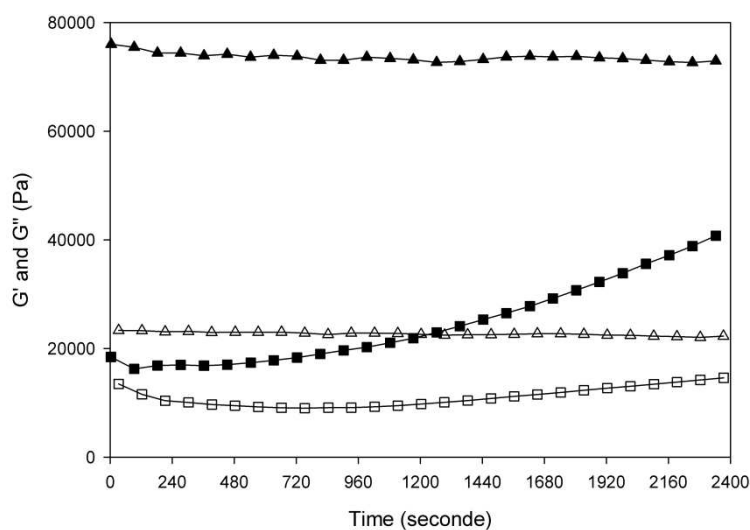


Figure 6: *Thermal stability for P(BMA-co-MA) with CaCO<sub>3</sub>/MA = 1.43 mol/mol and MA/BMA = 0.16 mol/mol at 200°C (triangle) and 240°C (square) observed by G' (black) and G'' (white) (Pa) vs time.  $f = 1 \text{ rad}\cdot\text{sec}^{-1}$  Temperature ramps at  $3^\circ\text{K}\cdot\text{min}^{-1}$ .*

### B-3.3 Calcium Carbonate dispersion

Since only low amounts of calcium carbonate are able to produce separated calcium carboxylate salts and clusters, the major remaining part is dispersed in the matrix. The CaCO<sub>3</sub> dispersion level is an important criterion that influences the mechanical and rheological properties. Since an ultra-turrax mixed all the reagents together, its

efficiency was observed by TEM photographs (Figure 7).  $\text{CaCO}_3$  grapes and agglomerates were destroyed as it is shown by comparison with the size distribution determined by Laser diffraction described in the experimental part. The concentration of these small agglomerates in the polymer matrix is influenced by the  $\text{CaCO}_3$  volume fraction in the formulation. The agglomerate size remains constant whatever the  $\text{CaCO}_3$  concentration (Figure 7). All the different formulations present  $\text{CaCO}_3$  agglomerates like grapes, homogeneously separated, with an average diameter near one micron or less. These grapes are composed by round grains linked together by physical or electrostatic interactions since small spaces, separating them, are perfectly visible (Figure 8). Isolated grains are also observed with diameters around 50 nm.

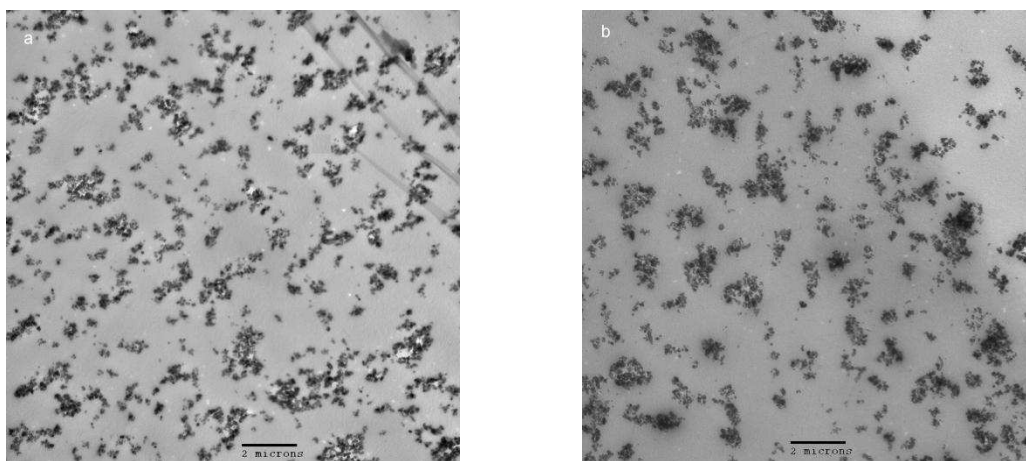


Figure 7: TEM photographs of  $\text{CaCO}_3$  dispersion in  $P(\text{BMA-co-MA})$  a: (2.50,0.16) and b: (1.00,0.16) with  $\times 7000$  growing,  $HV = 200 \text{ kV}$

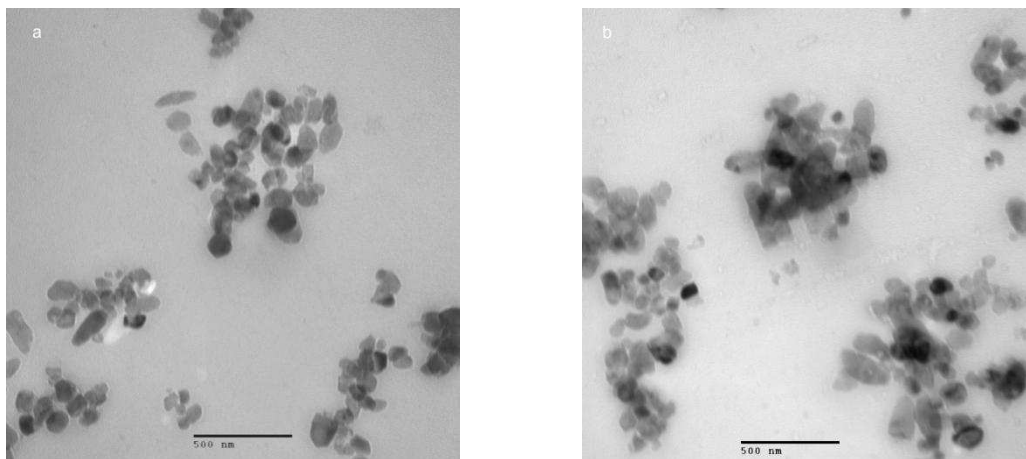


Figure 8: TEM photographs of  $\text{CaCO}_3$  dispersion in  $P(\text{BMA-co-MA})$  a: (2.50,0.16) and b: (1.00,0.16) with  $\times 50000$  growing,  $HV = 200 \text{ Kv}$

These TEM photographs demonstrate the mixing efficiency step since all the  $\text{CaCO}_3$  fillers are homogeneously dispersed in the matrix. By the highest magnification (Figure 8),  $\text{CaCO}_3$  agglomerates are therefore observed in round grains. In more, these grains are groups with spaces between them corresponding to the dispersion. These small spaces may be attributed to the existence of repulsive forces between them but at the same time, the grains remain linked because they are separated by small spaces avoiding a homogeneous dispersion of all the grains in the matrix (Figure 8a). They remain grouped in grapes. To explain such morphologies, repulsive forces between the grains are not enough. It is considered that it exists ionic polymer chains that interact at the surface of grains to separate them and acting as spacers without separating definitely the grains. This assumption means that it exists ionic sites at the grain surface to interact with the ionic polymer chains.

#### B-3.4 Solubility of PBMA-co-PMA/ $\text{CaCO}_3$ systems

Samples were synthesized in tubes to determine if  $P(\text{BMA-co-MA})$  copolymers with added  $\text{CaCO}_3$  are physically crosslinked. If a sample is swollen or insoluble, the network will be considered as strong and difficult or impossible to be reversibly destroyed at the used temperatures.

Without  $\text{CaCO}_3$ , all the copolymers are soluble in THF whatever were the molar and MA/BMA ratios between 0.10 and 0.35. The results of these solubility tests are grouped on the Figure 9, established with both the molar ratios controlling the  $P(\text{BMA-co-MA})$  copolymers structures and the filler rate that are respectively MA/BMA and  $\text{CaCO}_3/\text{MA}$  (Figure 9). The results are presented considering either the total solubility observed by a homogeneous clear solution or insoluble when at least a swelling was obtained.

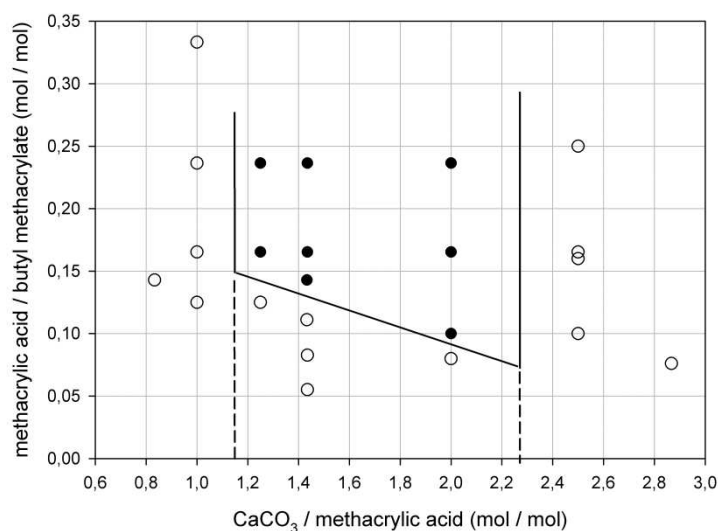


Figure 9: Solubility tests of *P(BMA-co-MA)* filled with  $\text{CaCO}_3$  in THF for 48 hours, ● insoluble or swollen sample, ○ soluble sample

The figure 9 shows an atypical behavior of the material in relation with both the expressed ratios, MA/BMA and  $\text{CaCO}_3/\text{MA}$ . With less than 10 mol% of MA in the copolymer chain, whatever the  $\text{CaCO}_3$  quantity, the materials are all soluble. Above 10 mol% of MA in the copolymer chain, the materials are soluble if  $\text{CaCO}_3$  is in default compared to the acid functions from MA. When  $\text{CaCO}_3$  is in excess ( $\text{CaCO}_3/\text{MA} > 1.0$  (mol/mol)), the materials become insoluble. This limit is, in theory, acceptable since  $\text{CaCO}_3$ , through its ionic form, is principally thought to interact with two acid functions and if an ionomer system is formed, two phases are expected, as described by Eisenberg<sup>[11,12]</sup>. In this study, only an unknown part of  $\text{CaCO}_3$  has to be efficient to form multiplets and clusters by its reaction with the acid. The resulting ionic moieties allow the multiplet formations and themselves the clusters. Then, the concentration of these multiplets must reach a limit to percolate and to form a physical network with strong interactions with the insolubility as result. This percolated system is dispersed in the ionic thermoplastic matrix filled with the  $\text{CaCO}_3$  grains and grapes.

More surprisingly, the materials become soluble again if the  $\text{CaCO}_3$  is more than twice the mole number of acid function ( $\text{CaCO}_3/\text{MA} > 2.0$  (mol/mol)). Consequently, it is not necessarily to increase the  $\text{CaCO}_3/\text{MA}$  ratio to continuously increase the network density that should keep the material finally insoluble. Very probably, for  $\text{CaCO}_3/\text{MA} > 2.0$  (mol/mol), to increase more the  $\text{CaCO}_3$  content finally destroys the

percolated and physical network because the  $\text{CaCO}_3$  volume fraction, that acts as a filler, is high enough to be in the way of the percolated clusters.

### **B-3.5 Structural analyses**

Dynamic mechanical analyses characterize the glass transition and the material behavior above  $T_g$  when clusters are formed in ionomers. From the model developed by Eisenberg, no intermediate regions exist between ion rich cluster region and regions with low multiplets contents. This model also justifies the glass temperature increase with the ion content. As it increases, the average distance between multiplets decreases and the size of the multiplets increases acting as cross-links as well as the size of the intercluster region decreases. Both these changes cause a reduction in mobility and the glass transition temperature is expected to increase. It is often observed. Below the glass transition temperature, the multiplets and clusters act as fillers.

#### **Filler content effect above the glass transition**

For all the used formulations with a constant MA content ( $\text{MA/BMA} = 16/100$  (mol/mol)), (Figure 10). the  $T_g$ , itself determined by the thermal analysis, is not affected by the  $\text{CaCO}_3$  content since the smallest used  $\text{CaCO}_3$  quantity shifts the  $T_g$ ,  $30^\circ\text{C}$  upper, compared to the sample without  $\text{CaCO}_3$ . This shift traduces a decrease of the mobility chains. A fraction of the  $\text{CaCO}_3$  reacted to produce ionic sites and consequently some interactions between the copolymer chains. The smallest used  $\text{CaCO}_3$  quantity ( $\text{CaCO}_3/\text{MA} > 1$  (mol/mol)) was sufficient to generate a shift at the maximum (Figure 10). Any  $\text{CaCO}_3/\text{MA}$  (mol/mol) inferior to 1 was tested. Then, the domain where this ratio increases the  $T_g$  from  $47$  to  $77^\circ\text{C}$ , was not established for the chosen MA/BMA ratio ( $16/100$  (mol/mol)).

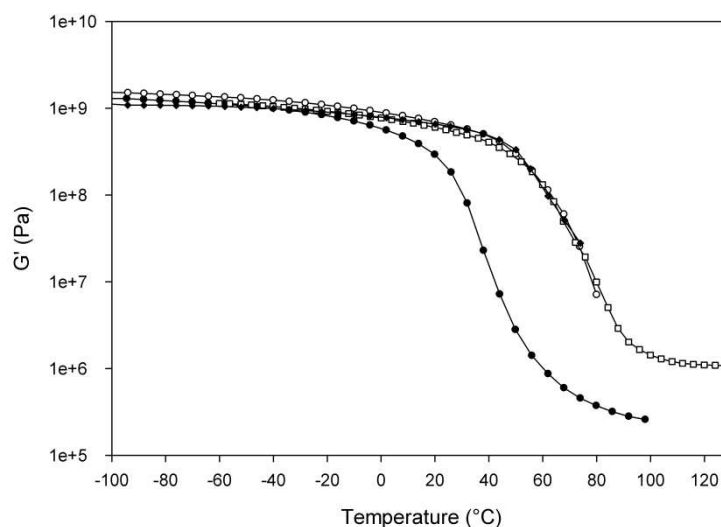


Figure 10:  $G'$  storage modulus (Pa) by rectangular torsion and temperature ramps at  $3^{\circ}\text{K}\cdot\text{min}^{-1}$  and  $1\text{ rad/s}$  with MA/BMA = 16/100 (mol/mol) at different  $\text{CaCO}_3$  contents ● : without  $\text{CaCO}_3$  ○  $\text{CaCO}_3/\text{MA} = 1$  (mol/mol) □  $\text{CaCO}_3/\text{MA} = 1.43$  (mol/mol) ◆  $\text{CaCO}_3/\text{MA} = 2.50$  (mol/mol)

As shown by the Figure 10, the glass plateau modulus is not significantly affected by the amount of the  $\text{CaCO}_3$ . On the contrary, above  $T_g$ , a clear difference between the filled and unfilled systems is observed whatever the state of  $\text{CaCO}_3$  reaction. This impact will be discussed further by dynamic analysis in the molten state.

It was demonstrated that  $\text{CaCO}_3$  reacts more easily with carboxylic acid functions above  $200^{\circ}\text{C}$  (Figure 6). From this reaction, the viscoelastic properties are not reversible after each first heating ramp and their return to lower temperatures don't allow to exactly retrieve the initial material properties. This is well observed by the storage modulus (Figure 11) which increases systematically above  $220^{\circ}\text{C}$  when  $\text{CaCO}_3$  is present in the sample. Only the sample without  $\text{CaCO}_3$  doesn't present this modulus increase above  $200/220^{\circ}\text{C}$ . In more, bubbles are well observed in samples filled with  $\text{CaCO}_3$  when they are removed after the tests, which logically corresponds to  $\text{CO}_2$  as product, formed during the  $\text{CaCO}_3$  reaction with the carboxylic functions.

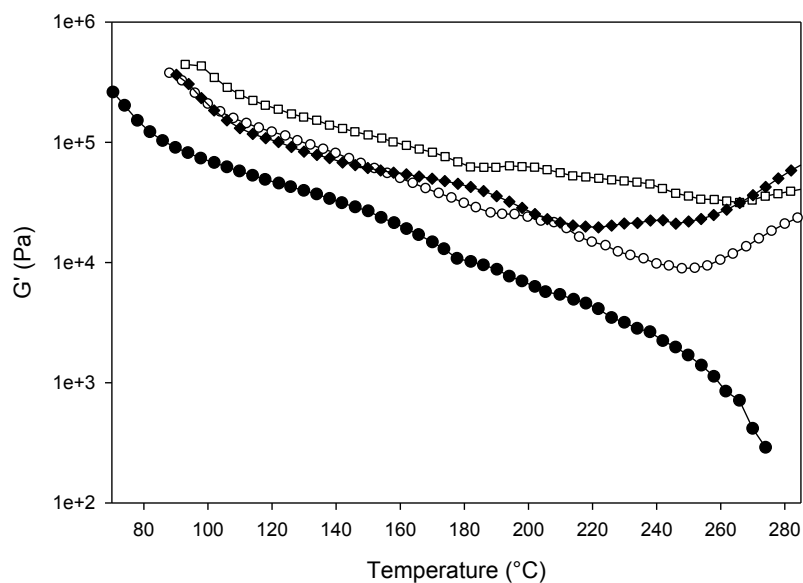


Figure 11:  $G'$  storage modulus (Pa) by parallel plates and temperature ramps at  $3^{\circ}\text{K}\cdot\text{min}^{-1}$  and  $1\text{ rad/s}$  with MA/BMA = 16/100 (mol/mol) ● : without  $\text{CaCO}_3$  ○:  $\text{CaCO}_3/\text{MA} = 1$  (mol/mol) □  $\text{CaCO}_3/\text{MA} = 1.43$  (mol/mol) ◆  $\text{CaCO}_3/\text{MA} = 2.50$  (mol/mol)

Figure 11 also shows evident differences between the samples below  $200^{\circ}\text{C}$ . All the samples, even without  $\text{CaCO}_3$ , exhibit the same modulus decrease, i.e. all the modulus curves are parallels. This vertical shift between the different samples is typically due to the filler effect of the  $\text{CaCO}_3$ . The  $\text{CaCO}_3$  filler effect is mainly influenced by the  $\text{CaCO}_3$  agglomerates but may also be affected by the concentration of the multiplets and clusters individually dispersed in the ionic main matrix in relation with the initial  $\text{CaCO}_3$  concentration and the thermal treatment which directly control the ionic moieties concentration. Only the storage modulus evolution of the sample without  $\text{CaCO}_3$ , is really different between  $70$  and  $110^{\circ}\text{C}$  since its  $T_g$  is  $30^{\circ}\text{C}$  lower than the others (Figure 10). To go further in the discussion of the analyses presented on Figure 11, it was necessary to highlight only the contribution of the ionic cluster to the complex shear modulus and subtract the  $\text{CaCO}_3$  filler hydrodynamic reinforcement brought by the non-dissociated  $\text{CaCO}_3$  aggregates. Without aggregate–aggregate interactions, the curves at different concentrations of  $\text{CaCO}_3$  aggregates must superimpose with the curve of the neat matrix following the general equation<sup>[44]</sup>:

$$G^*(\omega, \phi) = G^*(\omega, 0) \cdot f(\phi)$$

where  $\phi$  is the volume concentration of non-dissociated  $\text{CaCO}_3$  (Figure 8)

The function  $f(\phi)$  which actually represents the variations of the system viscosity normalized to the matrix viscosity is only dependent with the filler concentration and was already theoretically described by many authors<sup>[45, 46]</sup> on the basis of microstructural considerations. The Figure 12 presents the overlaid curves by vertical shifts with the sample without  $\text{CaCO}_3$  chosen as master curve.

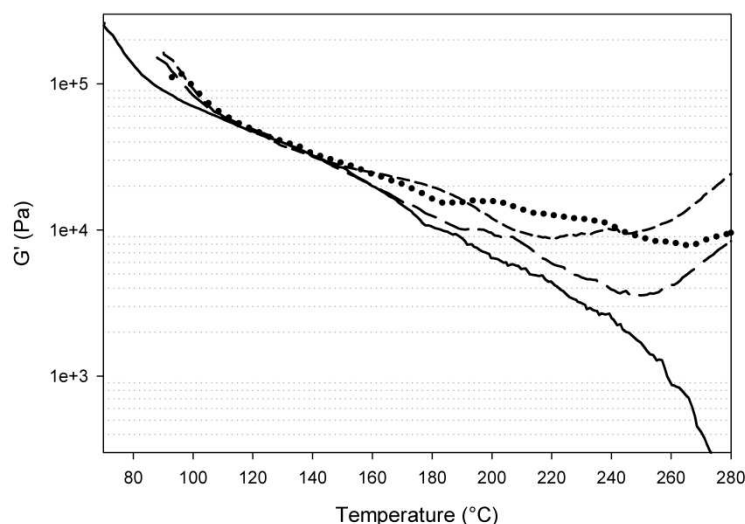


Figure 12:  $G'$  storage modulus (Pa) by parallel plates and temperature ramps at  $3^\circ\text{K}\cdot\text{min}^{-1}$  and  $1 \text{ rad/s}$  with  $\text{MA/BMA} = 16/100$  (mol/mol) line : without  $\text{CaCO}_3$  long dash:  $\text{CaCO}_3/\text{MA} = 1$  (mol/mol) Dotted:  $\text{CaCO}_3/\text{MA} = 1.43$  (mol/mol) Short Dash:  $\text{CaCO}_3/\text{MA} = 2.50$  (mol/mol)

The analysis of the variation of the storage modulus on figure 12 shows the differences between the systems according to the  $\text{CaCO}_3$  content. Two main regions are visible. Below  $140^\circ\text{C}$ , curves overlay is perfectly achieved indicating that the main impact of  $\text{CaCO}_3$  on the viscoelastic behavior is filler reinforcement. Above this temperature, rheological behavior of  $\text{CaCO}_3$  filled systems becomes significantly different to the unfilled matrix. Moreover, differences are clearly affected by the  $\text{CaCO}_3/\text{MA}$  ratio. Two phenomenons can be pointed out. Firstly, for the highest temperature (above  $240^\circ\text{C}$ ), an important increase of the storage modulus is observed which has been already discussed and is attributed of the increasing formation of ionic clusters. In the intermediate temperature range (around  $180^\circ\text{C}$ ), a new relaxation process is clearly visible. The relaxation time of this process, as its amplitude, is affected by the  $\text{CaCO}_3$  content. The more the  $\text{CaCO}_3$  concentration increases, the more the modulus associated to the process increases. In only one case, namely for

$\text{CaCO}_3/\text{MA} = 1.43$  (mol/mol) This relaxation process covers a wide range of temperature in comparison with the other compositions. In any case, the terminal flow observed for the unfilled system is not observed. These observations strongly suggest that this relaxation process is linked to the ionic cluster concentration. For low cluster concentration, only the relaxation process of isolated cluster is observed. Increasing the  $\text{CaCO}_3$  content, the percolation threshold of the ionic zone is reached and a global physical network is obtained. However, the highest  $\text{CaCO}_3$  content exhibits a surprising behavior as the behavior of not percolated ionic cluster is recovered. This behavior can be associated to the break of the ionic network by the presence of  $\text{CaCO}_3$  fillers. It was supposed that the high  $\text{CaCO}_3$  concentration blocks the possibility that ionic clusters percolate. An optimum of  $\text{CaCO}_3$  amount is then necessary in order to obtain the global physical network. These results perfectly agree with solubility tests and the RX analyses. Indeed, it was shown that both the samples ( $\text{CaCO}_3/\text{MA} = 1$  (mol/mol) and  $\text{CaCO}_3/\text{MA} = 2.50$  (mol/mol) show the ionic peak by RX and are soluble in THF. The sample with  $\text{CaCO}_3/\text{MA} = 1.43$  (mol/mol) is not soluble in THF which confirms the presence of a global ionic network.

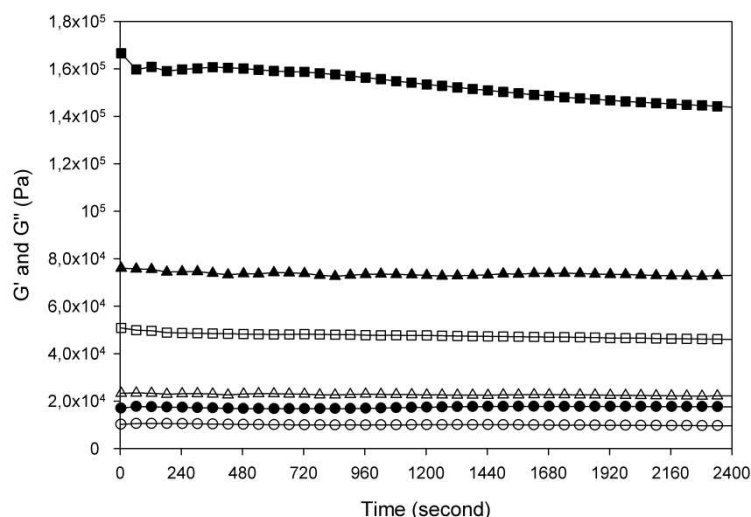


Figure 13: *thermal stability for P(BMA-co-MA) with MA/BMA = 0.16 (mol/mol). Storage modulus (black) and loss modulus (white) for  $\text{CaCO}_3/\text{MA} = 1.00$  mol/mol at 200°C (round),  $\text{CaCO}_3/\text{MA} = 1.43$  mol/mol at 190°C (triangle)  $\text{CaCO}_3/\text{MA} = 2.50$  mol/mol at 180°C (square) observed by  $G'$  (black) and  $G''$  (white) (Pa) vs time.  $f = 1 \text{ rad}\cdot\text{sec}^{-1}$ , strain = 2%*

To definitely confirm the discussion, the thermal stability of these different samples was studied in time near the temperature of the ionic cluster relaxation process (Figure 13). Then 200, 190 and 180°C were chosen for respectively  $\text{CaCO}_3/\text{MA} = 1.00, 1.43$  and  $2.50$  mol/mol; Thus, figure 13 shows clearly that the variation of the storage modulus in this temperature range is a true thermal activated relaxation process and not the kinetic disappearing of the ionic cluster. To summarize, these systems can be seen as two phases filled systems: A matrix of P(BMA-co-MA) filled with non dissociated  $\text{CaCO}_3$  aggregates and a dispersed phase of ionic cluster. The percolation of the dispersed phase is governed by the  $\text{CaCO}_3$  content and its dissociation state.

### MA content in the copolymer above the glass transition

At higher temperatures than  $T_g$  (Figure 14), a filler effect is observed again between 100 and 140°C; Indeed, if  $\text{CaCO}_3/\text{MA}$  is kept constant (1.43 (mol/mol), MA/BMA increases and the total  $\text{CaCO}_3$  content in the material increases. Four samples are presented on this Figure. Two samples are soluble in the THF (Figure 9) (○  $\text{CaCO}_3/\text{MA} = 1.43$  (mol/mol) + MA/BMA = 6/100 (mol/mol) and ●  $\text{CaCO}_3/\text{MA} = 2.50$  (mol/mol) + MA/BMA = 16/100 (mol/mol)). Both these samples exhibit the lowest modulus on the ionic plateau between 120°C and 190°C as expected since they have the lowest  $\text{CaCO}_3$  concentration in their formulation. For ○  $\text{CaCO}_3/\text{MA} = 1.43$  (mol/mol) + MA/BMA = 6/100 (mol/mol), it almost behaves like the reference without  $\text{CaCO}_3$  (Figure 11). Both the insoluble samples (□  $\text{CaCO}_3/\text{MA} = 1.43$  (mol/mol) + MA/BMA = 16/100 (mol/mol) and ◇  $\text{CaCO}_3/\text{MA} = 1.43$  (mol/mol) + MA/BMA = 25/100 (mol/mol)) behaves exactly like the insoluble samples previously discussed (Figure 12). Despite they are insoluble, they don't exhibit the ionic peak observed by X-ray (Figure 3) but clearly show the ionic plateau between 120 and 220°C (Figure 14). The solubility test in THF really appears as useful to estimate the structuration of the material.

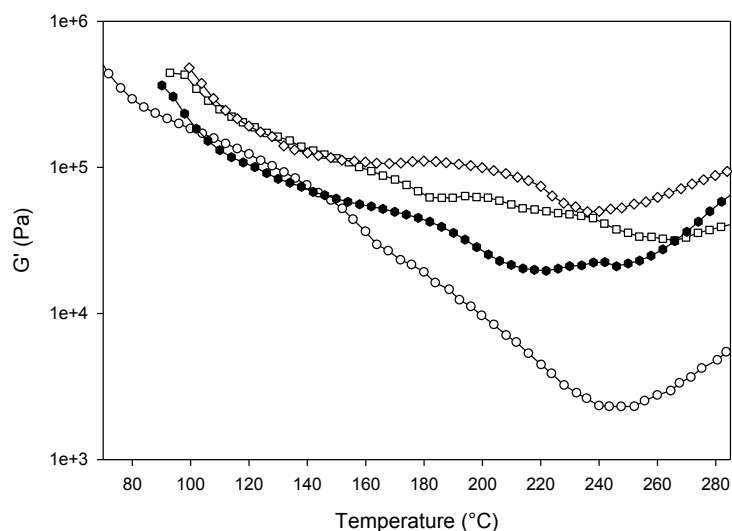


Figure 14:  $G'$  storage modulus (Pa) by parallel plates and temperature ramps at  $3^{\circ}\text{K}\cdot\text{min}^{-1}$  and  $1\text{ rad/s}$  with  $\text{CaCO}_3/\text{MA} = 1.43$  (mol/mol) :  $\circ$  MA/BMA = 6/100 (mol/mol)  $\square$  MA/BMA = 16/100 (mol/mol)  $\diamond$  MA/BMA = 25/100 (mol/mol)  $\bullet$   $\text{CaCO}_3/\text{MA} = 2.50$  (mol/mol) and MA/BMA = 16/100 (mol/mol)

## B-4 CONCLUSION

Calcium carbonate, generally used as filler in polymer materials, is able to generate ionic moieties with consequently the appearances of a plateau over the glass transition temperature of the polymer matrix. The ionic moieties are only constituted if the material is heated during its synthesis and long enough to generate a sufficient concentration of ionic moieties that produce percolated clusters. In more, the ionic moieties allow to disperse the  $\text{CaCO}_3$  fillers in grapes with a uniform repartition.

The X-Ray analysis as well as thermal and rheological analyses show that the material is organized with two phases, one corresponding to the cluster model developed by Eisenberg. The percolation of the cluster phase and the appearance of a crosslinked behavior is governed by peculiar conditions: at least 10 mol% of MA units are required in the copolymer chains and at least an excess of 20 mol% of  $\text{CaCO}_3$  vs MA. The large unreacted part of the  $\text{CaCO}_3$  behaves as a filler modifying the ionic plateau over  $T_g$ . More surprisingly, when  $\text{CaCO}_3/\text{MA}$  is superior to 2, the material loose its structure in two polymer phases. It is established now that these high filler contents disturb the structure of the cluster and ionic phase, losing its crosslinked material behavior. The  $T_g$  of the material can be adjusted only by the copolymer composition if a sufficient  $\text{CaCO}_3$  content is reached.

**ACKNOWLEDGMENT**

The authors thank the financial support from China Scholarship Council (state scholarship fund). This work benefited from the cooperation between East China University of Science and Technology (China) and Université Jean-Monnet Saint-Etienne (France).

## REFERENCES

- [1] Schneider, H. J. *Angewandte Chemie-International Edition* **2009**, 48, (22), 3924-3977.
- [2] Shimizu, L. S. *Polymer International* **2007**, 56, (4), 444-452.
- [3] Taubitz, J.; Luning, U. *European Journal of Organic Chemistry* **2008**, (35), 5922-5927.
- [4] Taubitz, J.; Luning, U. *Australian Journal of Chemistry* **2009**, 62, (11), 1550-1555.
- [5] Chen, L.; Yu, X. H.; Yang, C. Z.; Gu, Q. C.; Hu, T. D.; Xie, Y. N. *Journal of Polymer Science Part B-Polymer Physics* **1997**, 35, (5), 799-806.
- [6] Chen, J. D.; Carrot, C.; Chalamet, Y.; Majeste, J. C.; Taha, M. *Journal of Applied Polymer Science* **2003**, 88, (5), 1376-1383.
- [7] Ghosh, S. K.; De, P. P.; Khastgir, D.; De, S. K. *Journal of Applied Polymer Science* **2000**, 78, (4), 743-750.
- [8] Eisenberg, A.; Kim, J.-S., *Introduction to ionomers*. 1998; p 327.
- [9] Tant, M. R.; Wilkes, G. L. *Journal of Macromolecular Science-Reviews in Macromolecular Chemistry and Physics* **1988**, C28, (1), 1-63.
- [10] Mauritz, K. A. *Journal of Macromolecular Science-Reviews in Macromolecular Chemistry and Physics* **1988**, C28, (1), 65-98.
- [11] Eisenberg, A.; Hird, B.; Moore, R. B. *Macromolecules* **1990**, 23, (18), 4098-4107.
- [12] Eisenberg, A. *Macromolecules* **1970**, 3, (2), 147-154.
- [13] Hird, B.; Eisenberg, A. *Abstracts of Papers of the American Chemical Society* **1992**, 204, 40-PMSE.
- [14] Tsou, L.; Ma, X.; Sauer, J. A.; Hara, M. *Journal of Polymer Science Part B-Polymer Physics* **1998**, 36, (7), 1235-1245.
- [15] Kim, H. S.; Nah, Y. H.; Kim, J. S.; Yu, J. A.; Lee, Y. *Polymer Bulletin* **1998**, 41, (5), 569-575.
- [16] Kurian, T.; Datta, S.; Khastgir, D.; De, P. P.; Tripathy, D. K.; De, S. K.; Peiffer, D. G. *Polymer* **1996**, 37, (21), 4787-4793.

- [17] Datta, S.; De, P. P.; De, S. K. *Journal of Applied Polymer Science* **1996**, 61, (10), 1839-1846.
- [18] Song, J. M.; Oh, S. H.; Kim, J. S.; Kim, W. G. *Polymer* **2005**, 46, (26), 12393-12400.
- [19] Kim, S. H.; Kim, J. S. *Macromolecules* **2003**, 36, (7), 2382-2386.
- [20] Castagna, A. M.; Wang, W.; Winey, K. I.; Runt, J. *Macromolecules* **2011**, 44, (13), 5420-5426.
- [21] Capek, I. *Advances in Colloid and Interface Science* **2005**, 118, (1-3), 73-112.
- [22] Chu, B.; Wu, D. Q.; Macknight, W. J.; Wu, C.; Phillips, J. C.; Legrand, A.; Lantman, C. W.; Lundberg, R. D. *Macromolecules* **1988**, 21, (2), 523-525.
- [23] Galambos, A. F.; Stockton, W. B.; Koberstein, J. T.; Sen, A.; Weiss, R. A.; Russell, T. P. *Macromolecules* **1987**, 20, (12), 3091-3094.
- [24] Page, K. A.; Park, J. K.; Moore, R. B.; Sakai, V. G. *Macromolecules* **2009**, 42, (7), 2729-2736.
- [25] Hara, M.; Sauer, J. A. *Journal of Macromolecular Science-Reviews in Macromolecular Chemistry and Physics* **1994**, C34, (3), 325-373.
- [26] Leong, Y. W.; Abu Bakar, M. B.; Ishak, Z. A. M.; Ariffin, A.; Pukanszky, B. *Journal of Applied Polymer Science* **2004**, 91, (5), 3315-3326.
- [27] Nedev, M.; Podskoknieva, I. *Kautschuk Gummi Kunststoffe* **1991**, 44, (5), 439-441.
- [28] Papirer, E.; Schultz, J.; Turchi, C. *European Polymer Journal* **1984**, 20, (12), 1155-1158.
- [29] Zhang, J.; Bao, F. R.; Dai, D. P.; Zhou, N. L.; Li, L.; Lu, S.; Shen, J. *Chinese Journal of Inorganic Chemistry* **2007**, 23, (5), 822-826.
- [30] Sasaki, T.; Kawagoe, S.; Mitsuya, H.; Irie, S.; Sakurai, K. *Journal of Polymer Science Part B-Polymer Physics* **2006**, 44, (17), 2475-2485.
- [31] Andersson, M.; Suska, F.; Johansson, A.; Berglin, M.; Emanuelsson, L.; Elwing, H.; Thomsen, P. *Journal of Biomedical Materials Research Part A* **2008**, 84A, (3), 652-660.

- [32] Rakhmatullina, E.; Meier, W. *Langmuir* **2008**, 24, (12), 6254-6261.
- [33] Moon, J.; Park, M. *Polymer-Korea* **2009**, 33, (5), 477-484.
- [34] Yang, I. K.; Hu, C. C. *European Polymer Journal* **2006**, 42, (2), 402-409.
- [35] Sedlakova, Z.; Plestil, J.; Baldrian, J.; Slouf, M.; Holub, P. *Polymer Bulletin* **2009**, 63, (3), 365-384.
- [36] Kasselouri, V.; Dimopoulos, G.; Parissakis, G. *Cement and Concrete Research* **1995**, 25, (5), 955-960.
- [37] Kasselouri, V.; Dimopoulos, G.; Parissakis, G. *Cement and Concrete Research* **1995**, 25, (3), 477-484.
- [38] Brandrup, J.; Immergut, E. H.; Grulke, E. A.; Abe, A.; Bloch, D. R., *Polymer Handbook (4th Edition)*. John Wiley & Sons: 1999.
- [39] Rao, T. R. *Chemical Engineering & Technology* **1996**, 19, (4), 373-377.
- [40] Singh, N. B.; Singh, N. P. *Journal of Thermal Analysis and Calorimetry* **2007**, 89, (1), 159-162.
- [41] Maslen, E. N.; Streltsov, V. A.; Streltsova, N. R. *Acta Crystallographica Section B-Structural Science* **1993**, 49, 636-641.
- [42] Hara, M.; Sauer, J. A. *Korean Journal of Chemical Engineering* **1998**, 15, (4), 353-361.
- [43] Antony, P.; De, S. K. *Journal of Macromolecular Science-Polymer Reviews* **2001**, C41, (1-2), 41-77.
- [44] Agoudjil, B.; Bos, L.; Majeste, J. C.; Candau, Y.; Mamunya, Y. P. *Composites Part a-Applied Science and Manufacturing* **2008**, 39, (2), 342-351.
- [45] S.H., M.; E., P. P. *J. Colloid Interface Sci.* **1956**, 11, 80-95.
- [46] Krieger, I. M.; Dougherty, T. J. *Transactions of the Society of Rheology* **1959**, 3, 137-152.

## Chapter C

# Polystyrene supramolecular networks based on DA-AD hydrogen bonds

Yiping NI<sup>1,2,3</sup>, Frédéric BECQUART<sup>1,2,3</sup>, Mohamed TAHA<sup>1,2,3,\*</sup>, Ouissam ADIDOU<sup>1,2,3</sup>, Jean-Charles MAJESTE<sup>1,2,3</sup>, Jianding CHEN<sup>4</sup>

<sup>1</sup> Université de Lyon, F-42023, Saint-Etienne, France;

<sup>2</sup> CNRS, UMR 5223, Ingénierie des Matériaux Polymères, F-42023, Saint-Etienne, France;

<sup>3</sup> Université de Saint-Etienne, Jean Monnet, F-42023, Saint-Etienne, France;

<sup>4</sup> Laboratory of Advanced Materials Processing, East China University of Science and Technology, 200237 Shanghai, China

\*[MTAHA@univ-st-etienne.fr](mailto:MTAHA@univ-st-etienne.fr)

## Résume

Des réseaux supramoléculaires de polystyrène ont été synthétisés par copolymérisation radicalaire du styrène avec des monomères contenant des motifs donneur-accepteur (DA) par liaisons hydrogène doubles, soit le 2-méthacrylamidopyridine (MAP) ou le méthacrylamide (MAAM). Les pourcentages molaires de MAP et MAAM dans les copolymères étaient respectivement de 2% - 20% et 6% - 40%. Les liaisons hydrogène dans les copolymères ont été caractérisés par spectroscopie IRTF. Les températures de transition vitreuse ( $T_g$ s) de ces copolymères ont été modélisés par l'équation de Kwei, montrant des interactions secondaires dues à des liaisons hydrogène intermoléculaires. Les constantes d'association ( $K_{ass}$ ) de dimères DA-AD ont été indirectement calculées par spectroscopie  $^1H$ RMN par des molécules modèle de MAAM et MAP. Ces constantes ont été calculées avec des valeurs de  $6,75 \text{ m}^{-1}$  et  $16,75 \text{ M}^{-1}$  respectivement. Les analyses mécaniques dynamiques (DMA) ont été effectuées par des balayages en fréquence ou température à l'état fondu. Les copolymères Styrène - MAP ou styrène - MAAM avaient des modules plus hauts que le polystyrène de référence, mais la MAP a eu plus d'influence sur les propriétés des matériaux. Les copolymères de MAP ont eu un plateau qui est apparu vers  $150 \text{ }^\circ \text{C}$  prouvant la formation d'un réseau supramoléculaire.

## Abstract

Polystyrene supramolecular networks were prepared by radical copolymerization of styrene with monomers containing Donor-Acceptor (DA) moieties by double hydrogen bonds, either 2-methacrylamidopyridine (MAP) or methacrylamide (MAAM). The molar percentages of MAP and MAAM in the copolymers were respectively 2% - 20% and 6% - 40%. The hydrogen bonds in the copolymers have been characterized by FTIR spectroscopy. The glass transition temperatures ( $T_{gs}$ ) of these copolymers have been modeled by the Kwei equation showing secondary interactions due to intermolecular hydrogen bonds. The DA-AD association constants ( $K_{ass}$ ) have been indirectly calculated by  $^1\text{H-NMR}$  spectroscopy with model molecules of MAAM and MAP. These constants were respectively  $6.75 \text{ M}^{-1}$  and  $16.75 \text{ M}^{-1}$ . Dynamic Mechanical Analyses (DMA) by both frequency and temperature sweep tests, were carried out in the molten state. Styrene - MAP or styrene - MAAM copolymers had higher moduli than neat polystyrene but the MAP influences the materials properties distinctively to the MAAM. MAP copolymers had a second  $G'$  plateau that appeared at  $150^\circ\text{C}$  proving the formation of a supramolecular network.

**Keywords:** supramolecular, DA moiety, association constant, rheology

## C-1. Introduction:

Supramolecular chemistry is defined as the “chemistry of the non-covalent and intermolecular bonds”. In contrast to the covalent bonds, they have lower binding strength [1], but endow materials with reversible interactions typically dependent on temperature, solvent and pH [2-4]. At least two chemical moieties are able to form host-guest systems in dimers by single or multiple interactions [5]. Two different dimers must be distinguished: homodimers and heterodimers. Homodimers are necessarily composed of two identical moieties which are able to associate. Different kinds of interactions can be involved in supramolecular chemistry such as hydrogen bonds [6-8], ionic attractions [9], amphiphilic interactions [10], metal coordinations [11] or  $\pi$ - $\pi$  stackings [12].

Supramolecular polymers by hydrogen bonding association are extensively used to build polymer backbones by assembling non-covalent moieties [13] or polymer networks through intermolecular interactions between the chains. The dimers can be linked to the backbone or located at the end-chains [14]. A hydrogen bonding dimer is composed at least of a polarizable hydrogen - acceptor atom linked to an electronegative atom (A) that interacts complementarily with another dimer which is a nucleophilic donor (D). The total interaction energy of hydrogen bonds is the sum of several contributions, such as electrostatic energy, polarization energy, charge transfer, dispersion energy and exchange energy. It represents the total energy difference,  $\Delta E_{\text{HB}}$ , between the hydrogen-bonding system at equilibrium and the total energy of the free components [1]. It can reach  $120 \text{ kJ}\cdot\text{mol}^{-1}$  with a single hydrogen bond, almost half the value of covalent bond strength such as  $\sigma$  carbon-carbon bond, close to  $348 \text{ kJ}\cdot\text{mol}^{-1}$  [15]. Although hydrogen bonds are not the strongest non-covalent interactions, they are prominent in supramolecular chemistry due to their versatility and directionality. The determination of association constants  $K_{\text{ass}}$  is required to measure the reversible binding strength in supramolecular polymers (eqn.1) [16].

NMR spectroscopy is a common technique to determine  $K_{\text{ass}}$ .

The chemical shift ( $\delta$ ) of the labile protons, involved in hydrogen bonds, varies with the percentage of association with the donor, typically a carbonyl or the nitrogen atom [17]. Indeed, the observed chemical shift of a labile proton involved in hydrogen bonds is

located between  $\delta_h$ , corresponding to the chemical shift of this proton when no hydrogen bond exists, and  $\delta_c$  observed when this same labile proton is completely associated. The nature of the donor-acceptor system, but also the temperature, the solvent and its concentration influence the association's strength, and then the chemical shifts.

With heterodimer systems specifically,  $K_{ass}$  is obtained by Rose-Drago model which establishes a relationship between  $\delta$  and the host/guest mol ratio <sup>[16]</sup> (Eqn. 1). It is generally in the range of  $10 \sim 10^5 \text{ M}^{-1}$

$$\frac{1}{K} = \frac{\delta - \delta_h}{\delta_c - \delta_h} [H]_0 - ([H]_0 + [G]_0) + \frac{\delta_c - \delta_h}{\delta - \delta_h} [G]_0$$

Eq.1

Where  $[H]_0$  and  $[G]_0$  are respectively the initial concentrations of host and guest;  $\delta$  is the observed chemical shift of the interacting host/guest;  $\delta_h$  is the chemical shift of the free host;  $\delta_c$  is the chemical shift of the fully complexed host that is calculated by the equation and  $K_{ass}$ .

Chen <sup>[18]</sup>, based on the work of Horman <sup>[19]</sup> applied to caffeine, developed a model for homodimer systems (Eqn.2) working with single hydrogen bonds up to quadruple DADA-ADAD pairs <sup>[20, 21]</sup>.

$$\delta_{obs} = \delta_m + (\delta_d - \delta_m) \frac{\sqrt{1+8KC}-1}{\sqrt{1+8KC}+1}$$

Eqn. 2

Where  $\delta_m$  is the free moiety's chemical shift;  $\delta_d$  is the moiety's chemical shift that is fully dimerized;  $\delta_{obs}$  is the observed chemical shift;  $K_{ass}$  and  $C$  are respectively the association constant and the homodimer concentration.

Other common spectroscopic techniques, such as U.V. <sup>[22]</sup>, I.R. <sup>[23]</sup>, I.T.C. (isothermal titration calorimetry) <sup>[24]</sup> or infrequently, VPO (vapor pressure osmometry) <sup>[25]</sup> are also used to determine association constants.

Several works concern systems with multiple hydrogen bonds which greatly enhance the variety of dimers as well as the association constants <sup>[26-29]</sup>. Polymers with double hydrogen bonds based on amides could be achieved by radical copolymerizations <sup>[30-33]</sup>

or polycondensation [34]. These copolymers have a good water solubility due to the amide groups and the strength of intermolecular hydrogen bonds which have been qualitatively [30] or quantitatively [34] studied by NMR at different temperatures. 2-aminopyridine derivatives are also other kinds of double hydrogen bonding units. The N-H located in the ortho position of the pyridine ring also gives an array of the DA double hydrogen bonding homodimers.  $K_{\text{ass}}$  were calculated from 1 to 100  $\text{M}^{-1}$  [20, 34] and were sufficient to increase the storage modulus in the molten state [34] although they are close to single hydrogen bonding  $K_{\text{ass}}$ .

There are many specific multiple hydrogen-bond systems. Among them, ureidopyrimidone (UPy) derivatives [26, 28, 35-37] present four hydrogen bonds with strong associations. UPy can be in equilibrium between its two tautomers, AADD or ADAD patterns [38], both of which are self-associated in homodimers. These highly hydrogen-bonding motifs exhibit high binding constants around  $10^7 \sim 10^8 \text{M}^{-1}$  [14] which lead to physical networks with high rubbery modulus [36].

Two approaches were found in literature to prepare supramolecular assemblies based on polymers or copolymers synthesized by radical polymerization. Via the first approach, a functional copolymer was first synthesized with supramolecular moieties grafted onto the copolymer in a second step. Feldman prepared model networks from polymers bearing Upy moieties [39]. Butyl acrylate and 6-(tert-butoxycarbonylamino)hexyl acrylate were copolymerized by ATRP, with pendant butoxycarbonylamino groups to finally graft onto the Upy moieties. Subramani [40] prepared a triple hydrogen bonding moiety grafted onto a polystyrene backbone. Styrene and *p*-(chloromethyl) styrene were first copolymerized by radical polymerization with AIBN. The pendant chloromethyl groups were modified to obtain a diaminotriazine group as DAD moiety.

Via the second approach, a monomer bearing supramolecular moieties was first prepared then copolymerized with another monomer. McKee [41] reported the synthesis of the UPy methacrylate. This functional monomer was copolymerized with methyl methacrylate or 2-ethylhexyl methacrylate by free radical polymerization. Park [42] described the supramolecular network based on immiscible poly(butyl-methacrylate) (PBMA) and polystyrene blends. Two functional vinyl monomers, urea of guanosine (UG)

with ADDA moiety and 2,7-diamido-1,8-naphthyridine (DAN) with DAAD moiety were prepared by HEMA esterification and a substitution of 4-vinylbenzyl chloride. P(BMA-co-UG) and P(S-co-DAN) were respectively copolymerized and then mixed together in order to study the strong supramolecular associations at the interface between the immiscible PS and PBMA. Methacrylate UPy [43] was also studied through a similar method synthesizing P(BMA-co-UPy). Both dimerizations of UPy and its association with DAN-St were investigated.

These studies where strong interactions develop with  $K_{\text{ass}}$  between  $10^6$  and  $10^8$  are based on relatively complicated synthetic methods but such strong interactions are a good opportunity to obtain reversible cross-linked materials with good viscoelastic and mechanical properties. The aim of this study is to determine if double hydrogen bonding motifs, available commercially or easy to prepare, can reach such constant bindings. To answer these questions, DA moieties are chosen among amide and aminopyridine derivatives from respectively methacrylamide (MAAM) and 2-methacrylamidopyridine (MAP). These monomers will be comparatively copolymerized with some styrene. Structure-property relationships of these copolymers will be emphatically investigated and presented with spectroscopic analyses by IR and  $^1\text{H-NMR}$ . The influence of DA concentration in the copolymer chain will be analyzed by thermal and viscoelastic studies.

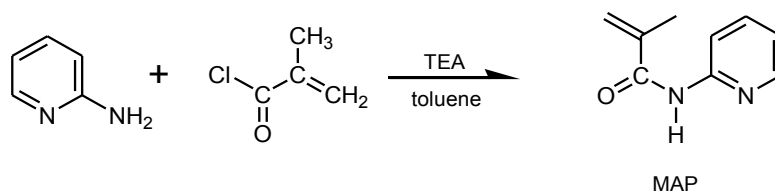
## **C-2. Experimental:**

### **C-2.1. Reagents**

2-aminopyridine (AP), methacryloyl chloride (MC), methacrylamide (MAAM), Styrene (St), dimethyl sulfoxide (DMSO), triethylamine (TEA) and 2,2'-Azobis(2-methylpropionitrile) (AIBN) were purchased from Aldrich. 2-acetamidopyridine (AcAP) was purchased from TCI Europe. Chloroform ( $\text{CHCl}_3$ ), anhydrous toluene, tetrahydrofuran (THF), ethanol and acetone were purchased from CARLO ERBA REAGENTS. Styrene was distilled under vacuum (0.2 mbar) at room temperature and stored at  $-23\text{ }^\circ\text{C}$  before its use. The other reagents were used as received.

### C-2.2. 2-methacrylamidopyridine (MAP) synthesis: monomer with DA moiety

MAP was synthesized through a method adapted from the work reported by Coskun [32, 33]: Methacryloyl chloride (10g, 0.064 mol) in 5 mL toluene was added dropwise to 2-aminopyridine (5g, 0.054mol) and triethylamine (10.91g, 0.108mol) in 60 mL toluene in a three-neck flask under argon atmosphere within 30 minutes at 0-5 °C and magnetically stirred for an additional hour. The reactive system was continuously mixed for 12 hours gradually raising the temperature to room temperature (around 20 °C). The precipitated side product was filtered off and abandoned. Filtrate was dried by distillation at room temperature under vacuum (0.2 Mbar) to remove the toluene and the methacryloyl chloride excess. The yielding dark-orange viscous MAP was dried under vacuum at 30 °C for 5 hours, with a yield of 40%.



Scheme 1: Synthesis of 2-methacrylamidopyridine (MAP) from 2-aminopyridine and methacryloyl chloride

### C-2.3. Copolymerization of P(MAAM-co-St) and P(MAP-co-St)

#### MAAM and styrene copolymerization in THF

Copolymers with different MAAM feeding ratio from 0 to 60 mol% were prepared by solution copolymerization with styrene. 20 g of the comonomers was added in a three-neck flask with 30 mL of THF. 1 mol% of AIBN was added with total comonomers' amount in reference. The mixture was refluxed under argon atmosphere for 8 hours. Then, the products containing 0 mol%, 15 mol% and 30 mol% of MAAM were precipitated with 200 mL of ethanol in beakers, and washed twice with ethanol. For copolymers containing more than 30 mol% of MAAM, the precipitation occurred in an acetone-water mixture with a 1:1 volume ratio. Finally, the copolymers were dried under vacuum at 140°C for 4 hours. Real MAAM ratios were calculated by NMR. Yields were between 80 and 96%.

## MAP and styrene Bulk copolymerization

Copolymers with different MAP feeding ratios from 0 to 20 mol% were prepared by bulk copolymerization with styrene. The MAP-St mixtures were placed in a two-neck flask under argon atmosphere, and 1 mol% AIBN was added with the comonomer amount in reference. The reactive system was heated at 70 °C with a silicone oil bath for 6 hours. The obtained copolymers were dried in an oven under vacuum (0.2 Mbar) at 140 °C for 3 hours. Yields were between 92 and 98%.

### C-2.4. Characterizations

#### Fourier transform infrared (FTIR) spectroscopy

FTIR spectra of P(MAAM-co-St) and P(MAP-co-St) copolymers were recorded with a Nicolet Nexus FTIR spectroscopy. Copolymers and Potassium bromide (KBr) were dried, mixed and pressed into pellets with the mass ratio 2 mg/160 mg. 32 scans were collected with a bandwidth of 4 cm<sup>-1</sup>. Typically the acquisitions were performed at room temperature, except when temperature ramps were chosen from 30°C to 210°C.

#### Nuclear magnetic resonance (NMR) spectroscopy

The <sup>1</sup>H-NMR analyses of P(MAAM-co-St) were performed with a Bruker Advance II spectrometer operating at 250 MHz and 300 K for 64 scans in DMSO-d<sub>6</sub> with TMS as an internal reference.

For binding constants determinations, <sup>1</sup>H and <sup>13</sup>C NMR analyses were respectively performed with a Bruker DRX400 spectrometer operating at 400 MHz and 100.6 MHz with a BBPO+ probe. These samples were acquired with 256 scans in CDCl<sub>3</sub> at 300K with TMS. Dilutions from 0.09 mol.L<sup>-1</sup> to 0.002 mol.L<sup>-1</sup> were operated between each acquisition.

AcAP CDCl<sub>3</sub> solution at 0.03 mol.L<sup>-1</sup> was also analyzed by <sup>1</sup>H-NMR spectroscopy at different temperatures with the same spectrometer. Spectra were recorded with the same parameters mentioned above but at 300 K and 315 K respectively, in order to determine K<sub>ass</sub>.

### **Size-exclusion chromatography (SEC)**

Number average molecular weight ( $M_n$ ), weight number average molecular weight ( $M_w$ ) and polydispersity index (PI) were obtained by size-exclusion chromatography.

For P(MAP-co-St) copolymers, the tests were conducted with equipment consisting of a Waters 515 HPLC pump, a refractive index-detector Waters 2414, a Wyatt viscometer, an auto sampler Waters 717 and three Waters Styrogel columns (HR1, HR2, HR3). 1.2-1.8 mg.mL<sup>-1</sup> samples were analyzed at room temperature in THF at 1 mL.min<sup>-1</sup>.

For P(MAAM-co-St) copolymers, samples were analyzed with a high temperature GPC (Waters Alliance GPC 2000) equipped with three SHODEX columns, HT803, HT804, and HT805 along with a refractometer coupled to a viscometer as detectors. The eluent was DMSO at 1 mL.min<sup>-1</sup> and 135°C. The concentration of each sample was 1-1.4 mg.mL<sup>-1</sup> in DMSO and dissolution was first achieved by heating at 90 °C for 120 minutes.

### **Thermal analysis**

Thermal transitions were determined by differential scanning calorimetry (DSC) with a TA Q10 device, by heating and cooling ramps from -50 to 200°C at 10°C.min<sup>-1</sup> under a nitrogen flow. The glass transition temperatures of the copolymers were measured by the second heating ramp.

### **Dynamic mechanical spectroscopy in the molten state**

Rheological measurements were carried out with two different pieces of equipment. Molten state rheology of P(MAP-co-St) copolymers was performed using a strain controlled Anton Paar Physica MCR 301 rotational rheometer, in the linear viscoelastic domain of the materials. Dynamic strains were applied using parallel plate geometry with 25mm diameter. The gap between the plates was fixed at 2mm. The temperature ramp was fixed at 3°C.min<sup>-1</sup> from 200°C to the minimum temperature at which samples become slipping and/or the transducer is overloaded. The frequency was fixed at 1 rad.s<sup>-1</sup> and the strain was fixed at 10%.

Molten state rheology of P(MAAM-co-St) copolymers was performed using a stress controlled SR5000 rheometer, also in the linear viscoelastic domain of the material. Dynamic stress was applied using 25mm parallel plate geometry. The ramp temperature was  $3^{\circ}\text{C}\cdot\text{min}^{-1}$  between  $120^{\circ}\text{C}$  and  $300^{\circ}\text{C}$ . The frequency was fixed at  $1\text{ rad}\cdot\text{s}^{-1}$  and the stress was typically chosen as 5000 Pa around  $200^{\circ}\text{C}$ .

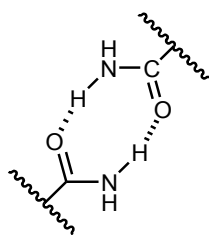
## C-3. Results and discussion

### C-3.1. Dimerization of self-assemblies

Self-assemblies by supramolecular interactions can occur between copolymer chains obtained by radical polymerization of styrene with functionalized comonomers. The number of the DA moieties as pendant groups was adjusted by the molar comonomer ratio.

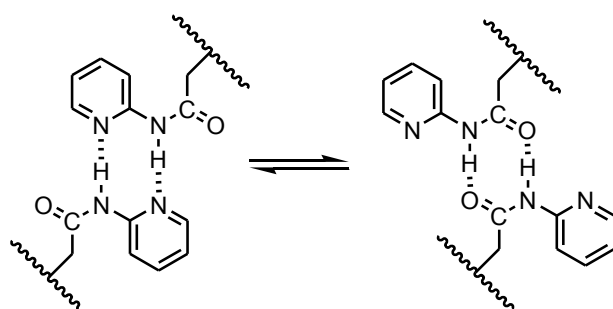
In this study, two monomers with self-assembling moieties were studied: methacrylamide (MAAM) and methacryloyl aminopyridine (MAP).

The capability of self-homodimerization via hydrogen bonds from amide was already described [20]. The homodimerization occurs with a cyclic conformation between both of the involved primary amide functions as shown in scheme 2.



Scheme 2. Self-homodimerization between P(MAAM-co-St) chains

The homodimerization between two MAP units is due to two kinds of hydrogen acceptors, nitrogen atoms from pyridine ring, or ketonic oxygen. Then, they can form two different structures in equilibrium with two hydrogen bonds per homodimer as it is shown in Scheme 3.



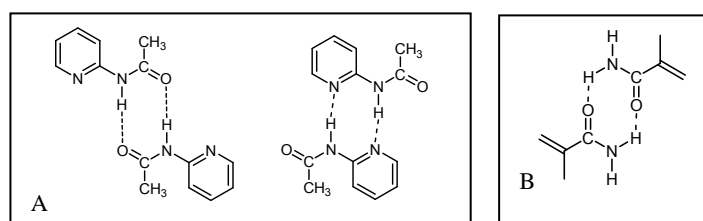
Scheme 3. Equilibrium self-homodimerization between P(MAP-co-St) chains

### C-3.2. Calculation of association constants $K_{\text{ass}}$

$K_{\text{ass}}$  value is the factor reflecting the strength of hydrogen bonds. Higher  $K_{\text{ass}}$  values mean that more stable assemblies are produced. It is also in relationship with the material plateau modulus in rheology. Strong hydrogen-bonding interactions influence this plateau [34]. The purpose of  $K_{\text{ass}}$  calculation is not only to calculate the binding strength in connection with the strength of the non-covalent network, but also to determine quantitatively whether intermolecular or intramolecular dimers are formed. In this study,  $K_{\text{ass}}$  was first calculated with simple model molecules before further complicated characterizations with supramolecular polymers since chains' entanglements and viscosity may affect the dimerization phenomenon.

2-acetamidopyridine (AcAP) was chosen as a model molecule because its structure is very similar to the MAP. It is able to form the same dimer associations as shown with scheme 4. MAAM is used directly.

As discussed in the introduction, Chen's equation [18] is applied to the homodimer formation. Since  $\delta_m$ ,  $\delta_d$ , and  $K$  are constant, the monomer concentration ( $C$ ) and  $\delta_{\text{obs}}$  are the variable.  $\delta_m$ ,  $\delta_d$ , and most importantly,  $K_{\text{ass}}$ , are obtained by fitting the experimental data with this equation.



Scheme 4. Possible homodimer structures between: A: AcAP homodimer; B: MAAM homodimer

Different monomer concentrations in  $\text{CDCl}_3$  were prepared 5 days before the analyses, and placed at room temperature for stabilization. NOESY  $^1\text{H-NMR}$  spectra were exclusively recorded for the lowest 2-AcAP concentration in order to deconvolve the doublet at 8.2 ppm to obtain the accurate chemical shift of N-H proton which is overlapped by a pyridine-ring proton. Curve fitting results of AcAP and MAAM are shown in figure 2 and  $K_{\text{ass}}$  values are listed in table 1.  $\delta_{\text{N-H}}$  proton has an upfield shift while the AcAP concentration decreases (figure 1). This can also be observed in other self-associated amides [20, 44]. The difference of  $\Delta \delta_{\text{N-H}}$  between intramolecular (folded) and intermolecular (unfolded) hydrogen bonds has been reported, concluding that the resonance of a folded hydrogen bond proton is narrow (approx. 0.2 ppm), while it is large (2-3 ppm) for a non-folded one [45]. The maximum of  $\Delta\delta$  for both AcAP and MAAM (table 1) exceeds 2 ppm, indicating that intermolecular hydrogen bonds are formed between dimers in chloroform.

$K_{\text{ass}}$  is influenced by the hydrogen-bonding number and array. Calculated  $K_{\text{AcAP}}$  and  $K_{\text{MAAM}}$  are based on the simple double hydrogen bonds (DA), so they are certainly weaker than those in typical triple hydrogen bond arrays which are mostly between 65 and 890  $\text{M}^{-1}$  [46]. Furthermore, the DA-AD homodimer is also predicted to have lower  $K_{\text{ass}}$  than DD-AA homodimer according to Beijer's theory [26]. But we can conclude that these values are in the suitable range of double hydrogen bonds from 1 to 100  $\text{M}^{-1}$  [20, 34, 44]. In particular,  $K_{\text{AcAP}}$  ( $16.75 \text{ M}^{-1}$ ) is in agreement with existing references according to which the  $K_{\text{ass}}$  of acylaminopyridine derivatives varies from 1.5 to 17  $\text{M}^{-1}$  [20], and comparatively higher than other N-H $\cdots$ N bonds (0.7-2.1  $\text{M}^{-1}$ ) in small molecule assemblies [47]. This value is also superior to  $K_{\text{MAAM}}$  calculated with the value of 6.75  $\text{M}^{-1}$ . The difference of the  $K_{\text{ass}}$  between AcAP and MAAM may be attributed to the supramolecular moieties' structures. In AcAP, double hydrogen bonds could be formed based on either N-H $\cdots$  N<sub>pyridine</sub> or N<sub>amide</sub>-H $\cdots$ O=C, while MAAM only have one formation based on the amide function. The interaction of N-H $\cdots$  N<sub>pyridine</sub> is reported as stronger

and more stable than amide in solid state [48] that may cause the  $K_{AcAP}$  to overwhelm  $K_{MAAM}$  with a higher association constant.

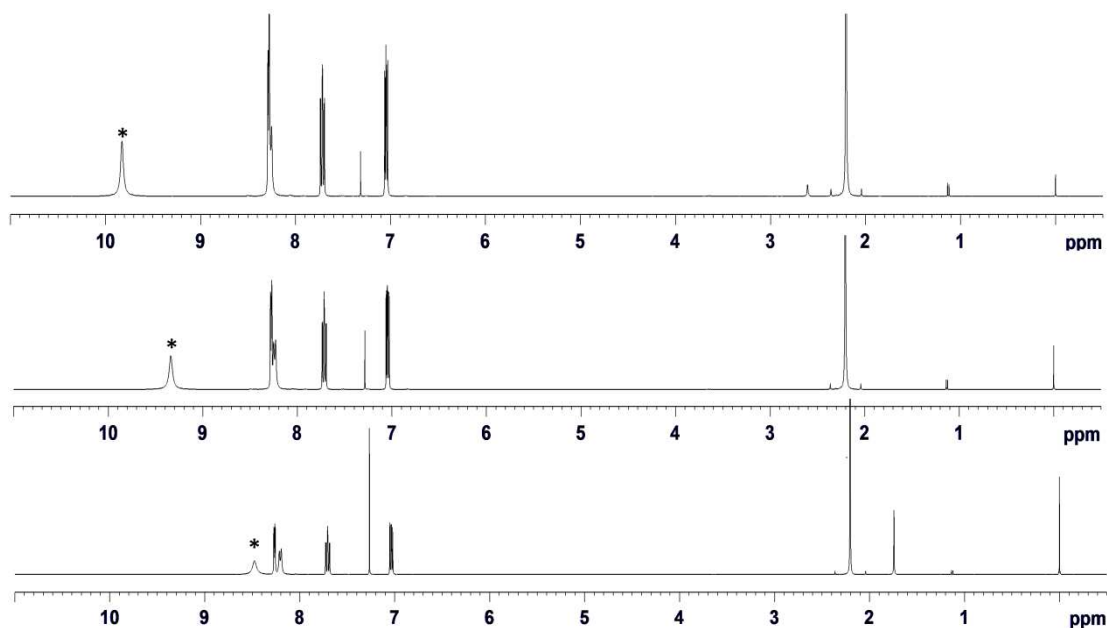


Figure 1.  $^1\text{H-NMR}$  Chemical shift of amide proton at different AcAP concentrations in  $\text{CDCl}_3$  and 300K. From upper to lower:  $0.0921 \text{ mol.L}^{-1}$ ,  $0.0417 \text{ mol.L}^{-1}$  and  $0.0088 \text{ mol.L}^{-1}$

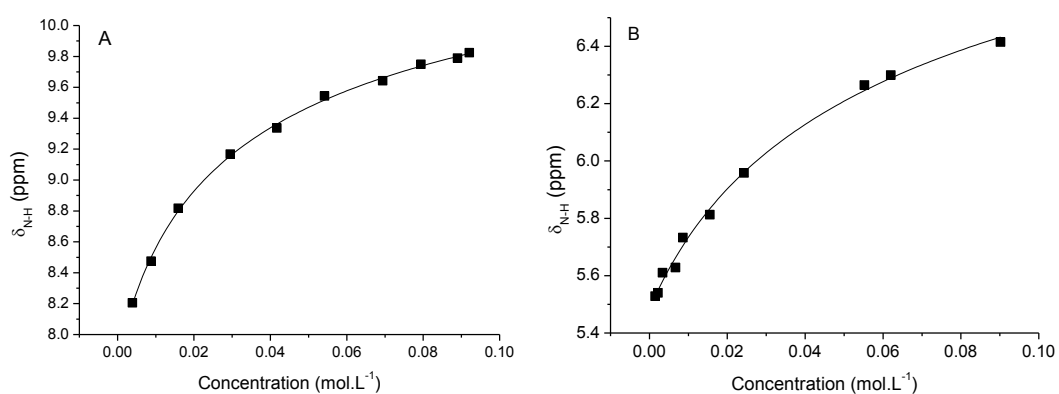


Figure 2.  $\delta_{\text{N-H}}$  fitting vs concentration in  $\text{CDCl}_3$  at 300K of A: AcAP; B: MAAM. ■ : experimental data and black line : fitted curve

Table 1.  $K_{\text{ass}}$ ,  $\delta_{\text{m}}$ ,  $\delta_{\text{d}}$  and  $\Delta\delta$  of monomers derived from curve-fits from Chen Model [18].

	$K_{\text{ass}}$ ( $\text{M}^{-1}$ )	$\delta_{\text{m}}$ (ppm)	$\delta_{\text{d}}$ (ppm)	$\Delta \delta$ (ppm)
<b>AcAP</b>	16.75	7.83	11.31	3.48
<b>MAAM</b>	6.75	5.48	7.71	2.23

These  $K_{\text{ass}}$  results from model molecules by NMR dilution experiments prove the dimerization of hydrogen-bonding DA moieties and their corresponding strength. So, when copolymers are synthesized, it exists a high probability to achieve simultaneously the networks' formation through DA-AD homodimerization which will be studied in the next characterizations.

### C-3.3. Characterization of hydrogen bonds in P(MAAM-co-St) and P(MAP-co-St) by FTIR

Hydrogen bonding occurs in amides containing a proton donor group -NH and a proton acceptor -C=O when the s orbital of the proton effectively overlaps the  $\pi$  orbital of the acceptor group possessing the lone pair. This interaction reduces the bond force constant of the acceptor, -C=O, and consequently decreases the frequency of the carbonyl absorption [49]. Furthermore, they are very sensitive to the concentration of intermolecular hydrogen-bonding groups[50]. It is reported that the absorptions resulting from intermolecular hydrogen bonds generally disappear at low concentrations (less than 0.01 M in nonpolar solvents) while that from intramolecular ones is persistent [49]. IR spectroscopy can be then used for qualitative characterizations of the studied systems. As discussed before, MAP and MAAM units can form homodimers by hydrogen bonding and consequently influence the involved carbonyl stretching by FTIR spectrometry. If carbonyls in amide functions are restricted by hydrogen bonds and transform to C=O...H-N, the carbonyl stretching may shift to lower frequency [51]. Another possibility is that the C=O band absorption splits into two peaks, one peak representing the hydrogen bonded C=O [34]. In this case, the intensity of bonded C=O is sensitive to the concentration of hydrogen bonds in the system [52].

#### Effect of MAAM concentration to P(MAAM-co-St) in FTIR spectra

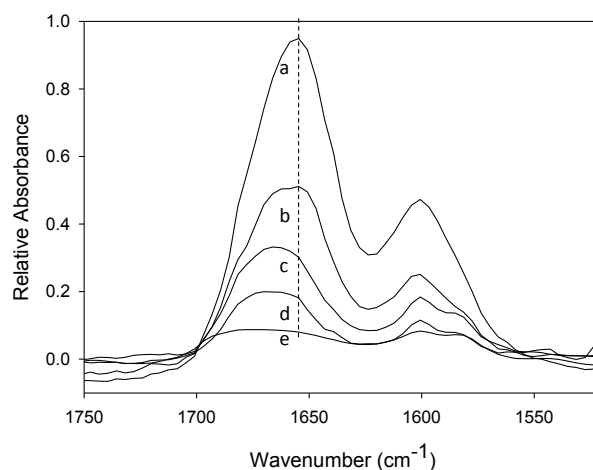


Figure 3. P(MAAM-co-St) IR spectra from 1750  $\text{cm}^{-1}$  to 1520  $\text{cm}^{-1}$  with different MAAM contents at room temperature. a: 40% MAAM; b: 30% MAAM c: 27% MAAM; d: 17% MAAM; e: 6% MAAM in mol fraction.

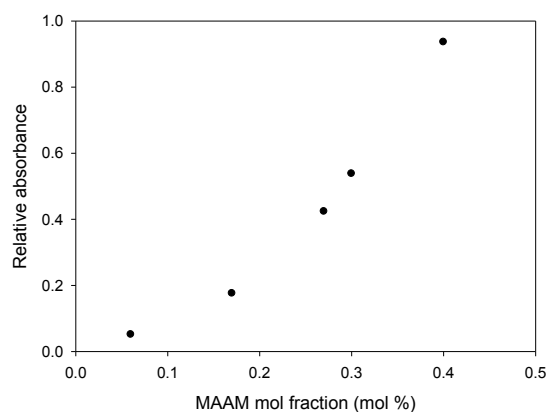


Figure 4. Relative absorption of carbonyl at 1670  $\text{cm}^{-1}$  with different mol fractions of MAAM

Figure 3 illustrates the influence of MAAM mole percentage in the copolymer backbone on the amide carbonyl absorbance around 1680  $\text{cm}^{-1}$ . In order to calibrate the carbonyl absorption with an internal standard, the styrene absorption at 790  $\text{cm}^{-1}$  corresponding to the C-H bending was chosen as a reference peak taking into account its mole percent in the copolymer. The relative absorption of the carbonyl was then calculated with the following relation:  $R = (A/A_{\text{st}}) \times X_{\text{st}}$

In which, R is the relative absorbance; A is the original absorbance;  $A_{\text{st}}$  is the absorbance of C-H from styrene at 690  $\text{cm}^{-1}$ ;  $X_{\text{st}}$  is the mol fraction of styrene in the copolymer.

When MAAM content increases, carbonyl absorption dramatically shifts to lower frequency from 1671  $\text{cm}^{-1}$  to 1655  $\text{cm}^{-1}$ . Only one peak corresponds to the C=O absorption. This peak is the barycenter of free and bonded C=O. Generally, the shift of

the C=O can be explained in two ways: either the hydrogen bonds' strength is weakened by the change of temperature, or the amount of hydrogen bonds in the system decreases. However, here only the latter explanation is acceptable since the temperature is not changed, which indicates that the C=O stretching absorption is influenced by the fact that intramolecular hydrogen bonds are being replaced by intermolecular ones.

When the MAAM content increases, absorbance of the carbonyl group also increases due to the increment of amide DA moiety shown in figure 4. Relative absorbance after calibration  $A_{C=O}/A_{St} \times X_{St}$  are illustrated in relation with MAAM contents. It proves that the sensitivity of MAAM influencing the hydrogen bond interactions is extremely intense with a high MAAM content above 30%.

Temperature-dependent absorption shift was recorded for 40% MAAM copolymers in order to study the temperature influence on the hydrogen bonds in the copolymers. The carbonyl absorbance peak slightly shifts to the higher wavenumbers during the heating process from 30°C to 180°C. The relating graph is not placed here since the shift is extremely mild. It shows that the hydrogen bonds are only gradually and slightly destroyed with the increase of temperature while strong hydrogen bonds still exist in the PMAAM segments.

### Effect of MAP concentration to P(MAP-co-St) in FTIR spectra

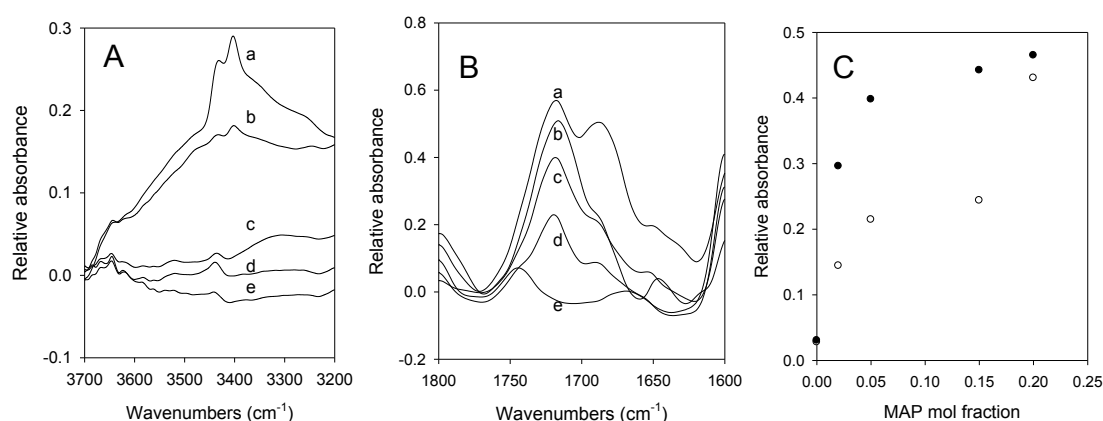


Figure 5. IR spectra (A and B) of P(MAP-co-St) with different MAP contents at room temperature: a) 20% MAP; b) 15% MAP; c) 5% MAP; d) 2% MAP; e) 0% MAP

C: Relative absorbance of C=O absorption: ●- for free C=O peaks at 1700 cm<sup>-1</sup>, ○- for H-bonded C=O at 1680 cm<sup>-1</sup>

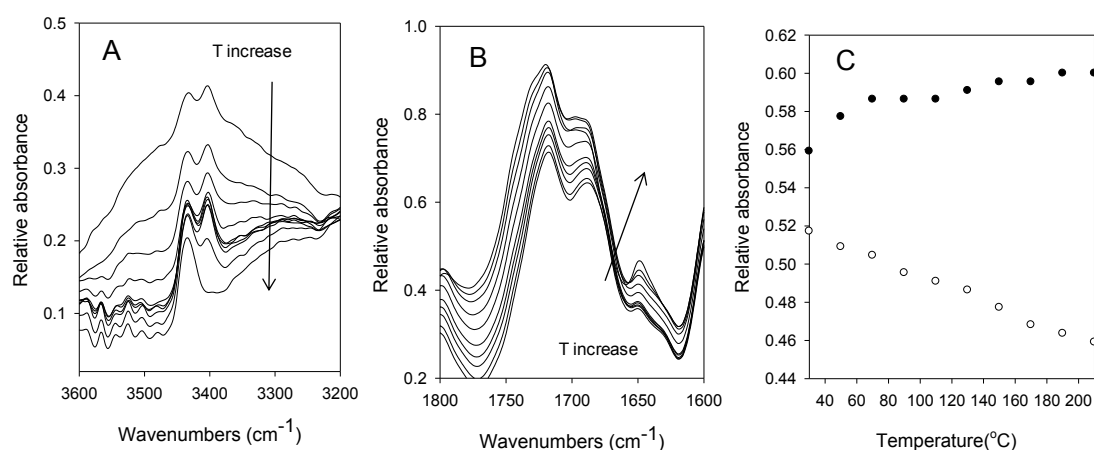


Figure 6. IR spectra (A and B) with 20 mol% MAP in P(MAP-co-St) at different temperatures (30~210°C)

C: Relative absorbance of C=O peaks: -●- for free C=O peaks at 1700 cm<sup>-1</sup>, -○- for H-bonded C=O at 1680 cm<sup>-1</sup>

Similar FTIR characterizations are applied for P(MAP-co-St) as well as for P(MAAM-co-St). N-H absorbance as well as C=O were investigated, with the N-H stretching vibration varying from 3600 to 3200 cm<sup>-1</sup> and carbonyl C=O stretching vibration varying from 1800 to 1600 cm<sup>-1</sup> respectively.

Figure 5A shows that for the N-H vibration, the absorbance intensity increases when MAP ratio in the copolymer is increased. This is reasonable since the more MAP involves the more hydrogen bonds. Two peaks in this domain are related to free N-H (two sharp peaks around 3450 cm<sup>-1</sup>) and one large peak between 3200 and 3700 cm<sup>-1</sup> for bonded N-H.

C=O absorption offers further information to characterize the hydrogen bonds (Figure 5B). In fact, it splits into two peaks attributed to the free C=O at 1710 cm<sup>-1</sup> and hydrogen-bonded C=O at 1685 cm<sup>-1</sup> respectively. It is different from those in a P(MAAM-co-St) system as discussed before where only one peak is observed. This phenomenon is because of the wavenumbers of these two C=O absorptions: if free C=O and bonded C=O have distinctive wavenumbers with a difference of dozens of cm<sup>-1</sup>, the peaks are difficult to be overlaid to form one identical peak. Absorption intensification is also observed in both peaks with an increasing MAP content which is normal and obeying Beer-Lambert law.

It is notable that although the intensity of both these peaks is influenced by the MAP content, the increment of hydrogen-bonded C=O absorbance is much more noticeable than that of free C=O absorbance in figure 5C. This means that the more MAP is induced, the stronger intermolecular hydrogen bonds instead of intramolecular ones are formed. The wavenumber of carbonyl absorption doesn't change a lot in this range of MAP concentration.

Figure 6 shows the temperature-dependent FT-IR spectra of 20 mol% MAP. With the increasing temperature, free C=O absorbance at  $1700\text{ cm}^{-1}$  slightly increases while hydrogen bonded C=O at  $1685\text{ cm}^{-1}$  shows a decrease in figure 6B and 6C. Intermolecular hydrogen bonds are thermo-responding so bonded carbonyl groups partially disassociate with the break of N-H...O=C interaction. Moreover, the shift of hydrogen bonded C=O stretching to a lower frequency (6B) also gives the evidence that hydrogen bonds between C=O and N-H were partly broken due to the high temperature. It is consistent with the intensity decline of N-H absorption at  $3410\text{ cm}^{-1}$  in figure 6A. All of these temperature dependence changes prove that the intermolecular hydrogen bonds in MAP are reduced but still exist even at higher temperatures.

The presence of hydrogen bonds in both P(MAAM-co-St) and P(MAP-co-St) was confirmed by FTIR spectroscopy here. The DA moieties influence as well as temperature responding influence were investigated through C=O absorption. The impact of MAP is more noticeable than MAAM which corresponds to their previous calculated  $K_{\text{ass}}$ .

#### **C-3.4. Solubility of P(MAAM-co-St) and P(MAP-co-St) with various DA moiety concentrations**

Formation of a cross-linked material can be determined by solubility tests. Uncross-linked polymers should be soluble in appropriate solvents, while cross-linked polymers can only be swelled. In this study, the copolymers using MAAM or MAP bearing associating moieties are expected to develop hydrogen bonds between the chains making the copolymer insoluble. Solvents of polystyrene were chosen for these tests (THF and  $\text{CHCl}_3$ ) and the amounts of MAAM or MAP are the only factors affecting the solubility of the copolymers.

As shown in scheme 1 and scheme 2, MAP or MAAM moieties have donor and acceptor neighbors that could self-assemble to DA-AD homodimers. After the copolymerization with styrene, both these DA-AD assemblies behave like crosslinking spots in the polymer networks. The results in table 2 and table 3 show that with an increasing molar ratio of the DA moiety in copolymers, the solubility changes from soluble to insoluble.

Table 2. Solubility of P(MAAM-co-St) in different solvents for different MAAM/styrene compositions.

	CHCl <sub>3</sub> (r.t.)	CHCl <sub>3</sub> (50°C)	THF (r.t.)	THF (50°C)	DMSO (r.t.)	DMSO (180°C)	M <sub>n</sub> /M <sub>w</sub> g.mol <sup>-1</sup>
<b>6% MAAM</b>	□	□	□	□	□	□	32703 / 51864
<b>17% MAAM</b>	□	□	□	□	□	□	38183 / 55377
<b>27% MAAM</b>	■	■	■	□	□	□	39273 / 76374
<b>30% MAAM</b>	■	■	■	■	□	□	25758 / 42858
<b>40% MAAM</b>	■	■	■	■	■	□	23410 / 47090

■ = insoluble; □=soluble

Table 3. Solubility of P(MAP-co-St) in different solvents for different MAAM/styrene compositions.

	CHCl <sub>3</sub> (r.t.)	THF(r.t.)	DMSO(r.t.)	DMSO(180°C)	M <sub>n</sub> /M <sub>w</sub> (g.mol <sup>-1</sup> )
<b>0% MAP</b>	□	□	□	□	18210 / 24090
<b>2% MAP</b>	□	□	□	□	18900 / 25860
<b>5% MAP</b>	■	■	□	□	-
<b>10% MAP</b>	■	■	■	□	-
<b>15% MAP</b>	■	■	■	□	-
<b>20% MAP</b>	■	■	■	□	-

■ = insoluble; □=soluble

This behavior also depends on the solvents' polarity. In less polar solvents such as CHCl<sub>3</sub> and THF, the assemblies are difficult to dissociate if intermolecular hydrogen bonds are strong and copolymers are insoluble in these solvents. In solvents with high polarity as DMSO, hydrogen bonds' interactions are weakened, and the solubility of these copolymers is enhanced. For insoluble copolymers, the increase of temperature will improve the solubility, i.e. for P(MAP-co-St). Some of the copolymers, soluble only at high temperature, precipitated again when the temperature dropped down, showing the thermo-responding properties and reversible solubility of these copolymers, which is a feature of supramolecular polymers.

Comparing MAAM and MAP, it is obvious that the latter has stronger interactions than the former in the medium-polar solvents, which is in agreement with  $K_{\text{ass}}$  results. Copolymers with a MAP content superior to 5 mol% are insoluble in CHCl<sub>3</sub> while in P(MAAM-co-St), this threshold is 17%.

Solubility tests of P(MAAM-co-St) and P(MAP-co-St) confirmed that the polymer networks were formed and controlled by adjusting the molar percentage of DA moiety in the copolymers. The networks based on MAP are stronger than those based on MAAM. They could only be broken at very high temperatures in a highly polar solvent such as DMSO. The threshold of P(MAP-co-St) which begins to show insolubility in THF is also lower as 5%, while in P(MAAM-co-St) it is 27%.

### C-3.5. Thermal properties of P(MAAM-co-St) and P(MAP-co-St)

Both P(MAP-co-St) and P(MAAM-co-St) copolymers show only one glass transition temperature.  $T_g$  obtained from both series cannot be fitted to Fox law. They are generally higher than predicted values from Fox equation because secondary interactions exist and restrict the chain motions and relaxations. In this case, Kwei equation (eq. 3) can represent experimental data [31, 53, 54].

$$T_g = \frac{W_1 T_{g1} + k W_2 T_{g2}}{W_1 + k W_2} + q W_1 W_2 \quad \text{Eq. 3}$$

Where  $T_{g1}$  and  $T_{g2}$  are the glass transition temperatures of the co-monomers and  $w_1$  and  $w_2$  their weight fractions.  $K$  and  $q$  are constants.  $Q$  value represents a measure of the interaction between both components. For  $k=1$ ,  $q=0$ , a simple additive rule is obtained.

In this case,  $T_g$  evolves linearly with monomer fraction, indicating that no specific interactions are involved in this copolymer system.

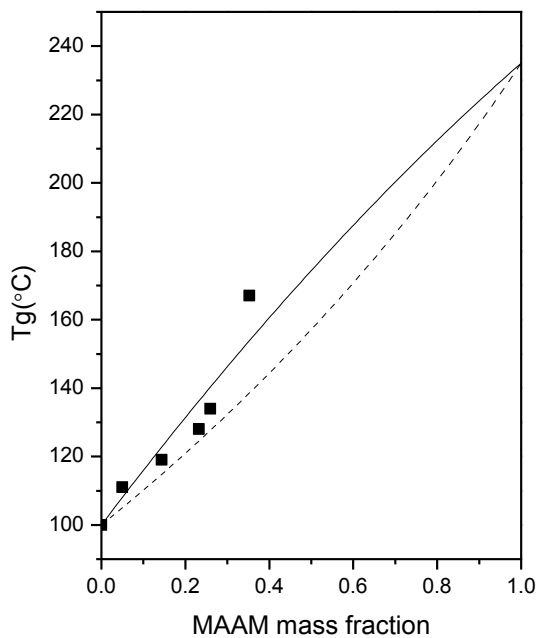


Figure 7. Glass transition temperature ( $^{\circ}\text{C}$ ) vs MAAM mass fraction in P(MAAM-co-St) copolymers, ■ experimental point; -- fits  $T_g$  respecting Fox equation;

— fits  $T_g$  respecting Kwei equation

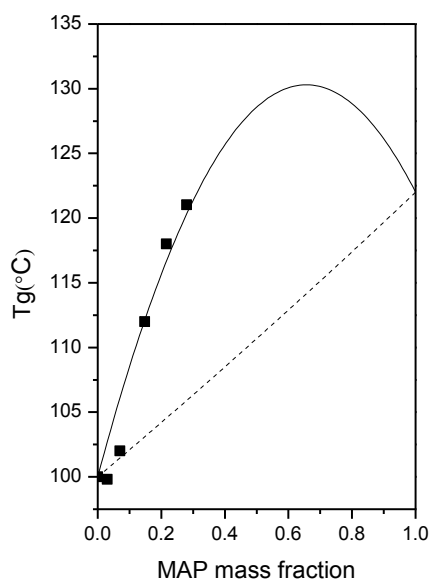


Figure 8. Glass transition ( $^{\circ}\text{C}$ ) vs MAP mass fraction in P(MAP-co-St) copolymers,

■ for experimental point; -- fits  $T_g$  respecting fox equation;

— fits  $T_g$  respecting Kwei equation

Differences of  $T_g$ s obtained from Fox equation and experimental values for P(MAAM-co-St) (in figure 7) are not obvious. Curve fitting results in figure 7 give  $k=1$ ,  $q=27.47$ . This high value represents the extent of secondary interaction between polymer chains and the existence of intermolecular hydrogen bonds [53].

$T_g$ s of P(MAP-co-St) perform a more distinct change depending on MAP mole fraction in figure 8. They are relatively close to the value calculated by Fox equation when MAP mole fraction is below 5%. For these samples, hydrogen bonding moieties are not sufficient for the association between the polymer chains. When MAP mole fraction is increased to 10%, 15% or even 20%, the differences of  $T_g$  between that predicted by Fox equation and the experimental data become more important. These differences are directly in relation with the MAP self-dimerization that increases the strengthening. Calculated constant  $q$  from curve-fitting for P(MAP-co-St) is 70.30, which is much higher than P(MAAM-co-St). Consequently, the dimerization between the DA moieties in the P(MAP-co-St) is much stronger than that in P(MAAM-co-St). Relative ratio of  $q_{\text{MAP-St}}$  and  $q_{\text{MAAM-St}}$  is in accordance with  $K_{\text{MAP-St}}$  and  $K_{\text{MAAM-St}}$  calculated by NMR spectroscopy.

Thanks to this interesting result, it can be seen that although neither  $T_g$ s obtained from P(MAAM-co-St) nor P(MAP-co-St) could obey the traditional Fox equation; their fitting with Kwei equation proves the existence of secondary interactions. The  $Q$  value derived from Kwei equations could be used as a measure of intermolecular interactions qualitatively.

### C-3.6. Structure analyses by dynamic rheology in the molten state

DMA (dynamic mechanical analyses) of P(MAAM-co-St) and P(MAP-co-St) copolymers are reported in this part. Since the differences of  $T_g$  have already been discussed above, only the viscoelasticity above  $T_g$  was analyzed here. The results of P(MAAM-co-St) and P(MAP-co-St) are discussed separately since they are quite different.

**P(MAAM-co-St) copolymers dynamic rheology****Frequency sweep**

Storage ( $G'$ ) and loss ( $G''$ ) moduli evolutions with angular frequency of P(MAAM-co-St) are shown in Figure 9. They were measured at least 30 °C above  $T_g$ . Since  $T_g$  in P(MAAM-co-St) varies from 100 °C to 167 °C, the testing temperature was set at 200 °C to ensure that all the thermoplastic samples suited the condition of molten state rheological analyses.

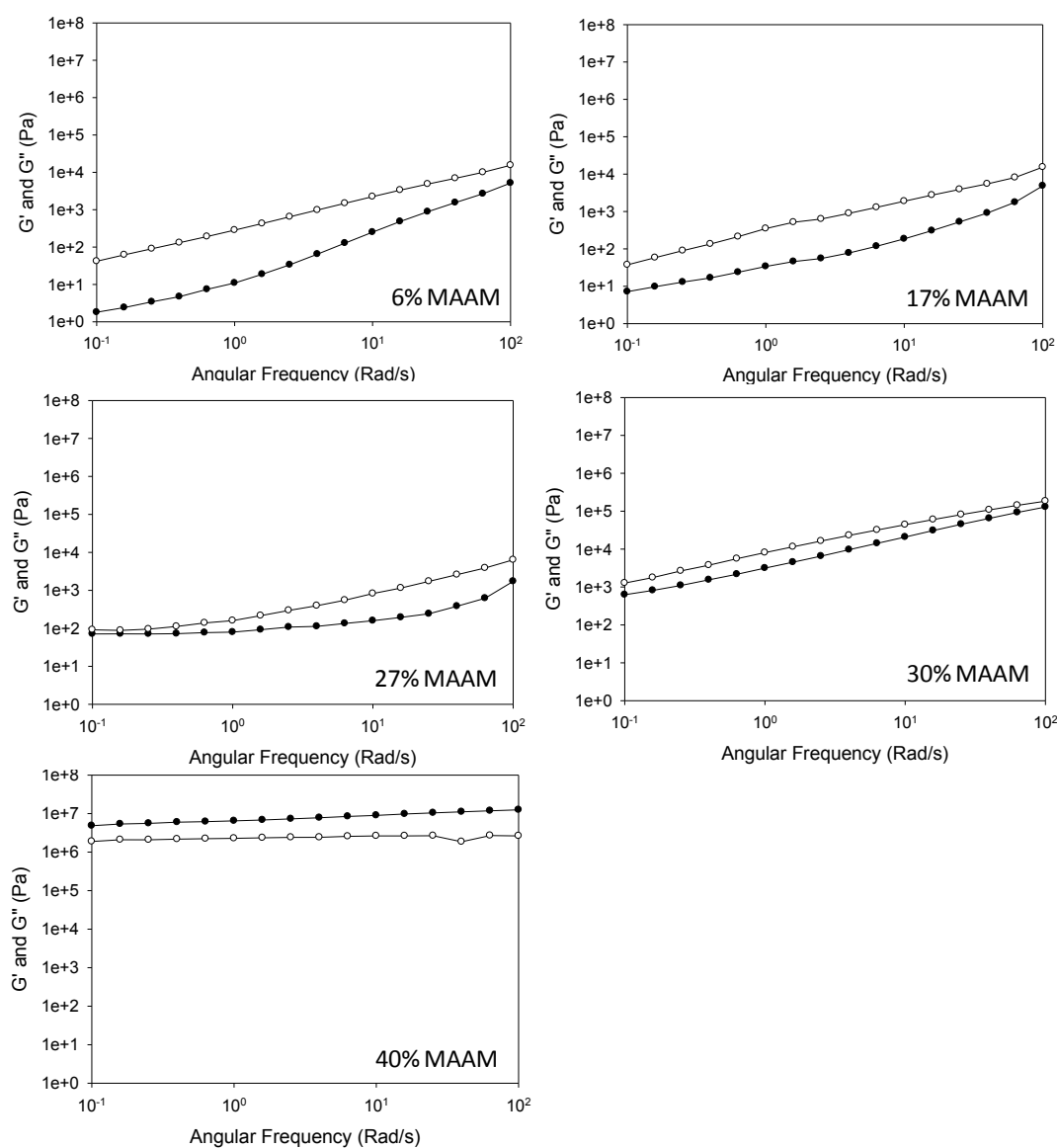


Figure 9.  $G'$  (●) storage modulus (Pa) and  $G''$  (○) loss modulus (Pa) of P(MAAM-co-St) in frequency sweep tests at  $T = 200^\circ\text{C}$  strain=10% for 6 mol%, 17 mol% and 27 mol% of MAAM; Strain =1% for 30 mol% of MAAM; Strain =0.1% for 40 mol% of MAAM.

Copolymers with MAAM contents inferior to 30% have parallel descending  $G'$  and  $G''$  curves from high to low frequency. Storage moduli are low ( $10^0$  to  $10^4$  Pa) and are depending on the frequency indicating that these materials are in the viscous states without a network formation. The interaction of DA moieties in MAAM is weak, and the mobility of polymer chains is barely restricted at the tested temperature. When the MAAM content in the copolymer increases (40 mol%), a considerable increase of moduli is obtained when comparing 30% MAAM to 27% MAAM. Furthermore, a plateau on the storage modulus appears and  $G'$  becomes higher than  $G''$  and almost independent from the frequency. Intermolecular interactions, in this sample are denser, and highly concentrated which limits polymer chain movements in a small range, indicating the formation of networks with rubbery-like performances.

### Temperature ramps

Storage ( $G'$ ) and loss moduli ( $G''$ ) evolutions in function of the temperature of P(MAAM-co-St) are shown in figure 10. Temperature ramp tests were subsequently performed for these copolymers in order to observe the full transition zones above the glass transition temperature.

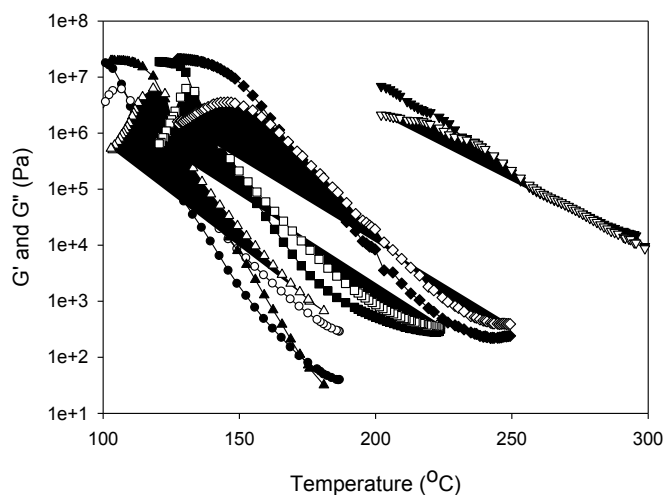


Figure 10.  $G'$  storage modulus (Pa) and  $G''$  loss modulus (Pa) of P(MAAM-co-St) in temperature ramp tests: ramping rate at  $3\text{ }^{\circ}\text{C}\cdot\text{min}^{-1}$ , frequency =  $1\text{ rad}\cdot\text{s}^{-1}$ , strain = 10%-0.1%, -●-  $G'$  of 6 mol% MAAM; -○-  $G''$  of 6 mol% MAAM; -▲- 17 mol%  $G'$  of MAAM; -△-  $G''$  of 17 mol% MAAM; -■- 27 mol%  $G'$  of MAAM; -□-  $G''$  of 27 mol% MAAM; -◆- 30 mol%  $G'$  of MAAM; -◇-  $G''$  of 20 mol% MAAM; -▼- 40 mol%  $G'$  of MAAM; -▽-  $G''$  of 40 mol% MAAM.

The crossover temperature at which  $G''$  overpasses  $G'$ , corresponds to the joint effect of the glass transition and the hydrogen bond interactions. It is obvious in the temperature-moduli graph that the addition of MAAM has a considerable effect shifting  $G'$  and  $G''$  curves, as well as the corresponding  $T_{\text{crossover}}$ , to high temperatures in figure 10. A second plateau attributed to hydrogen bond interactions appears in copolymers containing over 27% of MAAM. It shows that a part of DA associations still exists at high temperatures.

Although the plateau moduli are low ( $10^3$  Pa) in 27% MAAM and 30% MAAM and copolymers are in viscous states, with a further increment of MAAM content to 40%, the plateau modulus is increased to  $10^5$  Pa and the copolymer is in a rubbery state suggesting a high possibility of network formation. These results are in perfect concordance with those obtained in the frequency sweep tests and confirm the conclusions of the previous parts.

### P(MAP-co-St) copolymers dynamic rheology

#### Frequency sweep

$K_{\text{ass}}$  results showed that the association in P(MAP-co-St) was stronger than that in P(MAAM-co-St); thus a more distinctive influence of MAP on both the copolymers' structure and viscoelasticity is expected. Figure 11 shows the frequency-dependent  $G'$  and  $G''$  curves of various samples having different MAP contents.

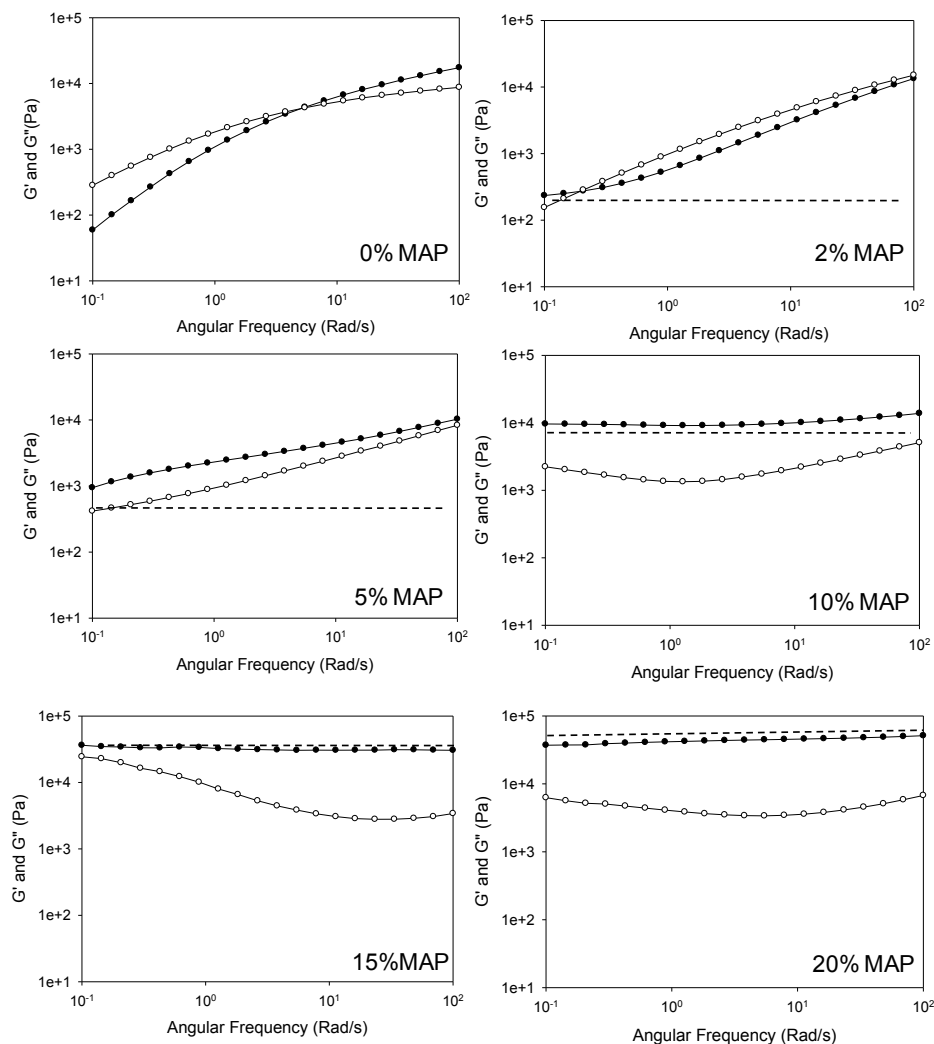


Figure 11.  $G'$  storage modulus (Pa) and  $G''$  loss modulus (Pa) of P(MAP-co-St) in frequency sweep tests:  $T = 200\text{ }^{\circ}\text{C}$ , strain=10%.  $\bullet$  : storage modulus  $G'$ ,  $\circ$  : loss modulus  $G''$ .

Obviously, the evolutions of  $G'$  moduli with MAP content are more noticeable than MAAM. Even a small amount of MAP influences both storage and loss moduli; addition of an auxiliary line (dash line in figure 11) helps to illustrate the MAP's effect. For the copolymer with 2 mol% MAP, the appearance of a plateau around  $5 \times 10^2$  Pa, only at low frequency, is due to the joint influence of MAP impact and neat PS performance. This

concentration of MAP is not so high that the slope coefficient of  $G'$  curve approaches to neat PS at high frequency. No network is formed in these two samples. With the increase of MAP content, the slope of  $G'$  curve is softened with a lower slope coefficient due to the elevation of MAP effect as shown from 0% MAP to 5% MAP. The plateau at low frequency range is more clearly observed, and is eventually independent of the frequency with further increment of MAP from 10% to 20%, showing the formation of networks. Ascending  $G'$  moduli due to MAP content prove that DA homodimerizations reduce the mobility of the polymer chains and reinforce the copolymer viscoelastic properties.

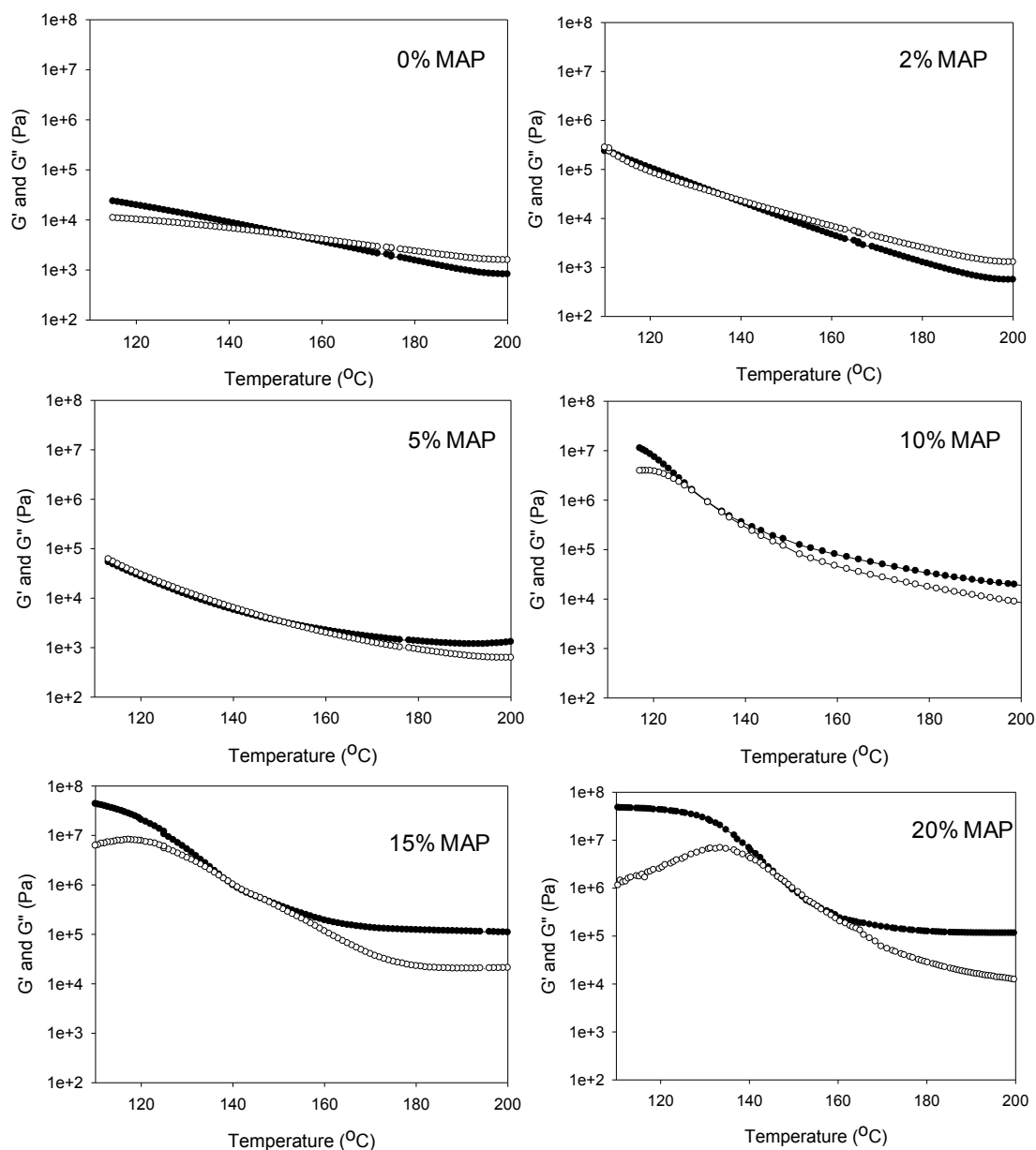


Figure 12.  $G'$  storage modulus (Pa) and  $G''$  loss modulus (Pa) of P(MAP-co-St) in temperature ramp tests: ramping rate =  $3\text{ }^{\circ}\text{C}\cdot\text{min}^{-1}$ , frequency =  $1\text{ rad}\cdot\text{s}^{-1}$ , strain = 10%,

● : storage modulus  $G'$ , ○ : loss modulus  $G''$

### Temperature ramps

Temperature dependent  $G'$  and  $G''$  of P(MAP-co-St) are shown in figure 12. Two important points need to be noticed with temperatures ranging from 110 to 200 °C. First, the increase of MAP content has a direct effect on the storage moduli increase although it is less obvious for copolymers with low MAP content (2-5 mol%). It is in accordance with the conclusion of frequency sweep tests that more MAP moieties could

better improve thermo-resistance properties. The further increase of MAP content, or more specifically the increase of DA hydrogen bond moieties from 5% to 20%, will lead to the second important observation: higher concentrations of DA-AD hydrogen bonding dimer block the chain movements and create a  $G'$  plateau at high temperatures. This plateau cannot be observed in the pure PS at the tested temperature range, whereas it appears in the copolymers with high MAP content (10-20 mol%) between 170-200 °C. This is unprecedented because although a few works [14, 34, 36] present the introduction of supramolecular interaction into polymer materials which transform materials from a viscous liquid to a rubbery-like state with high modulus around  $10^5$  Pa, they are normally limited at comparatively low temperature (30-120°C).

The selective appearance of a rubbery plateau in P(MAP-co-St) with MAP content higher than 5% MAP confirmed that the polymer network could be controlled by adjusting the molar ratio of DA moiety in the copolymers. The interaction, between MAP moieties by homodimerization, is strong and present in the copolymers even at high temperature.

#### **C-4. Conclusion**

Two supramolecular copolymers, P(MAAM-co-St) and P(MAP-co-St) were prepared by radical copolymerization between styrene and monomers bearing double hydrogen bonding moieties. Properties of the copolymer-assembled networks such as glass transition temperature and viscoelasticity behavior can be controlled by altering the comonomer composition. Both  $G'$  and  $G''$  moduli increased with increasing MAAM or MAP contents, and a plateau with high modulus appears in P(MAP-co-St) with MAP content above 10 mol%. These controllable properties were attributed to the strength of the dimers formed by hydrogen bonds. The hydrogen bonding strength has been quantified by  $^1\text{H-NMR}$  spectroscopy at different concentrations to obtain  $K_{\text{ass}}$  calculated at  $6.75 \text{ M}^{-1}$  for MAAM and  $16.75 \text{ M}^{-1}$  for MAP. Furthermore, the stronger hydrogen bond interaction of P(St-co-MAP), compared to P(St-co-MAAM), was proved by applying Kwei equation to  $T_g$  dependence against copolymer composition and by solubility tests. This study takes great advantage of simple synthesis procedures of the supramolecular polymers compared to common complicated synthetic methods that refrain potential developments. The resulting double association by homodimerization endows cross-

linked PS based copolymers with good properties above Tg from monomers industrially available or easy to prepare.

#### **ACKNOWLEDGMENT**

The authors thank the financial support from China Scholarship Council (state scholarship fund). This work benefited from the cooperation between East China University of Science and Technology (China) and Université Jean-Monnet Saint-Etienne (France).

## REFERENCES

- [1] Aakeröy, C.; Epa, K. *Topics in Current Chemistry* **2012**, 1-23.
- [2] Du, J. Z.; Tang, Y. P.; Lewis, A. L.; Armes, S. P. *Journal of the American Chemical Society* **2005**, 127, (51), 17982-17983.
- [3] Lee, O. S.; Stupp, S. I.; Schatz, G. C. *Journal of the American Chemical Society* **2011**, 133, (10), 3677-3683.
- [4] Ghosh, A.; Lee, W. B. *Macromol. Res.* **2011**, 19, (5), 483-486.
- [5] Lehn, J. M. *Angew. Chem.-Int. Edit. Engl.* **1988**, 27, (1), 89-112.
- [6] Binder, W. H.; Zirbs, R., Supramolecular polymers and networks with hydrogen bonds in the main- and side-chain. In *Hydrogen Bonded Polymers*, 2007; Vol. 207, pp 1-78.
- [7] Patra, D.; Ramesh, M.; Sahu, D.; Padhy, H.; Chu, C. W.; Wei, K. H.; Lin, H. C. *Polymer* **2012**, 53, (6), 1219-1228.
- [8] Wan, D. C.; Chen, F.; Kakuchi, T.; Satoh, T. *Polymer* **2011**, 52, (15), 3405-3412.
- [9] Chen, X. M.; Lu, X. M.; Cui, K.; Cui, W.; Wu, J.; Lu, Q. H. *Polymer* **2011**, 52, (14), 3243-3250.
- [10] Chiang, W. H.; Lan, Y. J.; Huang, Y. C.; Chen, Y. W.; Huang, Y. F.; Lin, S. C.; Chern, C. S.; Chiu, H. C. *Polymer* **2012**, 53, (11), 2233-2244.
- [11] Chen, Y. Y.; Lin, H. C. *Polymer* **2007**, 48, (18), 5268-5278.
- [12] Zou, G.; Wang, Y. L.; Zhang, Q. J.; Kohn, H.; Manaka, T.; Iwamoto, M. *Polymer* **2010**, 51, (10), 2229-2235.
- [13] Folmer, B. J. B.; Sijbesma, R. P.; Versteegen, R. M.; van der Rijt, J. A. J.; Meijer, E. W. *Advanced Materials* **2000**, 12, (12), 874-878.
- [14] Rieth, L. R.; Eaton, R. F.; Coates, G. W. *Angewandte Chemie-International Edition* **2001**, 40, (11), 2153-2156.
- [15] Adamson, A. W., *A textbook of physical chemistry*. Academic Press: 1986.

- [16] Schalley, C., *analytical methods in supramolecular chemistry*. wiley-vch Verlag GmbH & Co. KGaA, Weinheim: 2007.
- [17] Ilhan, F.; Gray, M.; Rotello, V. M. *Macromolecules* **2001**, 34, (8), 2597-2601.
- [18] Chen, J. S.; Rosenberger, F. *Tetrahedron Letters* **1990**, 31, (28), 3975-3978.
- [19] Horman, I.; Dreux, B. *Helvetica chimica acta* **1984**, 67, (3), 754-764.
- [20] Osmialowski, B.; Kolehmainen, E.; Dobosz, R.; Gawinecki, R.; Kauppinen, R.; Valkonen, A.; Koivukorpi, J.; Rissanen, K. *J. Phys. Chem. A* **2010**, 114, (38), 10421-10426.
- [21] Osmialowski, B.; Kolehmainen, E.; Kalenius, E.; Behera, B.; Kauppinen, R.; Sievaenen, E. *Structural Chemistry* **2011**, 22, (5), 1143-1151.
- [22] Bocian, W.; Kawecki, R.; Bednarek, E.; Sitkowski, J.; Pietrzyk, A.; Williamson, M. P.; Hansen, P. E.; Kozerski, L. *Chemistry-a European Journal* **2004**, 10, (22), 5776-5787.
- [23] Kao, D. Y.; Shu, W. T.; Chen, J. S. *J. Chin. Chem. Soc.* **2005**, 52, (6), 1171-1178.
- [24] Dethlefs, C.; Eckelmann, J.; Kobarg, H.; Weyrich, T.; Brammer, S.; Nather, C.; Luning, U. *European Journal of Organic Chemistry* **2011**, (11), 2066-2074.
- [25] Brammer, S.; Luning, U.; Kuhl, C. *European Journal of Organic Chemistry* **2002**, (23), 4054-4062.
- [26] Beijer, F. H.; Sijbesma, R. P.; Kooijman, H.; Spek, A. L.; Meijer, E. W. *Journal of the American Chemical Society* **1998**, 120, (27), 6761-6769.
- [27] Brunsveld, L.; Folmer, B. J. B.; Meijer, E. W.; Sijbesma, R. P. *Chem. Rev.* **2001**, 101, (12), 4071-4097.
- [28] Hirschberg, J.; Beijer, F. H.; van Aert, H. A.; Magusim, P.; Sijbesma, R. P.; Meijer, E. W. *Macromolecules* **1999**, 32, (8), 2696-2705.
- [29] De Greef, T. F. A.; Smulders, M. M. J.; Wolffs, M.; Schenning, A.; Sijbesma, R. P.; Meijer, E. W. *Chem. Rev.* **2009**, 109, (11), 5687-5754.
- [30] Oishi, T.; Lee, Y. K.; Nakagawa, A.; Onimura, K.; Tsutsumi, H. *Journal of Polymer Science Part a-Polymer Chemistry* **2002**, 40, (11), 1726-1741.

- [31] Kao, H. C.; Kuo, S. W.; Chang, F. C. *J. Polym. Res.-Taiwan* **2003**, 10, (2), 111-117.
- [32] Coskun, M.; Temuz, M. M.; Demirelli, K. *Polymer degradation and stability* **2002**, 77, (3), 371-376.
- [33] Coskun, M.; Barim, G.; Temuz, M. M.; Demirelli, K. *Polymer-Plastic Technology and Engineering* **2005**, 44, (4), 677-686.
- [34] Woodward, P. J.; Merino, D. H.; Greenland, B. W.; Hamley, I. W.; Light, Z.; Slark, A. T.; Hayes, W. *Macromolecules* **2010**, 43, (5), 2512-2517.
- [35] Corbin, P. S.; Zimmerman, S. C. *Journal of the American Chemical Society* **1998**, 120, (37), 9710-9711.
- [36] Lange, R. F. M.; Van Gorp, M.; Meijer, E. W. *Journal of Polymer Science Part a-Polymer Chemistry* **1999**, 37, (19), 3657-3670.
- [37] Hofmeier, H.; Hoogenboom, R.; Wouters, M. E. L.; Schubert, U. S. *Journal of the American Chemical Society* **2005**, 127, (9), 2913-2921.
- [38] Sontjens, S. H. M.; Sijbesma, R. P.; van Genderen, M. H. P.; Meijer, E. W. *Journal of the American Chemical Society* **2000**, 122, (31), 7487-7493.
- [39] Feldman, K. E.; Kade, M. J.; Meijer, E.; Hawker, C. J.; Kramer, E. J. *Macromolecules* **2009**, 42, (22), 9072-9081.
- [40] Subramani, C.; Dickert, S.; Yeh, Y. C.; Tuominen, M. T.; Rotello, V. M. *Langmuir* **2011**, 27, (4), 1543-1545.
- [41] McKee, M. G.; Elkins, C. L.; Park, T.; Long, T. E. *Macromolecules* **2005**, 38, (14), 6015-6023.
- [42] Park, T.; Zimmerman, S. C. *Journal of the American Chemical Society* **2006**, 128, (35), 11582-11590.
- [43] Park, T.; Zimmerman, S. C. *Journal of the American Chemical Society* **2006**, 128, (44), 14236-14237.
- [44] Sartorius, J.; Schneider, H. J. *Chemistry-a European Journal* **1996**, 2, (11), 1446-1452.

- [45] Hisamatsu, Y.; Fukumi, Y.; Shirai, N.; Ikeda, S.-i.; Odashima, K. *Tetrahedron Letters* **2008**, 49, (12), 2005-2009.
- [46] Zimmerman, S. C.; Corbin, F. S. *Molecular Self-Assembly* **2000**, 96, 63-94.
- [47] Plante, A.; Mauran, D.; Carvalho, S. P.; Page, J.; Pellerin, C.; Lebel, O. *J. Phys. Chem. B* **2009**, 113, (45), 14884-14891.
- [48] Chapkanov, A. G.; Zareva, S. Y.; Nikolova, R.; Trendafilova, E. *Collect. Czech. Chem. Commun.* **2009**, 74, (9), 1295-1308.
- [49] Silverstein, R.; Webster, F., *Spectrometric Identification of Organic Compound*. Wiley-India: 2006.
- [50] Milani, A.; Castiglioni, C.; Di Dedda, E.; Radice, S.; Canil, G.; Di Meo, A.; Picozzi, R.; Tonelli, C. *Polymer* **2010**, 51, (12), 2597-2610.
- [51] Chen, S. J.; Hu, J. L.; Zhuo, H. T.; Yuen, C. W. M.; Chan, L. K. *Polymer* **2010**, 51, (1), 240-248.
- [52] Kuo, S. W. *J. Polym. Res.* **2008**, 15, (6), 459-486.
- [53] Hsu, W. P. *Thermochim. Acta* **2006**, 441, (2), 137-143.
- [54] Slark, A. *Polymer* **1999**, 40, (8), 1935-1941.

## Chapter D

# Polyurea-urethane supramolecular thermo-reversible networks

Yiping NI <sup>1,2,3</sup>, Frédéric BECQUART <sup>1,2,3</sup>, Mohamed TAHA <sup>1,2,3\*</sup>, Jianding CHEN <sup>4</sup>

<sup>1</sup> Université de Lyon, F-42023, Saint-Etienne, France;

<sup>2</sup> CNRS, UMR 5223, Ingénierie des Matériaux Polymères, F-42023, Saint-Etienne, France;

<sup>3</sup> Université de Saint-Etienne, Jean Monnet, F-42023, Saint-Etienne, France;

<sup>4</sup> *Laboratory of Advanced Materials Processing, East China University of Science and Technology, 200237 Shanghai, China*

*\*correspondence: MTAHA@univ-st-etienne.fr*

## Résumé

De nouveaux réseaux polymères supramoléculaires polyurée-uréthane (PUU) ont été synthétisés à base de blocs tri-uret ou tétra-uret. La formation des réseaux étaient contrôlée par la conformation des motifs tri-uret ou tétra-uret, et leur concentration. La spectroscopie IRTF et des tests de solubilité ont montré que la présence significative de liaisons hydrogène est seulement observée pour les motifs tri-uret pour former des matériaux réticulés à température ambiante. La constante d'association par liaison hydrogène,  $K_{ass} = 95 \text{ M}^{-1}$ , a été calculée par  $^1\text{H}$ RMN pour les auto-associations des blocs tri-uret. L'analyse mécanique dynamique a confirmé que le tri-blocs uret permet de former des réseaux à température ambiante qui se défont entre 105 et 135 °C. Les blocs de tétra-uret ont une conformation pliée à température ambiante et à température relativement basse. Les polymères contenant ces motifs ne se réticulent à la température ambiante et au-dessous. L'augmentation de la température favorise la conformation pliée et mène à des liaisons hydrogène intermoléculaires et, à haute température, à des matériaux réticulés.

## Abstract

Novel polyurea-urethane (PUU) supramolecular polymer networks based on tri-uret and tetra-uret blocks were synthesized. The network formation was controlled through the conformation of hydrogen bonding moieties, and their concentration. FTIR spectroscopy and solubility tests showed the presence of significant hydrogen bonds only in tri-uret moieties and that these bonds conducted to cross-linked materials at room temperature. Hydrogen bonding association constant,  $K_{\text{ass}} = 95 \text{ M}^{-1}$ , was calculated using  $^1\text{H-NMR}$  for tri-uret blocks self-associations. Dynamic mechanical analysis confirmed that tri-uret blocks conducted to a network at room temperature and that de-cross-linking occurs between 105 and 135 °C. The tetra-uret blocks had a folded conformation at room and relatively low temperature. The polymers containing these moieties did not cross-link at room temperature and below. Temperature increase favored unfolded conformation and conducted to intermolecular hydrogen bonds and, at high temperature, to cross-linked materials.

### Keywords

Polyurea-urethane, hydrogen bonds, supramolecular, reversible networks, rheology

## D-1.Introduction

Conventional covalent bonded polymer networks with abundant advantages such as controllable thermal and mechanical properties have been widely researched for decades<sup>[1]</sup>. These networks are formed almost exclusively by covalent bonds and are generally irreversible. In contrast, supramolecular chemistry developed during the last few decades<sup>[2]</sup> is a popular study domain and is used by an increasing number of researchers for its innovative features like thermo-reversibility.

Supramolecular chemistry is defined as the chemistry of non-covalent and intermolecular bonds, “including the structures and functions of the moieties formed by association of two or more chemical species”<sup>[2]</sup>. These non-covalent interactions include hydrogen bonds<sup>[3-5]</sup>, amphiphilic interactions<sup>[6]</sup>, ionic attractions<sup>[7]</sup>, metal coordinations<sup>[8]</sup> and  $\pi$ - $\pi$  stacking<sup>[9]</sup> interactions. The supramolecular hydrogen bonds interaction is the most intensively studied<sup>[3, 10, 11]</sup> principally thanks to their versatility and directional property. The use of hydrogen bonds to prepare supramolecular polymer networks can endow the materials with reversible transformations from liquid (non-assembled state) to rubbery performance (assembled state)<sup>[12]</sup> depending on temperature or solvent concentrations<sup>[13, 14]</sup>. The directionality of hydrogen bond interactions induces the orientation of chain segments, leading to ordered conformations, and even thermotropic liquid crystalline materials<sup>[15]</sup>. Having these advantages, strengthened interactions with different hydrogen bonding pair numbers make the replacement of covalent bonds possible and therefore yield non-covalent cross-linked networks especially when the association constant  $K_{\text{ass}}$  is above  $10^7 \text{ M}^{-1}$ , as obtained for example in typical quadruple hydrogen bonding moiety like ureidopyrimidone (UPy)<sup>[16, 17]</sup>.

Polyurea-urethanes (PUU) have the potentiality to self-assemble through hydrogen bond supramolecular interactions<sup>[18]</sup>. PUU are often synthesized by alternating soft and hard segments along the molecular chains. Hard segments are usually synthesized from the

reactions of isocyanates and amines, while the soft segments are typically formed from polyesters, polyethers, or alkyl blocks. Urea groups contain both hydrogen donors (D) N-H and hydrogen acceptors (A) C=O which can either associate with complementary hydrogen bond moieties <sup>[19]</sup>, such as carboxylic groups <sup>[20, 21]</sup>, or form dimers or multimers among themselves <sup>[22, 23]</sup>.

Association constant,  $K_{\text{ass}}$ , is a useful parameter to quantify the strength of hydrogen bond interactions in a supramolecular network. Reversible supramolecular polymer networks are often based on triple or quadruple hydrogen bond pairs <sup>[24, 25]</sup>. These moieties have high association constants  $K_{\text{ass}}$  exceeding  $10^5 \text{ M}^{-1}$ . Polyurea and polyurethane supramolecular networks are comparatively less reported in literature although network formation is achievable.

Low molecular weight gelators based on the structure R-NHCONH-X-NHCONH-R have been synthesized and tested for their ability to cause gelation of organic solvents<sup>[22]</sup>. These urea compounds spontaneously form highly ordered fibers when absorbed on graphite and fibers from cooled homogeneous solutions through the formation of multiple intermolecular hydrogen bonds. The overall result is a long-term thermal stability of the structures. The gels formed by these urea compounds are stable but irreversibly disrupted by mechanical agitation. However, they can be restored by heating them above melting temperature, followed by cooling down to room temperature, indicating that the gel formation is thermo reversible.

In Wisse's study, bis-(ureido)butylene-based supramolecular fillers were incorporated in a poly( $\epsilon$ -caprolactone)-based polyurea in a modular approach via a "perfect-fit" principle <sup>[26, 27]</sup>. Although no network formation is indicated, stiffer materials are obtained without a decrease in tensile strength or elongation at break.

Moreover, the molecular features of fatty acid based self cross-linking polyurethane urea that influence the micro phase morphology and dynamic mechanical behavior of polymer

were exploited by Patel <sup>[28]</sup>. With higher urea contents, higher strength of hydrogen-bonding among urea linkages results in improved inter connectivity of hard segments.

Reversible polymer networks could be successfully achieved by the self-assembly of urea blocks in polyurea as discussed above. The network results in stiffer materials with high moduli, while it is thermo-reversible. However, the  $K_{\text{ass}}$  were not calculated in these studies. Recently, in a study on thermo-reversible polyurethane networks by Woodward<sup>[29]</sup>, the  $K_{\text{ass}}$  were calculated and varied from 7 to 45  $\text{M}^{-1}$  depending on the chemical structures of the polyurethanes. Viscometric analyses demonstrated that these bisurethane species assembled into extended hydrogen-bonded networks both in solution and in bulk, and the strength of the material is due to the crystallization of the end groups into hard micro domains that give the polymer a 3D network structure.

In this study, attempts to prepare polyurethane-co-urea supramolecular thermo-reversible networks were made. Readily commercially available monomers, urea and biuret, were used to build supramolecular interactions by tri-uret and tetra-uret blocks in one-step polycondensation. The effect of the temperature on the conformations of multiurets, and consequently hydrogen bonding, association constant, cross-linking, and de-cross-linking of the polymers will be analyzed. According to literature, a  $K_{\text{ass}}=100 \text{ M}^{-1}$  seems reasonable to obtain a supramolecular network with a thermo-reversibility within a temperature range of 100 to 160°C.

## D-2. Experimental Section

**Reagents.** Urea, biuret, glycerol, octan-1-ol, pentan-1-ol, 4,4'-Methylenebis(cyclohexyl isocyanate) (HMDI), phenyl isocyanate, anhydrous dimethyl sulfoxide (DMSO) were purchased from Sigma Aldrich and used as received. Glycerol was first dehydrated by molecular sieves 3 Å (rod shape, size 1/16 inch, Fluka) for 24 hours.

**Preparation of polyurea-urethane.** For urea-based (PU series) systems, urea, pentan-1-ol and glycerol (in table 1) were first magnetically mixed at 125 °C in a double-neck flask until a homogenous mixture was obtained. Then weighted HMDI was added dropwise with a syringe. The system was heated for 5-7 hours at 125 °C until the disappearance of the isocyanate absorption at 2238 cm<sup>-1</sup> by acquisition of samples withdrawn every 15 minutes.

**Table 1.** Formulations of PU series with different functionalities

PU series	Glycerol: urea: mono-alcohol: HMDI (mol ratio)	Glycerol mass%	Urea mass%	Pentan-1-ol mass%	HMDI mass%
PU F=1	1:1:3:4	6.3%	4.1%	18.0%	71.6%
PU F=2	1:2:3:5	5.1%	6.7%	14.8%	73.3%
PU F=3	1:3:3:6	4.4%	8.5%	12.5%	74.6%
PU F=4	2:4:4:9	5.9%	7.7%	11.2%	75.2%
PU F=5	3:5:5:12	6.6%	7.2%	10.6%	75.6%

For biuret-based (PU Bi series) systems, urea, octan-1-ol and glycerol (in table 2) were first magnetically mixed at 175 °C in a double-neck flask until a homogenous mixture was obtained. Then weighted HMDI was added dropwise with a syringe. The system was heated for 3-5 hours at 175 °C until the disappearance of the isocyanate absorption at 2238 cm<sup>-1</sup> by acquisition of samples withdrawn every 15 minutes.

**Table 2.** Formulations of PU Bi series with different functionality

PU Bi series	Glycerol: biuret: mono-alcohol: HMDI (mol ratio)	Glycerol mass%	Biuret mass%	Octan-1-ol mass%	HMDI mass%
PU Bi F=1	1:1:3:4	5.6%	6.3%	23.9%	64.2%
PU Bi F=2	1:2:3:5	5.1%	6.7%	14.8%	73.3%

PU Bi F=3	1:3:3:6	4.4%	8.5%	12.5%	74.6%
PU Bi F=4	2:4:4:9	5.9%	7.7%	11.2%	75.2%
PU Bi F=5	3:5:5:12	6.6%	7.2%	10.6%	75.6%

All the products were dried under vacuum (0.2 mbar) at 120 °C for 4 hours before further characterizations.

**Synthesis of polyurea assembling moiety models.** Two polyurea models, 1,1-2(N-Phenylaminocarbonyl)urea, and 1,1-2(N-Phenylaminocarbonyl)triuret, were synthesized specifically to calculate the association constant of dimers by <sup>1</sup>H-NMR.

1,1-2(N-Phenylaminocarbonyl)urea, 1, was synthesized by the reaction of phenyl isocyanate and urea. A solution of 2g (0.0333mol) of urea in 10mL DMSO was prepared by magnetic stirring in a single-neck flask at 70 °C. Then 7.93g (0.0666mol) phenyl isocyanate was added dropwise into the flask. The system was heated for 3 hours until the disappearance of the isocyanate absorption at 2238 cm<sup>-1</sup> controlled by FTIR. The solution was precipitated in 500 mL of deionized water and then filtered. Precipitate residues were dried at 70°C under vacuum (0.2 Mbar) for 8 hours.

1,1-2(N-Phenylaminocarbonyl)triuret ,2 was synthesized by the reaction of phenyl isocyanate and urea. A solution of 2g (0.0194mol) of biuret in 10mL DMSO was prepared by magnetic stirring in a single-neck flask at 70 °C. Then 4.62g (0.0388mol) phenyl isocyanate was added dropwise into the flask. The system was heated for 3 hours until the disappearance of the isocyanate absorption at 2238 cm<sup>-1</sup> monitored by FTIR. The solution was precipitated in 500 mL of deionized water and then filtered. Precipitate residues were dried at 70°C under vacuum (0.2 Mbar) for 8 hours.

### Characterizations

**FTIR spectroscopy.** FTIR spectra of polyurethane-urea were recorded with a Nicolet Nexus FTIR spectrometer. PUU and Potassium bromide (KBr) were dried, mixed and pressed

into pellets with a mass ratio 2 mg/160 mg. 32 scans were collected with a band width set at 4  $\text{cm}^{-1}$  at room temperature.

**Nuclear magnetic resonance (NMR) spectroscopy.** The  $^1\text{H}$ -NMR analyses of polyurea models 1 and 2 were performed with a Bruker Advance II spectrometer operating at 250 MHz, 300 K for 128 scans in  $\text{CDCl}_3$  and  $\text{DMSO-D}_6$  respectively with TMS as an internal reference. The binding constant was calculated by the spectra results in  $\text{CDCl}_3$  with dilutions varying from  $0.1 \text{ mol}\cdot\text{L}^{-1}$  to  $0.02 \text{ mol}\cdot\text{L}^{-1}$ .

The  $^1\text{H}$ -NMR analyses of PU Bi f=1 were performed with a Bruker DRX400 spectrometer operating at 400 MHz with a P-SEX probe operating at 300 K for 128 scans in  $\text{DMSO-d}_6$  with TMS as an internal reference.

The association of tri-uret or tetra-uret is assumed to be obtained by dimerization, so Chen's equation<sup>[30]</sup> was applied to calculate  $K_{\text{ass}}$ .

$$\delta_{\text{obs}} = \delta_{\text{m}} + (\delta_{\text{d}} - \delta_{\text{m}}) \frac{\sqrt{1+8K_{\text{ass}}C}-1}{\sqrt{1+8K_{\text{ass}}C}+1}$$

Where  $\delta_{\text{m}}$  is the monomer's chemical shift when they are free and not dimerized;  $\delta_{\text{d}}$  is the dimer chemical shift when all the monomers are dimerized;  $\delta_{\text{obs}}$  is the observed chemical shift;  $K_{\text{ass}}$  and  $C$  are respectively the association constant and the monomer concentration.

**Thermal analysis.** Thermal transitions were determined by differential scanning calorimetry (DSC) with a TA Q10 instrument, by heating and cooling ramps from  $-50$  to  $200 \text{ }^\circ\text{C}$  at  $10^\circ\text{C}\cdot\text{min}^{-1}$  under a nitrogen flow. The glass transition temperatures of the copolymers were measured by the second heating ramp.

**Rheology in molten states.** Molten state rheology of polyurethane-urea was performed on a strain-controlled ARES rheometer from Rheometrics in linear viscoelastic domain. They were performed using a parallel plate geometry with 25 mm diameter. The ramp temperature was  $1.5 \text{ }^\circ\text{C}\cdot\text{min}^{-1}$  between  $T_{\text{min}}$  and  $220^\circ\text{C}$ , in which  $T_{\text{min}}$  is the minimum temperature where the samples began slipping and/or transducer became overloaded. The frequency was fixed at

1 rad.s<sup>-1</sup> and the strain varied from 0.5 % at 100 °C to 10% around 160 °C. Above 160 °C, the strain was fixed at 10% to remain in the transducer's sensitivity range.

The tests were performed with a constant auto-tension by a normal force (20g).

### D-3. Results and discussion

**Synthesis and characterization of the PUUs with different functionalities.** PUUs were designed principally considering two aspects: the potential number of donor-acceptor assembling moieties in the zigzag unfolded conformation from tri-uret and tetra-uret blocks. The tri-uret blocks, named here PU series, were synthesized by reactions of urea with isocyanate. The tetra-uret blocks, named here PU Bi series, were synthesized by reactions of biuret with isocyanate. Their structures are given in Figure 1A. Multiple hydrogen donors (N-H group) with acceptors (C=O) endow PUU with self-assembling capacity. Secondly, the functionality defined as the number of multi-uret sequences in the prepolymer was adjusted by altering the stoichiometries of the different constituents of the reactive system (Table 1); the presence of multi-uret sequences in the prepolymer is symbolized by red rectangles in Figure 1B.

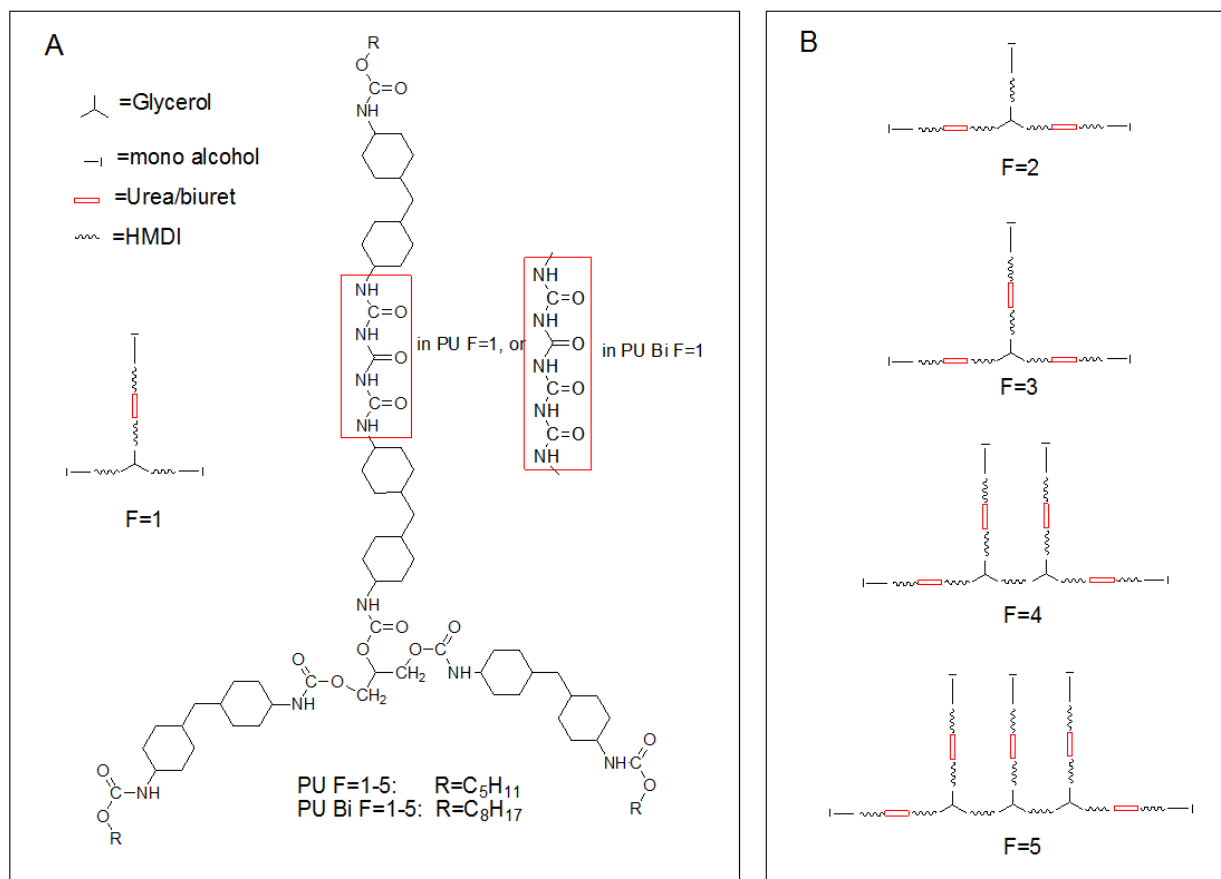


**Figure 1.** Expected structures of polyurea-urethane by structure design: A: Schematic structure and chemical structure of PU  $f=1$  and PU Bi  $f=1$ ; B: Schematic structures of PUU with different functionalities  $f=2-5$

**Solubility of PUU.** PUU based on both urea and biuret can lead under certain conditions to the formation of assembled polymer networks. The presence of a cross-linked material can be determined by simple solubility tests. If a sample cannot dissolve in a good solvent, polymer networks are then considered as formed. It is important to note that such experiments can only indicate a possibility of the presence or absence of a network, and such results must be confirmed by other analysis techniques.

For the PU series, the material having functionality equal to 1 was soluble in THF at room temperature, whereas the polymers having functionalities from 2 to 5 were insoluble. Under the same conditions, all the PU Bi were soluble in THF.

Considering that the various PU Bi have tetra-uret blocks and various PU have tri-uret blocks per function, the PU Bi's containing more donor acceptor moieties than equivalent PU's lead more readily to cross-linking in the case where the associations were intermolecular. Actually these results indicate that zigzag conformation is predominant for the various PU Bi while folded intramolecular interaction is predominant for PU (Figure 2). Equivalent results were also reported in literature for systems with more than four hydrogen bond moieties [31-33].

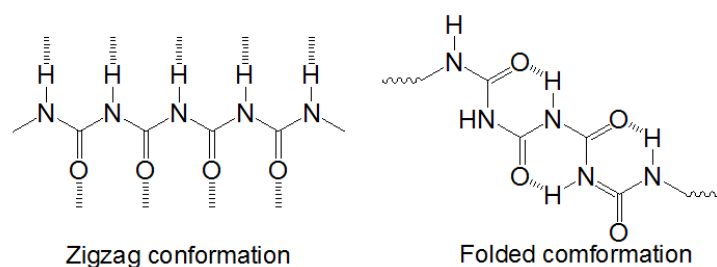


**Figure 2.** The zigzag and intramolecular bonded forms of tetra-urea segments in PU Bi series

**Qualitative characterization of hydrogen bonds in PUU by FTIR.** IR spectroscopy is widely used as an important experimental technique to determine the extent of hydrogen bonds in polymers containing amide blocks [34] and especially in PUUs [35]. Some researchers have shown that the quantitative measure of the hydrogen bonding strength determines the absorbance of peak absorption [36].

Upon the formation of hydrogen bonds formed between amide blocks, stretching involving the proton-donating groups (N-H) and the proton-accepting groups ( $-C=O$ ) are expected to have their absorption frequencies shifting towards lower energy, due to the reduction of the

bond force constant of the acceptor. The magnitude of these shifts, as well as changes in the absorption characteristics depend on the type (inter or intra) and the strength of the hydrogen bonds and the concentration of hydrogen bonding moieties in solvents [36, 37].

For the polyurea-urethane, two absorptions in PUUs will be influenced by the existence of hydrogen bonds: N-H stretching around  $3400\text{ cm}^{-1}$  and C=O stretching around  $1700\text{ cm}^{-1}$ , the latter being more obvious and easier to discuss due to its splitting from no hydrogen bonded amides, according to the existing studies [28, 38].

### Influence of tri-uret content in PU series at room temperature

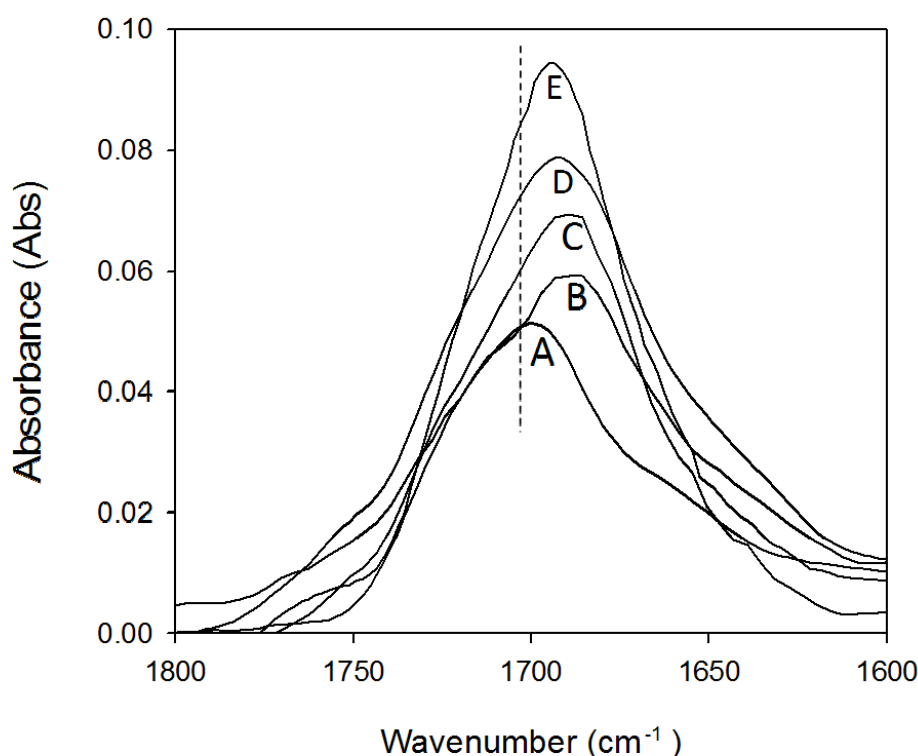


**Figure 3.** FTIR spectra of C=O absorption of PU series at room temperature: A: PU F=1; B: PU F=2; C: PU F=3; D: PU F=4; E: PU F=5.

In the present case, there is only one obvious absorption around  $1700\text{ cm}^{-1}$ . The other hydrogen bonded C=O at  $1650\text{ cm}^{-1}$  was considered as being overlaid by this absorption. The frequency of jointed C=O absorption is shifted depending on the synergy of both free C=O

and hydrogen-bonded C=O, so that the content of each is variational due to the sample formula.

FTIR spectra, with functionalities from 1 to 5 of PU series, are depicted in figure 3. Actually, it is the tri-uret mass percentage (table 1) instead of the functionalities that affects the carbonyl absorption. The C=O absorptions of PU F=1 with tri-uret content at 4.87 wt% is at  $1699\text{ cm}^{-1}$ . By increasing the tri-uret content to 6.71 wt% in PU F=2, the carbonyl absorption shifts dramatically to a lower wavenumber. This absorption shift was maximized in PU F=3 the carbonyl absorption of which is at  $1688\text{ cm}^{-1}$ . It is explained by the fact that the high concentration of tri-urea blocks in PU F=3 leads to the strengthened hydrogen bonding interaction. However for functionalities of PU F=4 and F=5, the C=O absorptions have a blueshift back to higher frequency ( $1693\text{ cm}^{-1}$ ) since they have lower tri-uret concentrations than PU F=3.

#### **Influence of tetra-uret content in PU Bi series at room temperature**

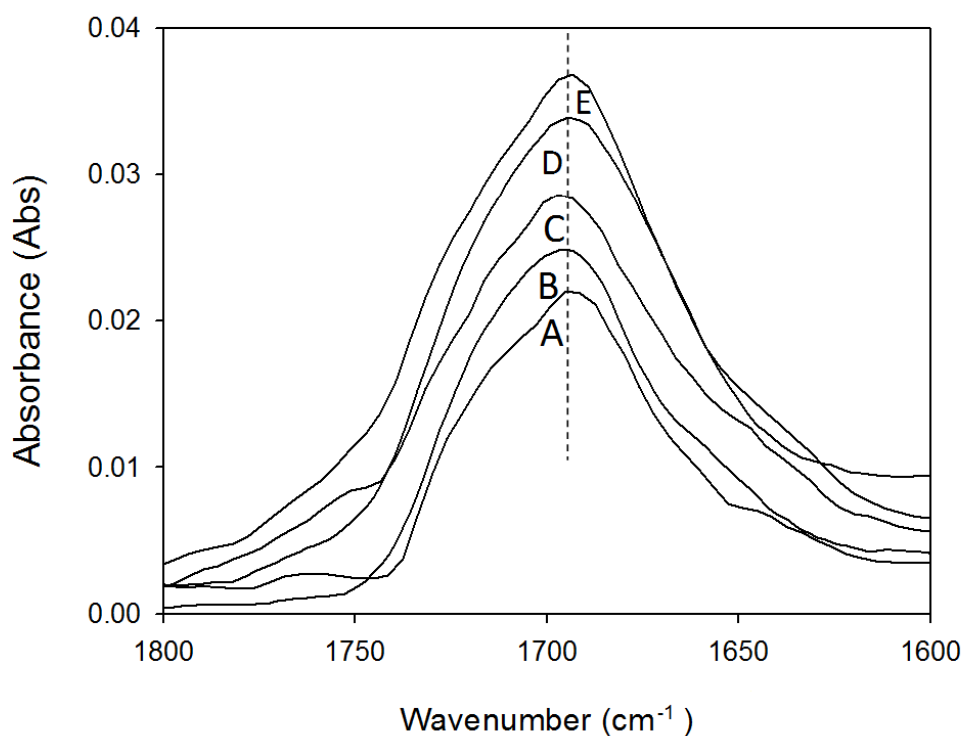
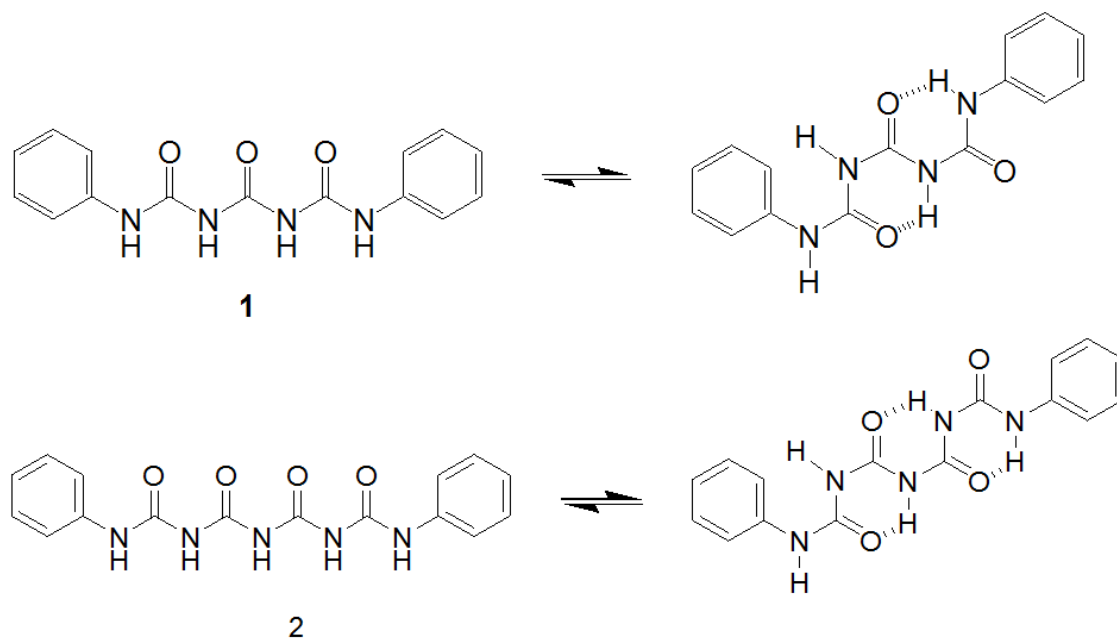


**Figure 4.** FTIR spectra of C=O absorption of PU Bi series at room temperature: A: PU Bi F=1; B: PU Bi F=2; C: PU Bi F=3 ; D: PU Bi F=4; E: PU Bi F=5.

In contrast to PU series, the difference observed on FTIR spectra of PU Bi series (Figure 4) is less distinct, indicating that hydrogen bonds in this series are only intramolecular or that the FTIR is not sensitive enough to detect possible intramolecular hydrogen bonds in this system even if a small difference is still visible between the 2 extreme concentrations in PU Bi F=1 and PU Bi F=3.

**Hydrogen bonds' association constant by  $^1\text{H-NMR}$ .** The association constant ( $K_{\text{ass}}$ ) calculation is characteristic of the strength of intermolecular hydrogen bonds' interactions. It is typically performed in  $\text{CDCl}_3$  solvent which has low polarity that shouldn't destroy the hydrogen bond associations. The chemical shift of labile protons, which is N-H in the present work, is tracked in dilution experiments.



**Scheme 1.** Supposed Chemical structure of polyurea models based on 1,1-2(N-Phenylaminocarbonyl)urea (**1**) and 1,1-2(N-Phenylaminocarbonyl)triuert , (**2**)

Two models containing tri-uret and tetra-uret blocks were respectively prepared as described in the experimental part and used for  $K_{\text{ass}}$  calculation. According to the solubility results of PU and PU Bi series, **1** is supposed to be in zigzag conformation while **2** is supposed to be in folded conformation in scheme 1. The chemical shifts of N-H proton in both of these models from  $^1\text{H}$  NMR spectra are listed in table 3.

**Table 3.** Concentration dependent labile N-H chemical shift of polyurea models at 300K in  $\text{CDCl}_3$

Model name	$\delta_{\text{N-H}}$ (ppm)		$\Delta \delta$ (ppm)
	With $C=0.11 \text{ mol.L}^{-1}$	With $C=0.03 \text{ mol.L}^{-1}$	
1	9.4385	9.3261	0.11ppm
2	9.3042	9.3241	-0.02ppm

$\Delta \delta_{\text{N-H}}$  between **1** and **2** in  $\text{CDCl}_3$ , at different concentrations when diluted, are also quite different, and this  $\Delta \delta_{\text{N-H}}$  reflects the association strength of the assembling moieties when their solutions are diluted at the same concentration. Dilution of **2** based on the tetra-uret doesn't change the  $\delta_{\text{N-H}}$  in large scale, indicating the weak interactions due to the predominantly folded conformation among **2**. Only **1** has an obvious upfield shift illustrated in figure 5, which indicates that tri-uret blocks are at least partially in unfolded conformations.  $K_{\text{ass}}$  is calculated by curve fitting method of Chen's equation<sup>[30]</sup> to obtain the value equal to  $95 \text{ M}^{-1}$ .

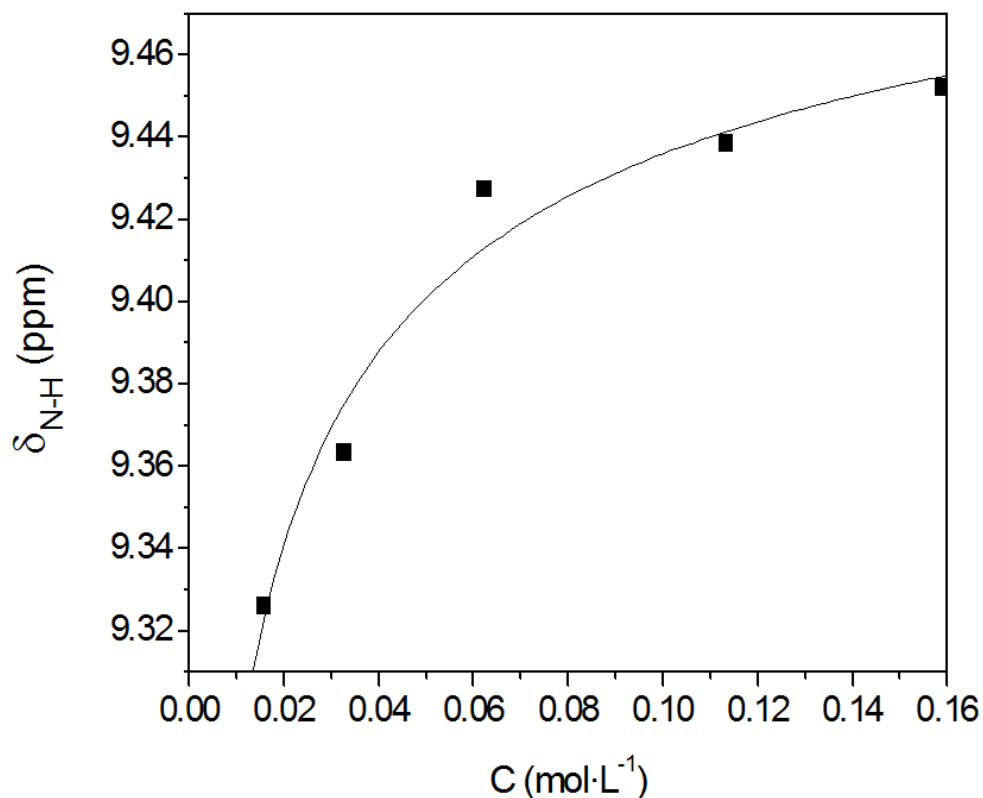


**Figure 5.**  $K_{\text{ass}}$  calculation by curve fitting of  $\delta_{\text{N-H}}$  vs concentration in  $\text{CDCl}_3$  at 300K of **1**:

— as curve-fitting result, ■ as experimental data

This  $K_{\text{ass}}$  value ( $95 \text{ M}^{-1}$ ) based on tri-uret blocks is comparable to other triple hydrogen bonding assemblies such as DAD-ADA pairs ( $65\text{-}130 \text{ M}^{-1}$ )<sup>[39]</sup>, but lower than assemblies with DDD-AAA pairs ( $>10^5 \text{ M}^{-1}$ )<sup>[40, 41]</sup>. Nevertheless our target to build stronger associations than urea block  $\text{-NH-CO-NH-}$  is accomplished, since the  $K_{\text{ass}}$  of the single-urea blocks was reported as  $6.9$  to  $45 \text{ M}^{-1}$ <sup>[29]</sup>. In addition, and seen that the associations' reversibility at a reasonable temperature is required in this study, associations higher than 100 should be avoided. From the obtained  $K_{\text{ass}}$  value, the conformation of tri-uret block associations in PU series is considered as composed of both DAD-ADA and DD-AA pairs (DD-AA  $K_{\text{ass}}=80\text{-}1000 \text{ M}^{-1}$ ).

**Structure analyses by dynamic rheology in the molten state.** Dynamic mechanical analyses (DMA) of PU and PU Bi series are studied in this part. These products were first analyzed by DSC. Each sample has a single  $T_g$  indicating that there is no phase separation. The obtained results are given in Table 4.

**Table 4.**  $T_g$  ( $^{\circ}\text{C}$ ) of PUU with different functionalities determined by DSC at  $10^{\circ}\text{K}\cdot\text{min}^{-1}$ .

	F=1	F=2	F=3	F=4	F=5
PU	79.5	102.4	105.9	117.4	122.4
PU Bi	75.5	88.4	95.3	114.0	116.1

#### **PU Bi series dynamic rheology**

The influence of the building blocks' functionality on the moduli evolutions with temperature was studied here. For the samples issued from prepolymers having F=2-5, successive heating and cooling ramps were made (Figure 6).

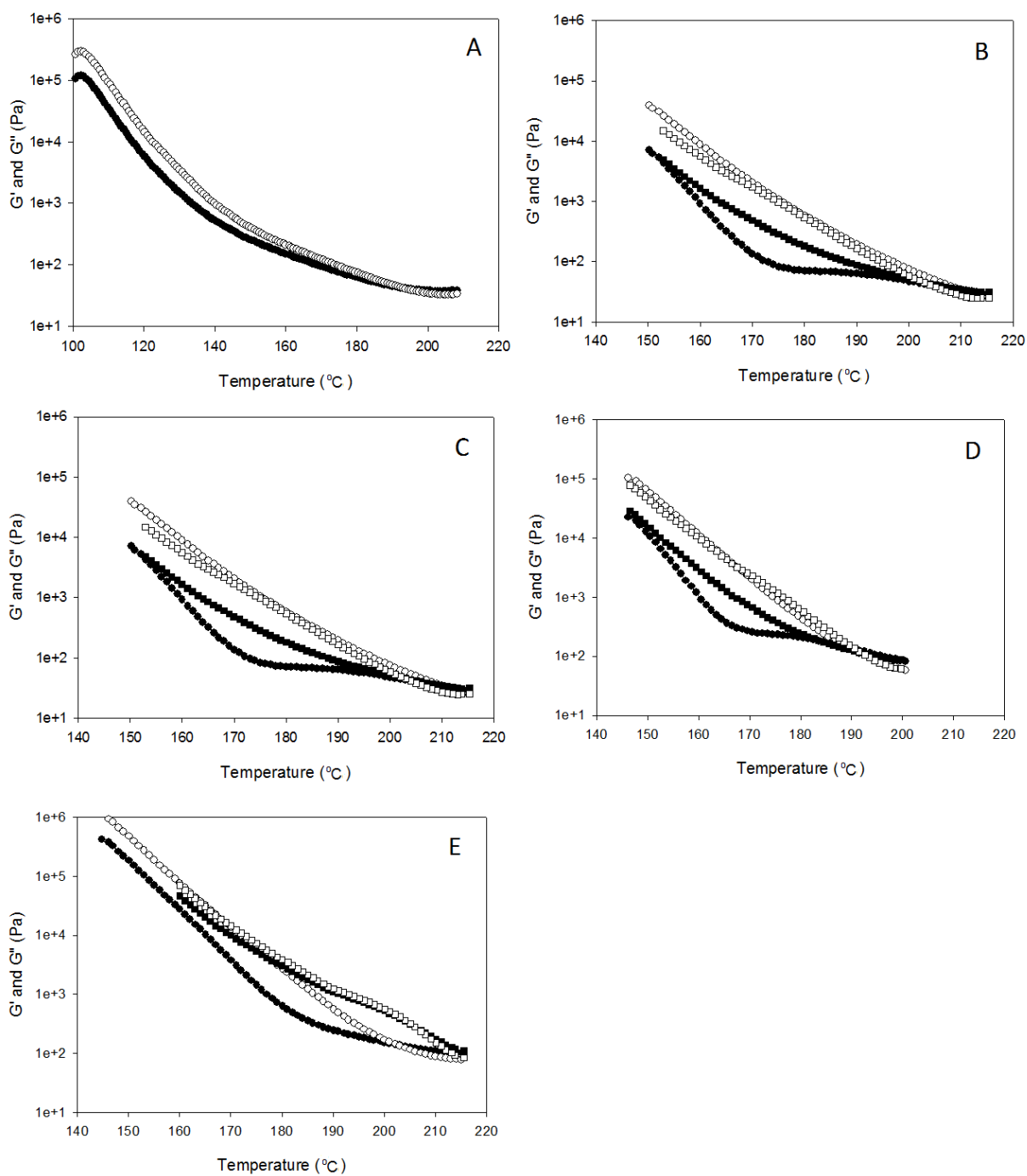


**Figure 6.**  $G'$  storage modulus (Pa) and  $G''$  loss modulus (Pa) of PU Bi series by temperature ramp tests at  $1.5\text{ }^{\circ}\text{C}\cdot\text{min}^{-1}$ , frequency =  $1\text{ rad}\cdot\text{s}^{-1}$ ,  $\bullet$ : storage modulus  $G'$  in heating ramp,  $\circ$ : loss modulus  $G''$  in heating ramp,  $\blacksquare$ : storage modulus  $G'$  in cooling ramp,  $\square$ : loss modulus  $G''$  in cooling ramp. A: PU Bi F=1; B: PU Bi F=2; C: PU Bi F=3; D: PU Bi F=4; E: PU Bi

F=5

The  $G'$  values are generally higher than those measured when cooling. This is due to the presence of intermolecular hydrogen bonds. Their dynamic association is different during heating and cooling leading to different moduli.

No network is present in this series with temperatures up to 180 °C, reflected by  $G''$  superior to  $G'$ . The density of intermolecular hydrogen bonds is not high enough to lead to cross-linked materials. Furthermore, hydrogen bonds in PU Bi series may not efficiently contribute to the network formation at low temperature, but they certainly influence the viscoelastic properties in PUU at high temperature. Linear polymers have a sharp decline for both  $G'$  and  $G''$  moduli when the temperature heating overpasses  $T_g$ , with  $G''$  being consistently above  $G'$ . For the studied materials,  $G'$  plateaus are observed around 170 °C indicating that hydrogen bonds are persistent. Their quantity increases when the functionality is between 1 and 5, leading to  $G'$  higher plateau moduli (Figure 7). It is important to note that for PU Bi samples with functionalities from 2 to 4,  $G'$  overpasses  $G''$  at higher temperature, proving that a network may be obtained at these temperatures.

All these results are coherent implying that the equilibrium unfolded/ folded conformations of tetra-uret segments (scheme 1) is in favor of the folded one at low temperature and that it is replaced by the unfolded conformation when the temperature increases, leading to more intermolecular interactions.

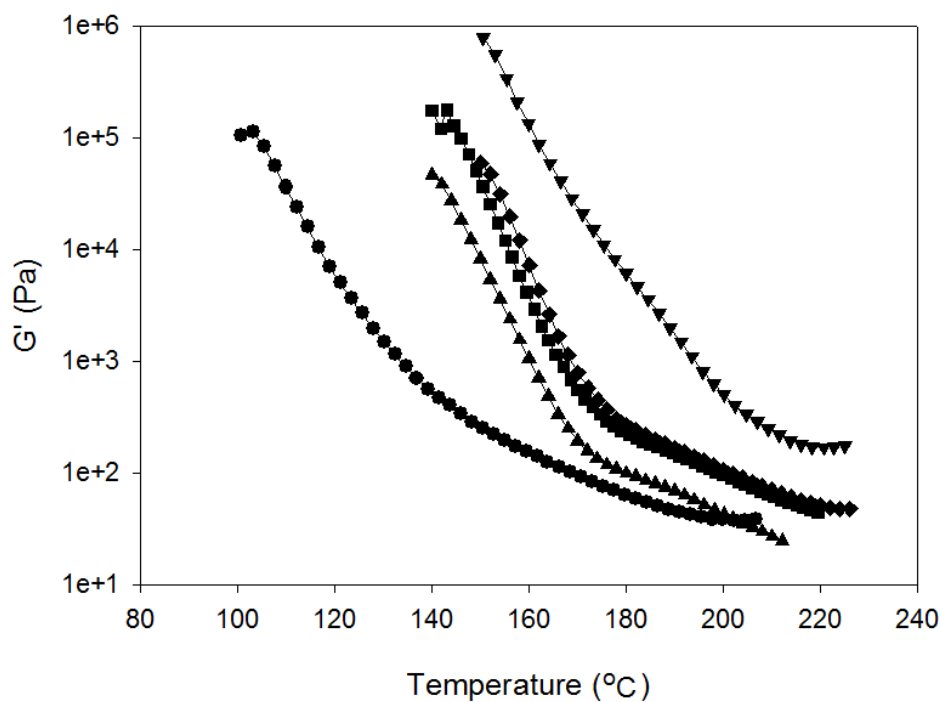


**Figure 7.**  $G'$  storage modulus (Pa) PU Bi series by temperature ramp tests at  $1.5\text{ }^{\circ}\text{C}\cdot\text{min}^{-1}$ , frequency =  $1\text{ rad}\cdot\text{s}^{-1}$ , ●: PU Bi  $f=1$ , ▲ : PU Bi  $f=2$ , ■:PU Bi  $f=3$ , ◆: PU Bi  $f=4$ , ▼: PU Bi  $f=5$ .

### PU series dynamic rheology

Temperature ramp tests of PU series having different functionalities were performed by one cooling followed by one heating ramp, except for PU  $f=1$ . Storage ( $G'$ ) and loss ( $G''$ ) moduli evolutions with temperature are shown in Figure 8.

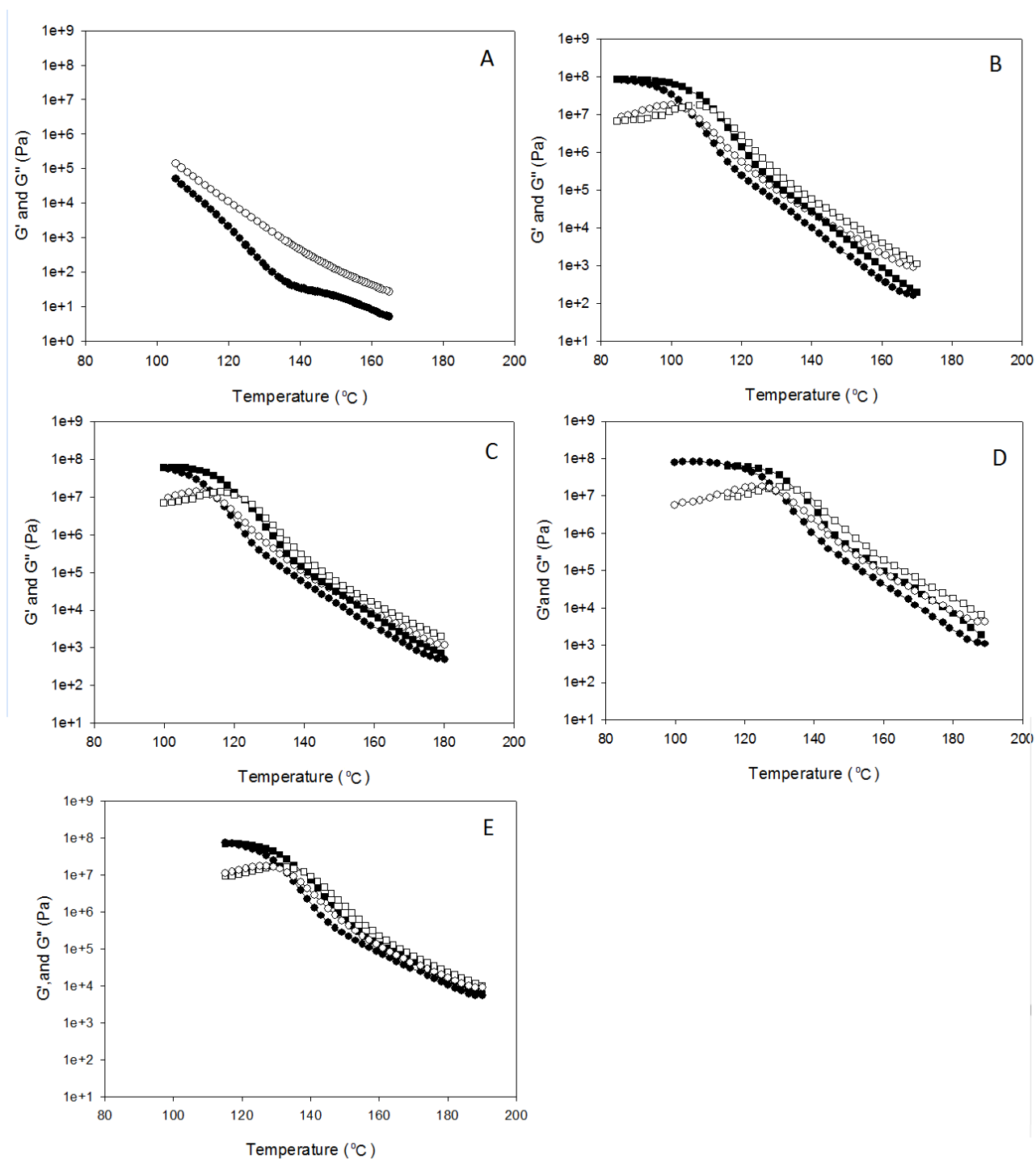


**Figure 8.**  $G'$  (Pa) storage modulus (Pa) and  $G''$  (Pa) loss moduli of PU series by temperature ramp tests at  $1.5\text{ }^{\circ}\text{C}\cdot\text{min}^{-1}$ , frequency =  $1\text{ rad}\cdot\text{s}^{-1}$ , round symbols for cooling ramp:  $\bullet$ :  $G'$ ;  $\circ$ :  $G''$ , square symbols for heating ramp:  $\blacksquare$ :  $G'$ ;  $\square$ :  $G''$ . A: PU F=1; B: PU F=2; C: PU F=3; D: PU F=4; E: PU F=5

For all the studied samples,  $G''$  is higher than  $G'$  at high temperature. During cooling, a clear crossover of  $G'$  and  $G''$  is obtained except for PU with  $f=1$ . These results confirm that at higher temperatures than  $T_{\text{crossover}}$ , hydrogen bonds are weakened. The intermolecular associations being broken, the polymer is a thermoplastic. During cooling, the hydrogen bonds are observed again and become stronger, and at temperatures below  $T_{\text{crossover}}$ , supramolecular interactions lead to cross-linked materials when the functionality is favorable.

When  $f=1$ , only a diblock or star like structure can be obtained. The  $T_{\text{crossover}}$  increases with increasing PU series functionality. This also confirms that higher functionality lead to higher crosslinking density.

During the heating cycle, the opposite behavior is observed and the network discards at temperature higher than  $T_{\text{crossover}}$ . Here also, since hydrogen bonds association are dynamic and different during heating and cooling cycles, different moduli are obtained and the curves do not overlap.

To confirm these observations, these cross-linking/ de-cross-linking can be observed for several cooling / heating cycles, experiments were made for the samples having  $f=3$  (Figure 9). The curves perfectly overlay for the different cycles leading to the conclusion that both the network dissociations and rebuilding processes, based on the hydrogen bonds, are thermally reversible.

These results show clearly that for the PU series, tri-uret blocks have a zigzag unfolded conformation leading to efficient supramolecular associations.

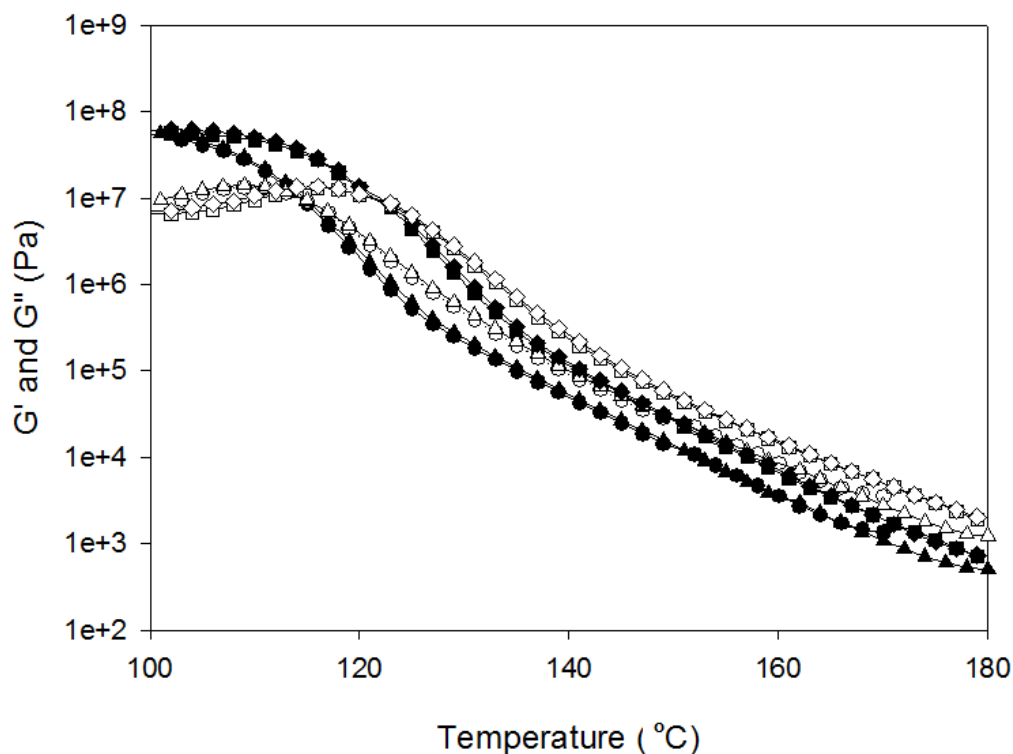


**Figure 9.** Reversibility of  $G'$  and  $G''$  crossover of PU  $f=3$  by ramps at  $= 1.5\text{ }^{\circ}\text{C}\cdot\text{min}^{-1}$ , frequency  $= 1\text{ rad}\cdot\text{s}^{-1}$ , strain  $= 10\%-0.1\%$ , 1<sup>st</sup> cooling ramp: ● for  $G'$  and ○ for  $G''$ ; first heating ramp: ■ for  $G'$  and □ for  $G''$ ; 2<sup>nd</sup> cooling ramp: ▲ for  $G'$  and △ for  $G''$ ; second heating ramp: ◆ for  $G'$  and ◇ for  $G''$

#### D-4. Conclusion

Polyurea-urethane supramolecular thermo-reversible networks were prepared using urea to obtain tri-uret blocks. The  $K_{\text{ass}}=95\text{ M}^{-1}$  was calculated by  $^1\text{H-NMR}$  with the Chen model.

At the lowest temperatures, the tri-uret blocks seem to have an unfolded conformation while tetra-uret blocks were folded. This folded conformation did not lead to a cross-linked material. At higher temperature, the tetra-uret conformation became at least partially unfolded leading to supramolecular interaction and consequently to cross-linked polymers.

**ACKNOWLEDGMENT**

The authors thank the financial support from China Scholarship Council (state scholarship fund). This work benefited from the cooperation between East China University of Science and Technology (China) and Université Jean-Monnet Saint-Etienne (France).

## REFERENCES

- [1] Beyer, M. K.; Clausen-Schaumann, H. *Chemical Reviews-Columbus* **2005**, 105, (8), 2921-2948.
- [2] Lehn, J. M. *Angew. Chem.-Int. Edit. Engl.* **1988**, 27, (1), 89-112.
- [3] Binder, W. H.; Zirbs, R., Supramolecular polymers and networks with hydrogen bonds in the main- and side-chain. In *Hydrogen Bonded Polymers*, 2007; Vol. 207, pp 1-78.
- [4] Gooch, A.; Nedolisa, C.; Houton, K. A.; Lindsay, C. I.; Saiani, A.; Wilson, A. J. *Macromolecules* **2012**, 45, (11), 4723-4729.
- [5] Lee, S. H.; Ouchi, M.; Sawamoto, M. *Macromolecules* **2012**, 45, (9), 3702-3710.
- [6] Ikkala, O.; ten Brinke, G. *science* **2002**, 295, (5564), 2407-2409.
- [7] Zare, P.; Stojanovic, A.; Herbst, F.; Akbarzadeh, J.; Peterlik, H.; Binder, W. H. *Macromolecules* **2012**, 45, (4), 2074-2084.
- [8] Burnworth, M.; Rowan, S. J.; Weder, C. *Macromolecules* **2012**, 45, (1), 126-132.
- [9] Zhao, L. H.; Png, R. Q.; Zhuo, J. M.; Wong, L. Y.; Tang, J. C.; Su, Y. S.; Chua, L. L. *Macromolecules* **2011**, 44, (24), 9692-9702.
- [10] Armstrong, G.; Buggy, M. *J. Mater. Sci.* **2005**, 40, (3), 547-559.
- [11] ten Brinke, G.; Ruokolainen, J.; Ikkala, O. *Hydrogen Bonded Polymers* **2007**, 113-177.
- [12] Lange, R. F. M.; Van Gorp, M.; Meijer, E. W. *Journal of Polymer Science Part a-Polymer Chemistry* **1999**, 37, (19), 3657-3670.
- [13] BOSMAN A W, S. R. P., Meijer E W. *Materials Today* **2004**, 7, (4), 34-39.
- [14] Bertrand, A.; Chen, S. B.; Souharce, G.; Ladaviere, C.; Fleury, E.; Bernard, J. *Macromolecules* **2011**, 44, (10), 3694-3704.
- [15] Kato, T.; Matsuoka, T.; Nishii, M.; Kamikawa, Y.; Kanie, K.; Nishimura, T.; Yashima, E.; Ujiie, S. *Angewandte Chemie-International Edition* **2004**, 43, (15), 1969-1972.
- [16] Feldman, K. E.; Kade, M. J.; Meijer, E.; Hawker, C. J.; Kramer, E. J. *Macromolecules* **2009**, 42, (22), 9072-9081.

- [17] Ware, T.; Hearon, K.; Lonnecker, A.; Wooley, K. L.; Maitland, D. J.; Voit, W. *Macromolecules* **2012**, 45, (2), 1062-1069.
- [18] Luo, N.; Wang, D. N.; Ying, S. K. *Polymer* **1996**, 37, (16), 3577-3583.
- [19] Chandran, S. K.; Nath, N. K.; Cherukuyada, S.; Nangia, A. *Journal of Molecular Structure* **2010**, 968, (1-3), 99-107.
- [20] Jordan, L. M.; Boyle, P. D.; Sargent, A. L.; Allen, W. E. *J. Org. Chem.* **2010**, 75, (24), 8450-8456.
- [21] Goswami, S.; Jana, S.; Dey, S.; Sen, D.; Fun, H. K.; Chantrapromma, S. *Tetrahedron* **2008**, 64, (27), 6426-6433.
- [22] VanEsch, J.; DeFeyter, S.; Kellogg, R. M.; DeSchryver, F.; Feringa, B. L. *Chemistry-a European Journal* **1997**, 3, (8), 1238-1243.
- [23] Kim, J. U.; Davis, R.; Zentel, R. *J. Colloid Interface Sci.* **2011**, 359, (2), 428-435.
- [24] Patra, D.; Ramesh, M.; Sahu, D.; Padhy, H.; Chu, C. W.; Wei, K. H.; Lin, H. C. *Polymer* **2012**, 53, (6), 1219-1228.
- [25] McKee, M. G.; Elkins, C. L.; Park, T.; Long, T. E. *Macromolecules* **2005**, 38, (14), 6015-6023.
- [26] Wisse, E.; Govaert, L. E.; Meijer, H. E. H.; Meijer, E. W. *Macromolecules* **2006**, 39, (21), 7425-7432.
- [27] Wisse, E.; Spiering, A. J. H.; van Leeuwen, E. N. M.; Renken, R. A. E.; Dankers, P. Y. W.; Brouwer, L. A.; van Luyn, M. J. A.; Harmsen, M. C.; Sommerdijk, N.; Meijer, E. W. *Biomacromolecules* **2006**, 7, (12), 3385-3395.
- [28] Patel, A. N.; Patel, M. M.; Dighe, A. *Progress in organic coatings* **2012**, 74, (3), 443-452.
- [29] Woodward, P. J.; Merino, D. H.; Greenland, B. W.; Hamley, I. W.; Light, Z.; Slark, A. T.; Hayes, W. *Macromolecules* **2010**, 43, (5), 2512-2517.
- [30] Chen, J. S.; Rosenberger, F. *Tetrahedron Letters* **1990**, 31, (28), 3975-3978.

- [31] Brammer, S.; Luning, U.; Kuhl, C. *European Journal of Organic Chemistry* **2002**, (23), 4054-4062.
- [32] Lafitte, V. G. H.; Aliev, A. E.; Horton, P. N.; Hursthouse, M. B.; Bala, K.; Golding, P.; Hailes, H. C. *Journal of the American Chemical Society* **2006**, 128, (20), 6544-6545.
- [33] Luning, U.; Kuhl, C.; Uphoff, A. *European Journal of Organic Chemistry* **2002**, (23), 4063-4070.
- [34] Milani, A.; Castiglioni, C.; Di Dedda, E.; Radice, S.; Canil, G.; Di Meo, A.; Picozzi, R.; Tonelli, C. *Polymer* **2010**, 51, (12), 2597-2610.
- [35] Mishra, A. K.; Narayan, R.; Raju, K. *Progress in organic coatings* **2012**, 74, (3), 491-501.
- [36] Kao, D. Y.; Shu, W. T.; Chen, J. S. *J. Chin. Chem. Soc.* **2005**, 52, (6), 1171-1178.
- [37] Silverstein, R.; Webster, F., *Spectrometric Identification of Organic Compound*. Wiley-India: 2006.
- [38] Teo, L. S.; Chen, C. Y.; Kuo, J. F. *Macromolecules* **1997**, 30, (6), 1793-1799.
- [39] Thalacker, C.; Miura, A.; De Feyter, S.; De Schryver, F. C.; Wurthner, F. *Organic & Biomolecular Chemistry* **2005**, 3, (3), 414-422.
- [40] Blight, B. A.; Camara-Campos, A.; Djurdjevic, S.; Kaller, M.; Leigh, D. A.; McMillan, F. M.; McNab, H.; Slawin, A. M. Z. *Journal of the American Chemical Society* **2009**, 131, (39), 14116-14122.
- [41] Zimmerman, S. C.; Corbin, F. S. *Molecular Self-Assembly* **2000**, 96, 63-94.

## Annexe

### Annexe 1. $M_c$ calculation of P(MAP-co-St)

$M_c$  (molecular weight between crosslinks) is the parameter that represents the crosslink degree of the polymers and which is also a sign concerning the strength of the network. In all the statistical methods, Flory-Rehner Equation is most extensively used to calculate the  $M_c$  between interpenetrating polymeric gel. It describes the swelling equilibrium of a lightly crosslinked polymer in terms of crosslink density and the quality of the solvent <sup>[1]</sup>:

$$M_c = \frac{d_p v_1 (v_2^{1/3} - v_2/2)}{\ln(1-v_2) + v_2 + \chi v_2^2} \quad \text{eq. 1}$$

Volume fraction of the polymer ( $v_2$ ) in the swollen gel is a measure of the amount of fluid that a gel can incorporate into its structure. It is calculated by the following equation <sup>[2]</sup>:

$$v_2 = \left[ 1 + \frac{d_p}{d_s} \left( \frac{M_a}{M_b} - 1 \right) \right]^{-1} \quad \text{eq. 2}$$

Where  $d_p$  and  $d_s$  are densities ( $\text{g. ml}^{-1}$ ) of the gel and solvent respectively.  $M_a$  and  $M_b$  are the masses ( $\text{g}$ ) of the swollen and dry gels respectively.  $v_2$  ( $\text{ml.mol}^{-1}$ ) is volume fraction of the swollen gel in the equilibrium state and  $\chi$  is the Flory-Huggins polymer solvent interaction parameter.

Solvent interaction parameter ( $\chi$ ) was calculated by Flory-Huggins theory. Equation used to calculate  $\chi$  value is given below <sup>[3]</sup>:

$$\chi = \frac{\ln(1-v_2) + v_2}{v_2^2} \quad \text{eq 3}$$

Recently  $M_c$  could also be derived from the value of this rubbery modulus of polymer based on the classical theory of rubber elasticity. This theory explains the relationship of modulus, temperature and crosslink density:

$$M_c = \rho RT / G_0 \quad \text{eq.4}$$

Where  $G_0$  is the modulus of rubbery plateau obtained from DMA;  $R$  is the gas constant;  $\rho$  is the density of polymer;  $T$  is the temperature in Kelvin degree. The affine model gives  $a = 1$ .

**Table Annexe-1.  $M_c$  calculation by two methods**

	Mc by Flory-Rehner equation (g.mol <sup>-1</sup> )	Mc by classic rubber elasticity theory (g.mol <sup>-1</sup> )
<b>0% MAP</b>	a	a
<b>2% MAP</b>	a	a
<b>5% MAP</b>	111174	b
<b>10% MAP</b>	9130	52132
<b>15% MAP</b>	2666	4175
<b>20% MAP</b>	1456	3080

<sup>a</sup>: soluble samples; <sup>b</sup>: no rubbery plateau observed in testing temperature range

The results from Flory-Rehner as well as classic rubber elasticity theory are listed in table 4. It is only calculated for MAP-St copolymers since hydrogen bonds interaction are more distinct in P(MAP-co-St) systems compared with P(MAAM-co-St). The samples of 0% MAP is pure PS and 5% MAP are soluble in the THF, so  $M_c$  calculation for these two samples is meaningless and not applied here. Both Flory-Rehner equation and rubber elasticity theory give the same tendency of  $M_c$ : with higher moieties concentrations in the copolymers, the crosslinking density is higher. This is corresponding to the association of MAP moiety discussed above that higher MAP represents more DA hydrogen bonds moieties along the polymer backbones and it increases the numbers of assemblies in the polymers. The assemblies entangled polymer chains, resulting in the reinforcement of network that is reflected in the decreasing  $M_c$  value.

The crosslinking performances due to the dimerization of MAP or MAAM were assumed at the beginning of discussion part, but until here we could finally conclude from the  $M_c$  result of P(MAP-co-St) that in addition to viscoelastic properties, this more intuitionistic characterization of polymer crosslinked networks also gives the proof that increasing DA moiety content has the direct and positive impact to the materials crosslinking density.

## Annexe 3. Network model through hydrogen bonds in the PUU

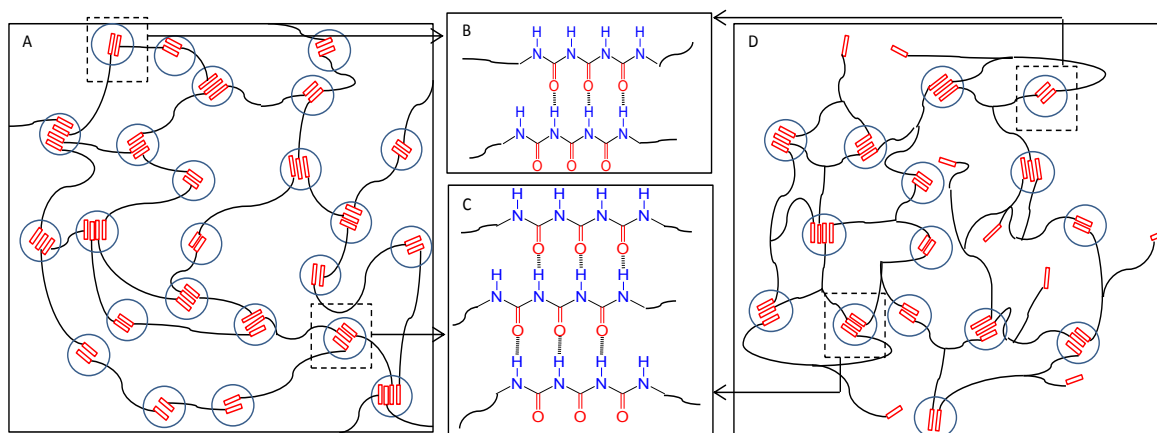


Figure annexe-2. Schematic demonstration of networks structure in crosslinking PU series:

A: crosslinked network in PU F=2; B: dimer conformation; C: trimer conformation; D: crosslinked network in PU F=3

The basic unit in tri-uret and tetra-uret is the urea NH-CO-NH- group. Association between single-urea groups and the application of the assemblies were reported in self-assembled supramolecular polymers <sup>[4]</sup>, but no references concerning networks based on tri-uret and tetra-uret blocks as in this study were found although it is expected to have higher association strength than single urea. As a result, we propose the network model illustrated in figure annexe-2.

Ideally, zigzagged tri-uret blocks in PU series have self-assembly capacity with its DDDD and AAA moieties. But self-association between tri-uret blocks forms as dimers (figure annexe-2B), trimers (figure annexe-2C), or multimers cannot be certainly determined. In dimerization assumption, the network formation depends on PUU functionalities: the network could only be assembled when functionalities equal to or greater than 3, since  $f=1$ , only small dimers are expected while with  $f=2$ , double interactions with two other moieties must lead to linear structures. But it is against the solubility tests that swollen samples are obtained with PU F=2. Therefore, the multimer conformations are supposed to exist in the PU series and functionalized as crosslinked spots suggested in figure annexe-2A. These multimers could be dimers or trimers or more complicated aggregates for the assembled moieties without limitation of moiety numbers. In this case, network formations can occur even with functionality of tri-uret (PU series) equal to 2. With further increment of functionality to 3

(figure annexe-2D) or more, the crosslinked spots are increased with more branched tri-uret blocks, resulting in the reinforcement of networks that is proved by IR, DSC, and rheological characterizations.

However, the tetra-uret blocks in PU Bi series performed differently. No networks are obtained due to the weaker hydrogen bonds than PU series according to FTIR and solubility tests. So the folded conformation among PUU molars is suggested. This folded formation can re-organize to zigzagged formation given by certain conditions and therefore endow the materials with higher modulus with stronger intermolecular hydrogen bonds interactions. This conformer transition of assemblies was confirmed by rheological analyses mention above.

### Annexe 3. Temperature dependent $^1\text{H}$ NMR in PU Bi F=1

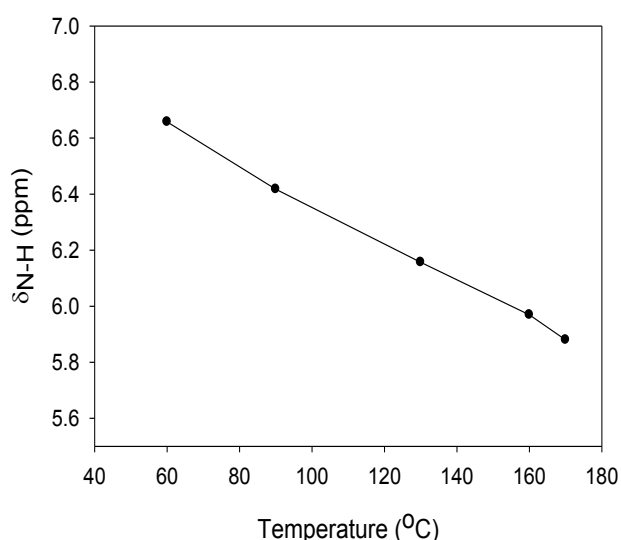


Figure annexe-3.  $\delta_{\text{N-H}}$  of PU Bi F=1 at different temperature in DMSO

In spite of its inapplicability in  $K_{\text{ass}}$  calculation, DMSO is suitable in temperature dependent  $^1\text{H}$  NMR shown in figure annexe-3 and table annexe-2 due to its high boiling point. Heating solution from 60 °C to 170 °C results in the shift of tetra-uret moiety  $\delta_{\text{N-H}}$  from 6.66 ppm to 5.88 ppm. This upfield shift represents the existence of hydrogen bonds among tetra-uret groups although they are not as strong as among tri-uret groups. Reduced  $\delta_{\text{N-H}}$  corresponding to the dissociation also respects the thermo-responsive essence of hydrogen bonds.

Table annexe-2. Concentration and temperature dependent  $\delta_{\text{N-H}}$  of PU Bi f=1 in DMSO

	$\delta_{N-H}$ (ppm)		$\Delta \delta$ (ppm)
	With C=0.23 mol.L <sup>-1</sup>	With C=0.02 mol.L <sup>-1</sup>	
60°C	6.6577	-	-
90°C	6.4177	6.4460	-0.0283
130°C	6.1568	-	-
160°C	5.9695	5.9953	-0.0258
170°C	5.8800	5.8854	-0.0085

## Annexe 2. PUU system reinforced with PVA

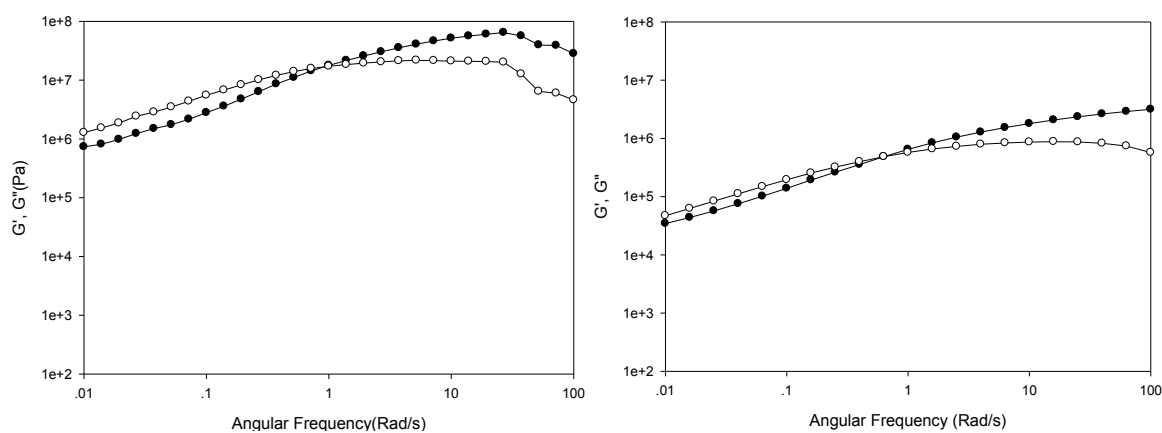


Figure annexe-4. Frequency ramp of: left: pu f=4 without PVA, right: PU

● = G'; ○ = G'', T=135 °C

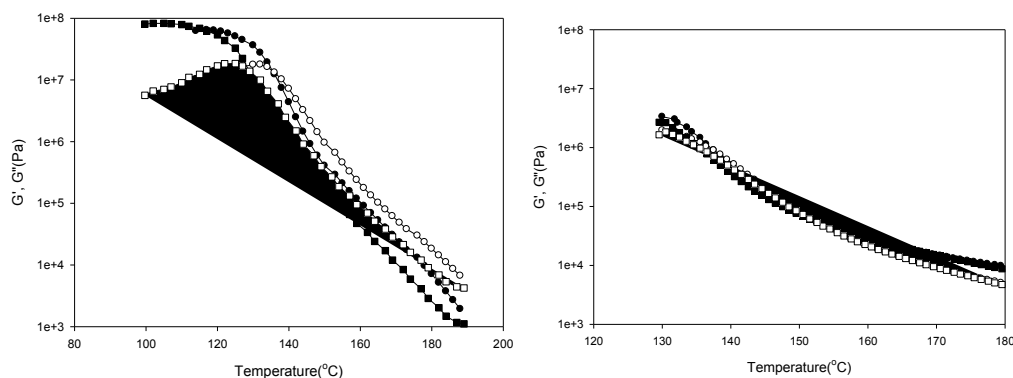
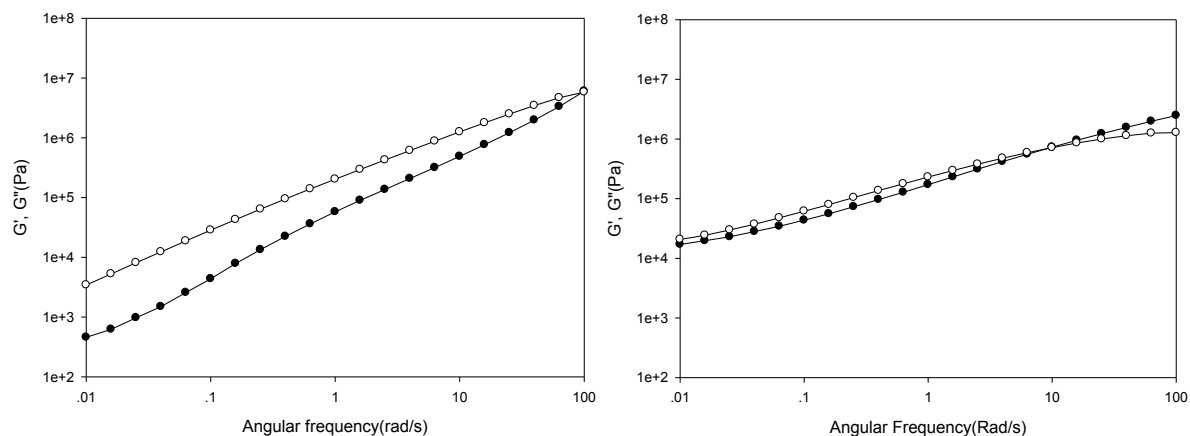


Figure annexe-5. Temperature ramp of: left: pu f=4 without PVA, right: PU f=4+PVA

● = G' during increasing ramp; ○ = G'' during increasing ramp; ■ = G' during decreasing ramp; □ = G'' during decreasing ramp;



**Figure annexe-6. Frequency ramp of: left: pu bi f=4 without PVA, right: PU bi f=4+PVA, modulus increase**

● =  $G'$ ; ○ =  $G''$  T=145

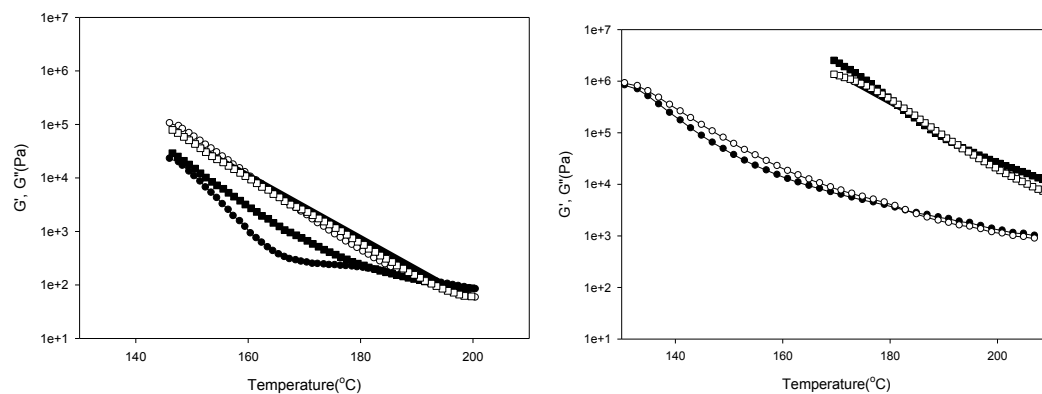


**Figure annexe-7. Temperature ramp of: left: pu bi f=4 without PVA, right: PU bi f=4+PVA, modulus increase**

● =  $G'$  during increasing ramp; ○ =  $G''$  during increasing ramp; ■ =  $G'$  during decreasing ramp; □ =  $G''$  during decreasing ramp;

[1] Flory, P. J., *Principles of polymer chemistry*. Cornell Univ Pr: 1953.

[2] Peppas, N. A.; Huang, Y.; Torres-Lugo, M.; Ward, J.; Zhang, J. *Annual Review of Biomedical Engineering* **2000**, 2, (1), 9-29.

[3] Ranjha, N. M.; Ayub, G.; Naseem, S.; Ansari, M. T. *Journal of Materials Science: Materials in Medicine* **2010**, 21, (10), 2805-2816.

[4] Pinault, T.; Andrioletti, B.; Bouteiller, L. *Beilstein J. Org. Chem.* **2010**, *6*, 869-875.

## General Conclusion

This Ph-D thesis focused on the preparation of polymer networks by different supramolecular interactions related to non-covalent bonds. Among which, ionic or hydrogen bonds interactions were chosen to be studied due to their binding strength. The materials crosslinked through supramolecular interactions were supposed to be reversibly responsive to external environment such as solvent, or temperature, with advantages in recycling and reuse.

The ionic interaction was firstly realized by introducing the  $\text{CaCO}_3$  to the BMA/MA copolymers to form the interaction between  $\text{Ca}^{2+}$  and  $\text{COO}^-$ .  $\text{CaCO}_3$ , was proved present in two phases by X-Ray analyses as well as thermal and rheological analyses. One phase corresponded to Eisenberg's model which first described a cluster phase in ionomers. The cluster percolation was observed when their concentration was high enough with the appearance of a crosslinked behavior. At least 10 mol% of MA units was required in the copolymer chains and at least an excess of 20 mol% of  $\text{CaCO}_3$  vs MA. The large unreacted part of the  $\text{CaCO}_3$  behaved as a filler, modifying the ionic plateau over  $T_g$ . More surprisingly, when  $\text{CaCO}_3/\text{MA}$  was superior to 2, the properties of the material decreased. It was established now that these high filler contents disturbed the structure of the ionic cluster phase, losing its crosslinked material behavior. The  $T_g$  of the material could be adjusted only by the copolymer composition if a sufficient  $\text{CaCO}_3$  content was reached.

The polymers networks based on the DA-AD double hydrogen bonds moieties in P(MAAM-co-St) and P(MAP-co-St) were respectively investigated. The rate of hydrogen bonding moieties was controlled by adjusting the molar ratio of the supramolecular monomers, MAAM or MAP, to the co-monomer St. Both  $G'$  and  $G''$  moduli were increased with increasing MAAM or MAP content, and plateau with high modulus appeared in crosslinked P(MAP-co-St) with MAP contents above 10 mol%, which was quite similar to the ionic polymer system. These controllable properties attributed to resistance of the double hydrogen bond interactions, could be qualitatively observed by FTIR, or quantitatively calculated from  $K_{\text{ass}}$  by  $^1\text{H-NMR}$  dilution experiments, resulting in  $6.75 \text{ M}^{-1}$  for MAAM and  $16.75 \text{ M}^{-1}$  for

MAP. Furthermore, the stronger hydrogen bonding interactions of P(MAP-co-St) when compared to P(MAAM-co-St), were also proved by Kwei equation in  $T_g$  studies and network solubility tests.

The study was consequently extended into PUU system. The moieties with capacity of association were tri-uret and tetra-uret blocks, which were derived from the reaction of urea or biuret with isocyanate respectively. PUU with tri-uret block was able to form PUU supramolecular thermo-reversible network with its  $K_{ass}$  equal to  $95 \text{ M}^{-1}$  by  $^1\text{H}$  NMR. The tri-uret blocks seemed to have an unfolded conformation at the lower temperatures, while tetra-uret blocks were folded. This folded conformation did not lead to cross-linked materials. At higher temperature, the tetra-uret conformation became at least partially unfolded leading to supramolecular interactions and consequently to cross-linked polymers. By synthesizing 1 to 5 units of tri-uret or tetra-uret blocks in one PUU structure, polymer network structures are modulated and controlled. Their potentials and advantages will be investigated by complementary study.

These supramolecular moieties had a great influence on the polymer network formation and therefore effected on reinforcement of materials. Studies concerning the structure of these networks in relation with the dynamics of their constructions would be in progress in further research.

## Conclusion Générale

Cette thèse est porte sur la synthèse de réseaux polymères by différents types d'interactions supramoléculaires par le biais de liaisons non-covalentes. Pour cela, des interactions ioniques et par liaisons hydrogène ont été retenues et étudiées par l'intermédiaire de leur résistance. Les matériaux réticulés par interactions supramoléculaires sont supposés l'être réversiblement soit par l'ajout de solvant soit par une modification de température avec l'avantage final de pouvoir être recyclés et réutilisés.

Les interactions ioniques ont été d'abord étudiées par l'introduction de carbonate de calcium ( $\text{CaCO}_3$ ) en mélange avec des copolymères synthétisés poly(méthacrylate de butyle –acide méthacrylique) (P(BMA-co-MA)) pour former des interactions entre des ions  $\text{Ca}^{2+}$  et des anions carboxylate  $\text{COO}^-$  formés in-situ par réaction partielle du carbonate de calcium avec les fonctions acide carboxylique. Il a été prouvé par R-X, analyses thermiques et rhéologiques, que le carbonate de calcium se retrouve présent dans deux phases Une phase correspond à celle décrite par le modèle d'Eisenberg, lequel décrit pour des ionomères, la formation d'une phase cluster nodulaire. La percolation de cette phase a été observée lorsque sa fraction était suffisante, s'accompagnant de l'apparition d'un comportement de matériau réticulé. Au moins 10% molaire d'acide méthacrylique dans le copolymère et au moins 20% molaire de carbonate de calcium ont été nécessaires pour atteindre la formation de réseaux caractérisés. Une part importante de carbonate de calcium est resté à l'état de charge, jouant également le rôle de charge, modulant la valeur de plateau caoutchoutique observé au-delà de la température de transition vitreuse. Plus surprenant, pour des rapports molaires carbonate de calcium – acide méthacrylique supérieurs à deux, les propriétés du matériau se dégradent. Il a pu être établi que pour des taux élevés en carbonate de calcium, sa fraction volumique devenant élevée, les charges encombrant le réseau percolé de la phase cluster et l'affaiblissent au point de provoquer sa rupture d'autant plus facilement que le taux augmente. Il a été également montré que la température de transition vitreuse peut être contrôlée par la composition du copolymère P(BMA-MA) si un taux suffisant de carbonate de calcium est atteint.

Des réseaux polymères formés par interactions supramoléculaires par la copolymérisation de styrène avec des monomères à motifs à double liaisons hydrogène DA (donneur-accepteur) comme la 2-méthacrylamidopyridine (MAP) et la méthacrylamide (MAAM) ont été

également étudiés. Le taux de motifs DA a été contrôlé par l'ajustement du rapport molaire des monomères supramoléculaires des copolymères poly(styrène-co-MAAM) et poly(Styrène-co-MAP). Les modules de perte et de conservation ont augmenté lorsque les taux de MAP et MAAM ont été augmentés dans les matériaux. Un module au plateau caoutchoutique a été clairement mis en évidence, prouvant la réticulation, lorsque le taux de MAP a dépassé 10% molaire, de manière similaire au système ionique déjà étudié. Les propriétés du matériau peuvent être contrôlées par la force des liaisons hydrogène qui se sont formées entre motifs en interaction. Ces interactions ont d'abord été mises en évidence qualitativement par spectroscopie Infra-Rouge, puis quantitativement par RMN  $^1\text{H}$  par le calcul de la constante d'association  $K_{\text{ass}}$ . Les constantes ont pour valeur  $6,75 \text{ M}^{-1}$  pour la MAAM et  $16,75 \text{ M}^{-1}$  pour la MAP montrant que les associations en dimères des motifs DA, se font avec des forces d'interaction supérieures avec le poly(Styrène-co-MAP) qu'avec le poly(styrène-co-MAAM). Ce résultat a également été confirmé par la validation du modèle de Kwei appliqué à l'évolution des températures de transition vitreuses observées ainsi que par des tests de solubilité.

L'étude a ensuite été poursuivie avec des nouveaux systèmes supramoléculaires poly(urée-uréthane) (PUU). De nouveaux monomères à multiples motifs triuret et tétrauret ont donc été synthétisés de manière originale et simple, par réaction entre l'urée ou la biuret avec de l'isocyanate (HMDI). Les PUU formés avec des motifs triuret ont permis de former des réseaux supramoléculaires thermo-réversibles avec une constante d'association  $K_{\text{ass}}$ , calculées par RMN  $^1\text{H}$ , de  $95 \text{ M}^{-1}$ . Les motifs triuret formés ont semblé avoir une conformation non repliée type zig-zag aux basses températures tandis que le motif triuret semble avoir une conformation repliée. Cette conformation repliée semble être la cause de la non-observation de la réticulation en raison d'un processus de dimérisation entre motifs moins favorables. A plus haute température, un changement partiel de conformation des motifs tétrauret en zigzag, semble s'opérer, permettant l'observation d'une réticulation par l'apparition de liaisons supramoléculaires fortes. Ces motifs supramoléculaires ont une grande influence sur la formation de réseaux permettant le renforcement des propriétés rhéologiques et potentiellement mécaniques de matériaux polymères. A partir des structures synthétisées avec de 1 à 5 motifs triuret ou tétrauret, les propriétés des réseaux formés ont pu être modulées et contrôlées. Des études complémentaires permettront d'explorer davantage leur potentiel.

## Abstract

Supramolecular polymer networks are prepared basing on two different supramolecular interactions, ionic interaction and hydrogen bonds interaction. Ionic interaction was introduced in P(BMA-co-MA) with  $\text{CaCO}_3$  as a filler. The presence of  $\text{Ca}^{2+}$  is confirmed with X-ray diffraction by the appearance of specific ionic peak. The hydrogen bond interaction was introduced by two approaches. One is to first prepare a supramolecular monomer bearing DA moiety then supramolecular polymer P(MAAM-co-St) and P(MAP-co-St) are prepared by polyaddition. In the other approach, the supramolecular polymer is synthesized by one-step PUU polycondensation from the reagent containing multiple-hydrogen-bond sequence. The presence of intermolecular hydrogen bonds is detected by FTIR qualitatively, and the strength, quantified as  $K_{\text{ass}}$ , is calculated by  $^1\text{H-NMR}$  for different moieties respectively. Solubility tests indicate that the introduction of supramolecular interaction in the traditional polymers leads to the crosslinking in different extents. Consequently, materials are strengthened showing better thermo-endurance property and higher modulus when the content of supramolecular moiety is increased. Furthermore, rheological analysis is performed to investigate the viscoelasticity and to track the thermo-reversibility.

### Keywords:

Supramolecular, networks, ionic interactions, hydrogen bonds, association constants, rheology

## Résumé

Des réseaux polymères supramoléculaires ont été préparés à partir de deux types d'interactions supramoléculaires différentes, ionique et par liaisons hydrogène. Les interactions ioniques ont été introduites dans des P(BMA-co-MA) par l'introduction de  $\text{CaCO}_3$  comme charge capable de se décomposer partiellement pour former des cation  $\text{Ca}^{2+}$ . La présence de  $\text{Ca}^{2+}$  a été confirmée par diffraction de rayons X par l'observation d'un pic ionique caractéristique. Les interactions par liaisons hydrogène ont été introduites selon deux approches. L'une a été de préparer d'abord un monomère supramoléculaire avec un motif DA (donneur-accepteur) pour ensuite le copolymériser en polymères supramoléculaires P(MAAM-co-St) et P(MAP-co-St) par polyaddition. Par l'autre approche, le polymère supramoléculaire a été synthétisé par polycondensation de PUU, monomères contenant des liaisons hydrogène multiples. La présence de liaisons hydrogène intermoléculaires a mise en évidence par IRTF qualitativement, et la constante d'association  $K_{\text{ass}}$  a été calculée par  $^1\text{H}$ -RMN pour les motifs d'association. Des tests solubilité ont indiqué que la génération d'interactions supramoléculaires dans les polymères conduit à des réticulations. En conséquence, les matériaux sont renforcés et présentent une meilleure thermo-résistance et des modules plus élevés lorsque la fraction motifs supramoléculaire est augmentée. En outre, Des analyses rhéologiques ont été réalisées pour étudier la viscoélasticité et la thermo-réversibilité de ces systèmes physiquement réticulés.

### Mots clés:

Supramoléculaire, réseaux, l'interaction ionique, liaison hydrogène, constant association, rhéologie